

PhD PROCEEDINGS

ANNUAL ISSUES OF THE DOCTORAL SCHOOL

FACULTY OF INFORMATION TECHNOLOGY & BIONICS

2023

PhD PROCEEDINGS

ANNUAL ISSUES OF THE DOCTORAL SCHOOL

FACULTY OF INFORMATION TECHNOLOGY & BIONICS  
PÁZMÁNY PÉTER CATHOLIC UNIVERSITY

# PhD PROCEEDINGS

ANNUAL ISSUES OF THE DOCTORAL SCHOOL  
FACULTY OF INFORMATION TECHNOLOGY & BIONICS  
2023



PÁZMÁNY *1635*  
— s i n c e

PÁZMÁNY UNIVERSITY *e*PRESS  
BUDAPEST, 2023

© PPKE Információs Technológiai és Bionikai Kar, 2023

HU ISSN 2064-7271

Kiadja a Pázmány Egyetem eKiadó  
Budapest, 2023

Felelős kiadó  
Rev. Mons. Dr. Kuminetz Géza  
a Pázmány Péter Katolikus Egyetem rektora

The publication of this volume was supported by  
the New National Excellence Program of the Ministry for Innovation and Technology

Cover image by Imre Gergely Jánoki: *Monitoring setup for simultaneous ECG, photoplethysmography and speckle plethysmography measurements of an anesthetized rat model animal.*

# Contents

<b>Introduction</b> . . . . .	<b>8</b>
<b>PROGRAM 1: BIONICS, BIO-INSPIRED WAVE COMPUTERS, NEUROMORPHIC MODELS</b> . . . . .	<b>9</b>
<b>Investigation of the intracortical effects of infrared neural stimulation</b> . . . . . <i>Zsófia BALOGH-LANTOS</i>	<b>10</b>
<b>Comparison of commonly used single cell migration parameters</b> . . . . . <i>Gréta Lilla BÁNYAI</i>	<b>11</b>
<b>Investigation of the effect of sensor placement on machine learning using 3D hand models</b> . . . . . <i>Eszter BIRTALAN</i>	<b>12</b>
<b>Early emergence of resistance to increased chromosome missegregation – a quantitative biology approach</b> . . . . . <i>Camilla CANCRINI</i>	<b>13</b>
<b>Structural and functional investigation of the postsynaptic Homer protein</b> . . . . . <i>Fanni FARKAS</i>	<b>14</b>
<b>Modelling the intracellular biochemical mechanisms of long-term potentiation in a CA1 pyramidal cell spine head</b> . . . . . <i>Gábor FARKAS</i>	<b>15</b>
<b>Growing yeast in microfluidic devices</b> . . . . . <i>Tünde Éva GAIZER</i>	<b>16</b>
<b>Extraction of PDMS electromagnetic parameters at microwave frequencies</b> . . . . . <i>Máté KÁLOVICS</i>	<b>17</b>
<b>Medial septal contributions to supra-theta oscillations</b> . . . . . <i>Barnabás KOCSIS</i>	<b>18</b>
<b>Dermatological comparison of the skin of C57BL/6J hairy and SKH1 nude mice</b> . . . . . <i>Dorottya KOCSIS</i>	<b>19</b>
<b>Possibilities of multicellularity in yeast</b> . . . . . <i>Valentina MADÁR</i>	<b>20</b>
<b>Molecular pathological characterisation of lung cancer using PET/CT imaging</b> . . . . . <i>Vilmos MADARAS</i>	<b>21</b>
<b>Shared representations for microbiome data: empowering predictive disease classification through transfer learning</b> . . . . . <i>Zsófia MOLNÁR</i>	<b>22</b>

<b>Review on the applicability of postnatal phonocardiogram processing techniques for fetal signals</b> . . . . .	<b>23</b>
<i>Kristóf MÜLLER</i>	
<b>Structural modeling of the interaction between dynein light chain molecule and the postsynaptic density scaffold protein GKAP</b> . . . . .	<b>24</b>
<i>Eszter NAGY-KANTA</i>	
<b>The role of extracellular vesicles in melanoma progression</b> . . . . .	<b>25</b>
<i>Afrodité NÉMETH</i>	
<b>Toxin production and sensitivity of different yeast strains</b> . . . . .	<b>26</b>
<i>Biborka PILLÉR</i>	
<b>Theoretical and applied studies on the cyclic movements of human limbs</b> . . . . .	<b>27</b>
<i>Balázs RADELE CZKI</i>	
<b>Examination of protein phase separation via in vitro and in silico methods</b> . . . . .	<b>28</b>
<i>András László SZABÓ</i>	
<b>Growth laws: from bacteria to yeast</b> . . . . .	<b>29</b>
<i>Giorgio TALLARICO</i>	
<b>A Hamiltonian representation of semi-discretized nonlocal flows</b> . . . . .	<b>30</b>
<i>Mihály András VÁGHY</i>	
<b>Structural characterization of the postsynaptic Drebrin protein</b> . . . . .	<b>31</b>
<i>Soma VARGA</i>	
<b>Yeast models of neurodegenerative diseases using whole-cell simulations</b> . . . . .	<b>32</b>
<i>Áron WEBER</i>	
<b>PROGRAM 2: COMPUTER TECHNOLOGY BASED ON MANY-CORE PROCESSOR CHIPS, VIRTUAL CELLULAR COMPUTERS, SENSORY AND MOTORIC ANALOG COMPUTERS</b> . . . . .	<b>33</b>
<b>Head restrained mouse behavior experiments</b> . . . . .	<b>34</b>
<i>Boldizsár Zsolt BALOG</i>	
<b>Progress report on robust epidemic model control by feedback linearization and state estimation</b> . . . . .	<b>35</b>
<i>Balázs CSUTAK</i>	
<b>Improvement possibilities of SVM algorithms for open-set recognition</b> . . . . .	<b>36</b>
<i>Lóránt Szabolcs DAUBNER</i>	
<b>Automatic stencil program generation from C++ to OPS DSL</b> . . . . .	<b>37</b>
<i>Balázs DRÁVAI</i>	
<b>Adapting the open-set recognition method to various time-series data</b> . . . . .	<b>38</b>
<i>András Pál HALÁSZ</i>	
<b>Comparison of the effect of combinations of non-pharmaceutical restrictions on the spread of COVID-19</b> . . . . .	<b>39</b>
<i>Gergely HORVÁTH</i>	
<b>Remote Cardio-Respiratory Monitoring of Neonate Rats under Asphyxia with Combined Photo- and Speckle-plethysmography</b> . . . . .	<b>40</b>
<i>Imre Gergely JÁNOKI</i>	

<b>Development of a soft resistive sensor to measure the arterial blood pressure waveform</b> . . . . .	<b>41</b>
<i>Rizal MAULANA</i>	
<b>A torque measurement process to compare biological and exosuit assisted wrist strength</b> . . . . .	<b>42</b>
<i>Katalin SCHÄFFER</i>	
<b>Utilizing the OP2 domain-specific library for adaptive multi-precision computing</b> . . . . .	<b>43</b>
<i>Bálint SIKLÓSI</i>	
<b>Time symmetric tracking of yeast cells using convolutional neural networks</b> . . . . .	<b>44</b>
<i>Gergely SZABÓ</i>	
PROGRAM 3: FEASIBILITY OF ELECTRONIC AND OPTICAL DEVICES, MOLECULAR AND NANOTECHNOLOGIES, NANO-ARCHITECTURES, NANOBIONIC DIAGNOSTIC AND THERAPEUTIC TOOLS . . . . .	<b>45</b>
<b>A Design and measurement of a compact retrodirective array</b> . . . . .	<b>46</b>
<i>András ESZES</i>	
<b>Modeling of VO<sub>2</sub> oscillator-based devices</b> . . . . .	<b>47</b>
<i>Mitra MOAYED</i>	
<b>Processing of time-independent and time-dependent signals using Oscillatory Neural Networks</b> . . . . .	<b>48</b>
<i>Tamás RUDNER</i>	
PROGRAM 4: HUMAN LANGUAGE TECHNOLOGIES, ARTIFICIAL UNDERSTANDING, TELEPRESENCE, COMMUNICATION . . . . .	<b>49</b>
<b>Gathering dataset for abstractive question answering using ChatGPT</b> . . . . .	<b>50</b>
<i>Kamran IBIYEV</i>	
<b>Abstractive Arabic text summarization with reinforcement learning</b> . . . . .	<b>51</b>
<i>Mram KAHLA</i>	
<b>Topology management and control in multipath wireless sensor networks</b> . . . . .	<b>52</b>
<i>Bálint Áron ÜVEGES</i>	
PROGRAM 5: ON-BOARD ADVANCED DRIVER ASSISTANCE SYSTEMS . . . . .	<b>53</b>
<b>Real-time foreground segmentation for surveillance applications in NRCS Lidar Sequences</b> . . . . .	<b>54</b>
<i>Marcell KÉGL</i>	
<b>Right ventricle segmentation in 3D echocardiographic recordings using deep neural networks</b> . . . . .	<b>55</b>
<i>Bálint MAGYAR</i>	
<b>Spatial completion of sparse lidar point cloud sequences</b> . . . . .	<b>56</b>
<i>Örkény Ádám H. ZOVÁTHI</i>	
<b>Appendix</b> . . . . .	<b>57</b>

# Introduction

It is our pleasure to publish this Annual Proceedings again to demonstrate the genuine multidisciplinary research done at the Jedlik Laboratories by young talents working in the Roska Tamás Doctoral School of Sciences and Technology of the Faculty of Information Technology and Bionics at Pázmány Péter Catholic University. The scientific results of our PhD students outline the main recent research directions in which our faculty is engaged. We also appreciate the support of the supervisors and consultants, as well as that of the five collaborating National Research Laboratories of the Loránd Eötvös Research Network, Semmelweis University and the University of Pannonia. The collaborative work with the partner universities, especially Katolieke Universiteit Leuven, Politecnico di Torino, Technische Universität München, University of California at Berkeley, University of Notre Dame, Universidad de Sevilla, Università di Catania, Université de Bordeaux and Universidad Autónoma de Madrid is gratefully acknowledged.

We acknowledge the support of numerous institutes, organizations and companies:

- Loránd Eötvös Research Network (ELKH),
- National Research, Development and Innovation Office (NKFIH),
- Hungarian Academy of Sciences (MTA),
- UNKP Programme, Ministry for Innovation and Technology, Hungarian Government,
- KDP Programme, Ministry for Innovation, and Technology, Hungarian Government,
- Gedeon Richter Co.,
- Office of Naval Research (ONR) of the US,
- NVIDIA Ltd.,
- Verizon Computer Vision Group (Eutecus Inc.), Berkeley, CA,
- MorphoLogic Ltd., Budapest,
- Analogic Computers Ltd., Budapest,
- AnaFocus Ltd., Seville,

and several other companies and individuals.

Needless to say, the resources and support of the Pázmány Péter Catholic University are gratefully acknowledged.

Budapest, June 2023.

GÁBOR PRÓSZÉKY

Chairman of the Board of the Doctoral School

GÁBOR SZEDERKÉNYI

Head of the Doctoral School



# PROGRAM 1

## BIONICS, BIO-INSPIRED WAVE COMPUTERS, NEUROMORPHIC MODELS

Heads: Tamás FREUND, Zsolt LIPOSITS, Sándor PONGOR

# Investigation of the intracortical effects of infrared neural stimulation

Zsófia BALOGH-LANTOS

(Supervisor: Zoltán FEKETE)

Pázmány Péter Catholic University, Faculty of Information Technology and Bionics

50/a Práter street, 1083 Budapest, Hungary

lantos.zsofia@itk.ppke.hu

**Abstract**—Infrared neuromodulation (IRN) is a technique that has been researched for more than a decade. Many experiments showed how it is possible to stimulate cells in cell cultures and nerve preparations. During these experiments, an optrode device was used to stimulate the nerves in the cortex of rats. Besides this device, a spatially dense Neuropixels electrode was implanted to record the action potentials. To determine the effects of IRN, single units were extracted from the high-density cortical recordings. Changes in the firing rates of single neurons were examined to investigate the changes in neural functions.

**Keywords**—infrared neuromodulation; electrophysiology; spike detection

## I. INTRODUCTION

A large number of individuals with different neurological disorders, like depression, Parkinson's disease, and epilepsy draw attention to these life-altering diseases [1]. This is why it is important to treat these diseases or their symptoms. Infrared neuromodulation uses pulsed or continuous infrared light to create temperature changes in the neural tissue. This temperature gradient causes the neurons to either suppress or elicit action potentials. Many biophysical and molecular effects are hypothesized behind the mechanism of INM. However, a clearer picture can only be obtained with in-depth theoretical explanations combined with experimental results.

## II. METHODS

The experiments used a sensing and intervention system to investigate the effect of tissue temperature modulation on neuronal function in four anesthetized rats. The inhibition and stimulation of cellular activity were achieved by spatially localized delivery of infrared radiation through an integrated optrode device [2]. In addition, a Neuropixels [3] electrode was included to record the intracortical signals. During the experiments, continuous infrared light was delivered to the brain tissue with the optrode device. For the spike detection Kilosort, a MATLAB-based template matching framework was used [4]. This is an automated method that uses the raw data to detect the spikes, getting more accurate waveforms. After using Kilosort, the spike clusters were manually curated and separated into single unit activity spike clusters. To analyze the data, custom MATLAB scripts were used. The average firing rate and relative firing rate of all detected cells was calculated.

Figure 1 shows the heatmap of the normalized relative firing rates of all cells. Each row represents one cell, sorted according to the channels, which corresponds to the depth of the detected cells. As the figure shows, some of the cells were inhibited, and some of them were excited.

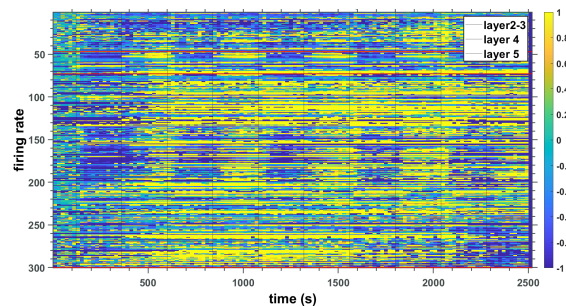


Fig. 1. Heatmap of the normalized relative firing rates

## III. DISCUSSION

During this research, the effect of infrared neuromodulation on neuronal cell activity was investigated. The data was recorded on the channels of the Neuropixels electrode used in the experiments and the obtained data were analyzed according to different parameters. The results show that the effect of infrared neuromodulation causes changes in neural function. It was demonstrated, that cells can be inhibited or excited.

This analysis will allow us to obtain more precise information about the propagation of the induced signals and their origin. These will help to elucidate the biophysical background of infrared neuromodulation, thus bringing us closer to the application of infrared stimulation in the therapy of neurodegenerative diseases.

## IV. ACKNOWLEDGEMENT

This research was supported by the National Research, Development and Innovation Office – NKFIH – through the grant no. TKP2021-EGA-42.

## REFERENCES

- [1] Z. Fekete, Á. C. Horváth, and A. Zátanyi, "Infrared neuromodulation: a neuroengineering perspective," *Journal of Neural Engineering*, vol. 17, no. 5, p. 051003, 2020.
- [2] Á. C. Horváth, S. Borbély, Ö. C. Boros, L. Komáromi, P. Koppa, P. Barthó, and Z. Fekete, "Infrared neural stimulation and inhibition using an implantable silicon photonic microdevice," *Microsystems & nanoengineering*, vol. 6, no. 1, p. 44, 2020.
- [3] N. A. Steinmetz, C. Aydin, A. Lebedeva, M. Okun, M. Pachitariu, M. Bauza, M. Beau, J. Bhagat, C. Böhm, M. Broux, *et al.*, "Neuropixels 2.0: A miniaturized high-density probe for stable, long-term brain recordings," *Science*, vol. 372, no. 6539, p. eabf4588, 2021.
- [4] M. Pachitariu, N. A. Steinmetz, S. N. Kadir, M. Carandini, and K. D. Harris, "Fast and accurate spike sorting of high-channel count probes with kilosort," *Advances in neural information processing systems*, vol. 29, 2016.

# Comparison of commonly used single cell migration parameters

Gréta Lilla BÁNYAI

(Supervisor: Tamás Márton GARAY)

Pázmány Péter Catholic University, Faculty of Information Technology and Bionics

50/a Práter street, 1083 Budapest, Hungary

banyai.greta.lilla@itk.ppke.hu

**Abstract**—Cancer metastases, relying on cell migration, are accounting for 90% of the fatal outcome in tumor patients. Hence, study of cell migration is essential to seek possible treatments [1]. Migration can be examined with different type of parameters, which aimed to show different characteristics of the cell movement. Some treatments may have different effects on these parameters. This study aimed to examine sensitivity of various migration parameters with help of a random walk model. Based on our simulations the average speed and total travel distance were the most sensitive and mean square displacement (MSD) the most insensitive to the changes in migration.

**Keywords**—cell migration, videomicroscopy, displacement, traveled distance, mean velocity, MSD, maximal displacement, persistent random walk model

## I. INTRODUCTION

Cell migration is involved in many biological processes, such as the formation of metastasis in cancer patients. During metastasis the tumor cell migrate from the primary tumor-site to another location to form metastasis by entering the bloodstream or lymphatic system [2] [3]. One of the widely used methods for investigating cell migration is timelapse videomicroscopy, which can examine cell motility independently from proliferation or invasion. Crucial, but not often addressed part of the investigations is to properly process the data extracted from the cell tracking, since many interrelated parameters can be calculated, and different parameters can paint different picture of the cell’s migratory behavior [4].

## II. PREVIOUS RESULTS

According manually processed videomicroscopic images evaluation of the consistence between migration parameters showed that the assessed effect – namely, that the given treatment stimulates or inhibits cell migration – might be dependent on the calculated parameter. For a more comprehensive analysis we used a simulation in which we implemented the basic elements of the cell migration measurement in an environment free from external influences.

## III. SIMULATION OF RANDOM WALK AND MIGRATION PARAMETERS

Random walk model was simulated in MATLAB. With the help of a single variable, the model can increase or decrease the speed and alter the probability of changing the direction of the simulated cell movement. A total of 100 control measurements were simulated. For the treatments that increase and decrease the migration speed, we performed 200-200 measurements with different concentrations, each of which contained 20 parallel measurements. In each case, the migration was recorded at 96 points, representing a 24-hour measurement with a 15-minute video rate.

Five commonly used migration parameters were calculated from the position of the cells at a given time point: Mean square displacement (MSD), displacement, maximal displacement, total traveled distance and average velocity, then statistical significance were determined for each parameter by comparing the area under the curve (AUC) of the control measurement to the treatments.

## IV. RESULTS AND SUMMARY

	MSD	$d_{displ}$	$d_{max}$	$d_{total}$	$v_{av}$
Increased velocity	2.36	2.16	1.77	1.14	1.13
Decreased velocity	0.31	0.40	0.51	0.88	0.89

TABLE I  
TREATMENT CONCENTRATION WHERE THE PARAMETERS SHOWED SIGNIFICANT CHANGE

In summary, by examining at what concentration the parameters can reliably show the effect of the treatment, we set up an order of how sensitive the tested parameters are. We observed that the parameters show a significant difference in sensitivity. The most sensitive were the total traveled distance and the average speed. Although it is ideal to be able to detect minimal effect of treatment with these parameters, but due to their excessive sensitivity, they can react sensitively to changes resulting from different the cell tracking method as well. Maximal displacement, which was in the middle of the sensitivity order has an advantage that it produces less errors and is not overly insensitive. Surprisingly, the MSD, which is often used in practice, was the least sensitive, and produced, not independently from its minor sensitivity, more false positive results.

## V. ACKNOWLEDGEMENTS

The authors acknowledge the support of the National Research, Development and Innovation Office – NKFIH – through grant no. TKP2021-EGA-42. I would like to extend my thanks to Márton Bese Naszlady from Pázmány Péter Catholic University for his help with the development of the program.

## REFERENCES

- [1] C. Hayot, O. Debeir, P. Van Ham, M. Van Damme, R. Kiss, and C. Decaestecker, “Characterization of the activities of actin-affecting drugs on tumor cell migration,” vol. 211, no. 1, pp. 30–40, 2006.
- [2] X. Trepast, Z. Chen, and K. Jacobson, “Cell migration,” *Compr Physiol.*, vol. 2, no. 4, pp. 2369–2392, 2012.
- [3] C. D. Paul, P. Mistrionis, and K. Konstantopoulos, “Cancer cell motility: lessons from migration in confined spaces,” *Nat Rev Cancer*, vol. 17, p. 131–140, 2010.
- [4] C. Carmona-Fontaine, H. Matthews, and R. Mayor, “Directional cell migration in vivo,” *Cell Adhesion & Migration*, vol. 2, no. 4, pp. 240–242, 2008.

# Investigation of the effect of sensor placement on machine learning using 3D hand models

Eszter BIRTALAN

(Supervisor: Miklós KOLLER)

Pázmány Péter Catholic University, Faculty of Information Technology and Bionics  
50/a Práter street, 1083 Budapest, Hungary  
birtalan.eszter@itk.ppke.hu

**Abstract**—The use of tactile sensors in hand prostheses is an increasingly popular trend in robotics as it can increase both the sample efficiency and performance of a grasp learning algorithm using a neural network. However, recent experiences seem to show that their positioning and number are highly influential in this process. This study aims to investigate these effects when it comes to training with a deep reinforcement learning algorithm and provide a comparative overview of the subject.

**Keywords**—tactile sensor, tactile sensor density, tactile sensor distribution, 3D hand simulation, deep reinforcement learning.

## I. INTRODUCTION

The most well-known sensation we assign to the human hand is touch. It helps us explore our environment and interact with it in our everyday lives without much conscious oversight. In recent years researchers began to investigate how tactile information could be used effectively in hand prostheses and found that adding such information to their simulations makes task training with deep reinforcement learning (DRL) more efficient and increases performance [1]. Other research groups were able to identify different activity patterns on high-density tactile gloves when grasping, lifting, and moving everyday objects [2], [3] and were able to successfully classify these patterns. They also noted how similar patterns appear when grasping different objects, a phenomenon that may be exploited for efficient robotic hand control. Melink et al. also noted that not only were the tactile sensors active unevenly, but their data also seemed to contribute differently to learning each task. When performing the same learning scheme with a higher and lower number of sensors they experienced a significant reduction in performance. These suggest that both the density and distribution of tactile sensors have a strong effect on task learning, however, as of yet there is no comprehensive study of the exact nature of this effect. This research aims to help with the closing of this gap in the literature.

## II. METHODS

To investigate these effects I set up a simulation environment containing a 3D hand model equipped with tactile sensors. The model learns to grasp and lift different objects using a DRL algorithm (Fig 1) using a similar grasp type to initially ease the task. In the future, I will change both the number and positioning of these sensors and examine the effect this will have on the learning process. The hand will also be equipped with a soft cover that should passively help the grasping process by conforming to the shape of the object and thus establishing a larger grasping area, similar to the UB IV hand design [4].

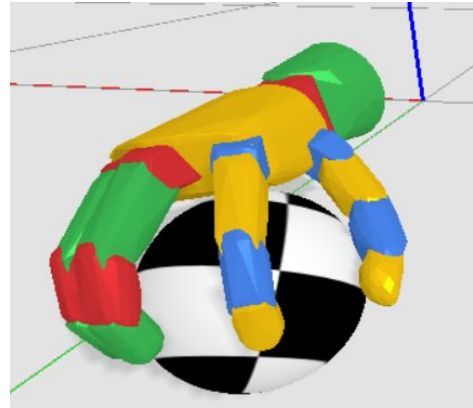


Fig. 1. A representation of the experimental setup.

## ACKNOWLEDGEMENTS

This research was supported by the National Research, Development and Innovation Office – NKFIH – through the grant no. TKP2021-NKTA-66.

## REFERENCES

- [1] A. Melnik, L. Lach, M. Plappert, T. Korthals, R. Haschke, and H. Ritter, “Using tactile sensing to improve the sample efficiency and performance of deep deterministic policy gradients for simulated in-hand manipulation tasks,” *Frontiers in Robotics and AI*, vol. 8, 2021. DOI: 10.3389/frobt.2021.538773.
- [2] S. Sundaram, P. Kellnhofer, Y. Li, J.-Y. Zhu, A. Torralba, and W. Matusik, “Learning the signatures of the human grasp using a scalable tactile glove,” *Nature*, vol. 569, pp. 698–702, 2019. DOI: 10.1038/s41586-019-1234-z.
- [3] J. Cepriá-Bernal and A. Pérez-González, “Dataset of tactile signatures of the human right hand in twenty-one activities of daily living using a high spatial resolution pressure sensor,” *Sensors*, vol. 21, no. 8, p. 2594, 2021. DOI: 10.3390/s21082594.
- [4] C. Melchiorri, G. Palli, G. Berselli, and G. Vassura, “Development of the ub hand iv: Overview of design solutions and enabling technologies,” *IEEE Robotics & Automation Magazine*, vol. 20, no. 3, pp. 72–81, 2013. DOI: 10.1109/MRA.2012.2225471.

# Early emergence of resistance to increased chromosome missegregation – a quantitative biology approach

Camilla CANCRINI

(Supervisor: Andrea CILIBERTO)

Pázmány Péter Catholic University, Faculty of Information Technology and Bionics  
50/a Práter street, 1083 Budapest, Hungary  
cancrini.camilla@itk.ppke.hu

**Abstract**—In my research project, I aim to learn more about how cells react to chromosome missegregation-causing events. This topic is of the utmost importance since such events occur to cells treated with antimetotics, a family of drugs frequently employed to treat cancer. Antimetotics alter microtubule dynamics, which hinders cancer cells' capacity to divide. These drugs activate the mitotic checkpoint, which prevents cells from entering mitosis and channels them towards cell death. However, it can happen that cells eventually bypass this checkpoint barrier and start to multiply at high rates of chromosome missegregation. While some cells die, others are capable of reproducing once more and producing resistant offspring. The objective of my project is to develop a mathematical framework for predicting the behavior of cells in response to induced missegregation (i.e. treatment with antimetotics). The outcome will be a phase-space diagram, that we will refer to as *survival map* (see Fig. 1), that will show whether cells will become resistant to induced missegregation or go extinct. The result of the population will depend on how the initial population size ( $N_0$ ) and missegregation rate ( $\rho$ ) interact. These two parameters can be modulated experimentally.

**Keywords**—Missegregation; Drugs resistance; Mathematical Model.

## I. INTRODUCTION

*Missegregation* refers to the process by which an erroneous number of chromosomes are distributed to daughter cells, and *aneuploidy* refers to the result of this process, which is a set of chromosomes differing from those found in wild-type cells. Missegregation can be caused by external stimuli (such as drugs, high temperatures, etc.) or it can happen spontaneously as a result of errors made during cell division. Aneuploidy has been linked to a variety of human diseases, including Down's syndrome, cancer, stress, and drug resistance. Antimetotics, a family of drugs used to treat cancer, induce errors in the segregation of chromosomes by damaging the mitotic spindles. This may stop cell cycle of cancer cells, arresting them in mitosis, and eventually leading to apoptosis (a process of cellular self-destruction). Unfortunately, the drug is not always able to achieve this result. Indeed, cells resistant to such treatments are cells that manage to go ahead in the cell cycle despite not having corrected the errors induced by the drug. This generates, at least initially, aneuploid cells. As can be understood, the result may therefore be paradoxical: not only tumor cells are not killed but the situation could also worsen due the introduction of further karyotype heterogeneity and complexity within the tumor population. Additionally, considering that it is well-known that aneuploidy often has a negative impact on fitness, the fact that aneuploidy promotes tumour cells survival and can consequently be advantageous under some circumstances, is what is known as 'aneuploidy

paradox' [4]. To rationalise how cells respond to this paradox in different conditions, I plan to develop a mathematical model of missegregation that might be used for predicting the outcome of a tumor population in response to induced missegregation as in the case upon treatment with antimetotics. To start, I suppose the fate of cells populations to depend from the interaction between two parameters: the initial population size ( $N_0$ ) and the missegregation rate ( $\rho$ ). Since I aim at always having a feedback for my model from experimental data, it is important for me to find strategies to modulate these two parameters experimentally. Last year I set up an experimental protocol for the modulation of  $N_0$ . This year I instead set up a protocol for  $\rho$  modulation. This was done for yeast haploid cells during the first semester. The plan was to create different strains, each one characterised by a unique rate of missegregation. During the second semester I instead tested the acquired strains, in order to confirm the different values of missegregation rates, and worked on the mathematical framework.

The future plan is to evolve these strains and use them to complete the *survival map* (see Fig. 1) as well as keep developing the mathematical model.

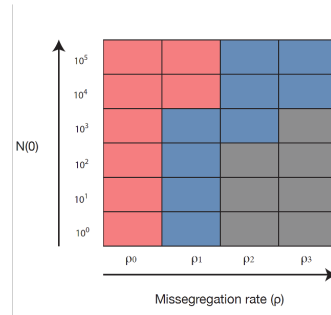


Fig. 1: Survival map. Each color represents a possible fate for a population of cells. For example, red color could represent extinction, blue color could represent resistance via aneuploidy whereas grey color represents resistance via point mutation.

## REFERENCES

- [1] KIMMEL GJ, BECK RJ, YU X, ET AL., *Intra-tumor heterogeneity, turnover rate and karyotype space susceptibility to missegregation-induced extinction.*, PLoS Comput Biol.; 19(1):e1010815 (2023).
- [2] PAVANI M, BONAIUTI P, CHIROLI E, ET AL., *Epistasis, aneuploidy, and functional mutations underlie evolution of resistance to induced microtubule depolymerization.*, EMBO J. (2021).
- [3] SCHENK, M.F., ZWART, M.P., HWANG, S. ET AL., *Population size mediates the contribution of high-rate and large-benefit mutations to parallel evolution.*, Nat Ecol Evol 6, 439–447 (2022).
- [4] SHELTERER JM, AMON A., *The aneuploidy paradox: costs and benefits of an incorrect karyotype.*, Trends Genet. 2011;27(11):446-453. doi:10.1016/j.tig.2011.07.003.

# Structural and functional investigation of the postsynaptic Homer protein

Fanni FARKAS

(Supervisor: Zoltán GÁSPÁRI)

Pázmány Péter Catholic University, Faculty of Information Technology and Bionics

50/a Práter street, 1083 Budapest, Hungary

farkas.fanni@itk.ppke.hu

**Abstract**—The postsynaptic density (PSD) is a complex protein network located beneath the postsynaptic membrane. The Shank and Homer scaffold proteins play a pivotal role in maintaining the central PSD, emphasizing the significance of their interactions for proper protein network formation. In addition, Homer1 interacts with mGluR1 $\alpha$ 5 subunits through their carboxy-terminals, enabling regulation of their postsynaptic localization, translation, and intracellular signaling. Mutations in these proteins have been linked to various neurodegenerative diseases. My research focuses on conducting a detailed structure-function characterization of the Homer1 protein using NMR spectroscopy and other biophysical methods.

**Keywords**—PSD; HOMER1; EVH1; NMR; interaction

## I. INTRODUCTION

The postsynaptic density (PSD) is positioned beneath the postsynaptic membrane of neurons and constitutes a large protein complex characterized by numerous interactions. These proteins play a vital role in various cognitive processes, including learning and memory formation [1]. Neurodevelopmental disorders significantly impact these aspects, leading to impairments in cognition, learning, and memory. Such disorders include autism spectrum disorder (ASD) and schizophrenia, where alterations in postsynaptic density proteins at excitatory synapses contribute to the pathology [2]. The scaffolding proteins, particularly Homer and Shank proteins, provide the structural framework for this protein network. Homer has the ability to form tetramers and facilitate the development of PSD complexes. EVH1 domain of Homer plays a crucial role in protein interactions. In order to comprehend the mechanistic workings of this dynamic structure and its involvement in neural processes, an in-depth analysis of its constituent proteins and their interactions is crucial. NMR spectroscopy serves as a prominent technique for investigating the three-dimensional structure and dynamics of proteins at the atomic level. When examining intrinsically disordered protein segments, NMR emerges as the preferred method, albeit necessitating specific conditions such as a highly concentrated protein sample, low pH, and minimal buffer components. [3]

## II. METHOD

The production of recombinant Homer protein (EVH1 domain) and its two mutant variants (M65I and S97L) was carried out in competent *E. coli* cells. The cells were cultured in LB to produce unlabelled protein sample and minimal media, labeled with  $^{13}\text{C}$  and  $^{15}\text{N}$  isotopes to produce labelled version as for NMR measurement. Following ultrasonic homogenization, the protein was purified using immobilized metal affinity chromatography (IMAC) utilizing a Fast Protein Liquid Chromatography (FPLC) system. To prepare a suitable

protein sample for NMR analysis, a buffer exchange was performed, followed by an Ion Exchange Chromatography (IEC) step using an S column. Subsequently, size exclusion chromatography (SEC) was employed to optimize the conditions (pH, NaCl level, etc.) suitable for NMR analysis. The results were evaluated using SDS-PAGE. Finally, the NMR-compatible sample was sent to Debrecen for NMR measurements. For the refinement of the structural model obtained for Homer EVH1, molecular dynamics calculations with the GROMACS software suite were performed. Several different force fields, protocols were applied along with different combinations of experimental and geometry restraints.

## III. RESULTS

The expression and purification of three EVH1 domains (wild type, and two point mutants) in both unlabelled and isotopically labelled forms was successfully achieved. Through the purification process and subsequent concentration, a highly concentrated sample was prepared, suitable for NMR measurements. Additionally, for further experiments aimed at modeling and understanding the behavior of human Homer, the complete DNA and amino acid sequence of Homer were designed and ordered. These sequences will be instrumental in our ongoing research efforts. I have performed exploratory molecular dynamics calculations on the existing EVH1 structural model, generated previously in our group. Optimization of the protocols is still in progress in order to improve the quality of the obtained conformers.

## ACKNOWLEDGEMENTS

I would like to express my gratitude to Dr. Zoltan Gaspari and Dr. Balint Peterfia for the invaluable guidance and support provided throughout my research endeavor. I am very grateful for your time, patience, and encouragement, which have played a significant role in this research. Thank you for your contributions and for being an exceptional mentor. This research was supported by the National Research, Development and Innovation Office – NKFIH – through the grant no. TKP2021-EGA-42 .

## REFERENCES

- [1] Y. Vyas and J. M. Montgomery, “The role of postsynaptic density proteins in neural degeneration and regeneration,” *Neural Regeneration Research*, vol. 11, no. 6, p. 906, 2016.
- [2] A. Banerjee, J. A. Luong, A. Ho, A. O. Saib, and J. E. Ploski, “Overexpression of homer1a in the basal and lateral amygdala impairs fear conditioning and induces an autism-like social impairment,” *Molecular autism*, vol. 7, no. 1, pp. 1–15, 2016.
- [3] A. Bax and G. M. Clore, “Protein nmr: boundless opportunities,” *Journal of Magnetic Resonance*, vol. 306, pp. 187–191, 2019.

# Modelling the intracellular biochemical mechanisms of long-term potentiation in a CA1 pyramidal cell spine head

Gábor FARKAS

(Supervisor: Szabolcs KÁLI)

Pázmány Péter Catholic University, Faculty of Information Technology and Bionics  
50/a Práter street, 1083 Budapest, Hungary  
farkas.gabor@itk.ppke.hu

**Abstract**—Long-lasting increase in the strength of synaptic communication is called long-term potentiation (LTP), the candidate mechanism of cellular-level learning. A sophisticated system of intracellular signaling pathways in the spine heads of postsynaptic dendrites remarkably takes part in the formation, maintenance, and expression of LTP. Using computational modelling combined with experimental results, possible mechanisms of LTP were revealed. Our results suggest that the permanent phosphorylation of AMPA receptors could be the principal mechanism of long-lasting synaptic strengthening.

**Keywords**—CA1 pyramidal cell, long-term potentiation, intracellular signaling, biochemical mechanisms

## I. INTRODUCTION

Besides the biophysical features of neurons, intracellular biochemical signaling pathways also contribute to the formation of complex neuronal functions such as activity-dependent synaptic plasticity. Modelling a network of subcellular cascades can help to understand the underlying molecular mechanisms of synaptic changes, such as long-term potentiation, the mechanism of action of different plasticity induction protocols and the roles of the different molecules, and pathways.

## II. METHODS

A computational model of the plasticity-related intracellular signaling pathways was created based on the model described in [1]. The one-compartmental model is located in a dendritic spine head of a CA1 pyramidal neuron and contains the main signaling pathways that establish hippocampal LTP: the CaMKII, the PKA and the PKC cascades. The model was used to fit experimental data gathered from papers in which the effects of the inhibition of the mentioned kinases were investigated in CA1-Schaffer collateral synapses. The Python-based model was simulated in the reaction-diffusion submodule of the Neuron simulation environment [2], and the model parameters were optimized with the Neuroptimus optimization software tool [3]. Such optimizations require powerful computational resources, so the Neuroscience Gateway (NSG) [4] – a portal providing high-performance supercomputers for computational neuroscientific tasks – was used.

## III. RESULTS

Five different possible components of LTP were identified in our results that are marked with the small colorful numbers in Figure 1. The figure illustrates the numbers of different AMPA receptor subunits whose phosphorylation state and number in the postsynaptic membrane determine the total synaptic conductance, a measure of synaptic changes.

## Numbers of different membrane-bound AMPA receptor subunits

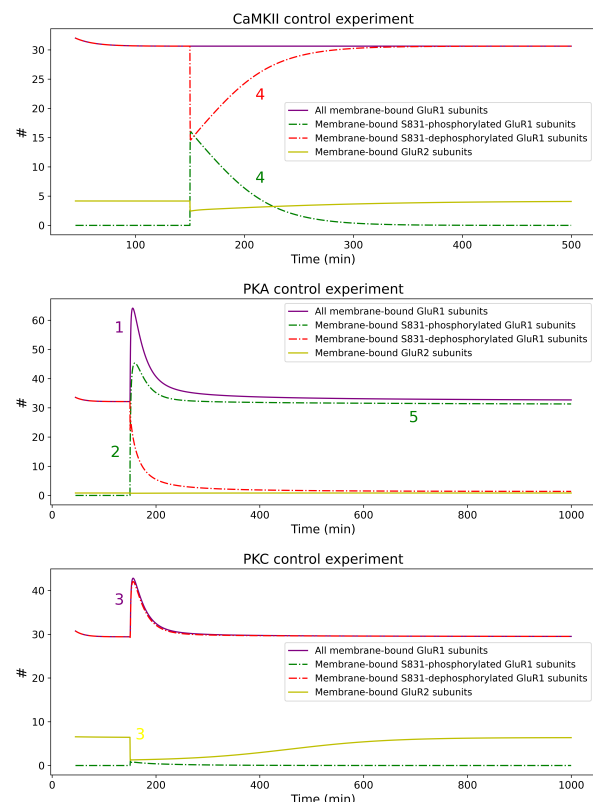


Fig. 1. Numbers of different AMPA receptor subunits in control cases with the small colorful numbers marking the possible mechanisms of LTP. 1.) Fast GluR1 insertion into the membrane (PKA S845-phosphorylation dependent), 2.) Fast GluR1 S831-phosphorylation mainly by CaMKII, but also by PKC, 3.) Slower GluR1 – GluR2 exchange in the membrane (PKA S845-phosphorylation and PKC S880-phosphorylation), 4.) Slower GluR1 S831-dephosphorylation by PP1, 5.) Permanent GluR1 S831-phosphorylation by autophosphorylated CaMKII (PKA – I1 – PP1 – CaMKII disinhibition).

## REFERENCES

- [1] T. Mäki-Marttunen, N. Iannella, A. Edwards, G. Einevoll, and K. Blackwell, “A unified computational model for cortical post-synaptic plasticity,” *eLife*, vol. 9, p. e55714, 07 2020.
- [2] R. McDougal, M. Hines, and W. Lytton, “Reaction-diffusion in the neuron simulator,” *Frontiers in Neuroinformatics*, 11 2013.
- [3] M. Mohacsi, M. Torok, S. Sárny, and S. Kali, “A unified framework for the application and evaluation of different methods for neural parameter optimization,” 07 2020, pp. 1–7.
- [4] S. Sivagnanam, A. Majumdar, K. Yoshimoto, V. Astakhov, A. Bandrowski, M. Martone, and N. Carnevale, “Introducing the neuroscience gateway,” *CEUR Workshop Proceedings*, vol. 993, 01 2013.

# Growing yeast in microfluidic devices

Tünde GAIZER

(Supervisor: Attila CSIKÁSZ-NAGY)

Pázmány Péter Catholic University, Faculty of Information Technology and Bionics

50/a Práter street, 1083 Budapest, Hungary

gaizer.tunde.eva@itk.ppke.hu

**Abstract**—Research with yeast have had a substantial contribution to our understanding of many cellular processes and well as is of high importance in biotechnological and food industry. One of the important research areas is aging. Aging is a fundamental biological process that affects all living organisms and has a significant impact on human health and society. In this paper I introduce the possibilities offered by the improvements in microfluidic technologies to increase our knowledge about aging. I introduce my developmental work toward an in-house yeast aging device in collaboration with the Biomicrofluidics Research Team. I have successfully observed aging yeast for over 50 hours including characteristics specific to aging and cell death.

**Keywords**—yeast; microfluidics; aging

## I. INTRODUCTION

*Saccharomyces cerevisiae*, commonly known as budding yeast, has been a powerful model organism for studying the molecular mechanisms of many processes in eukaryotic cells for over 60 years. Among these evolutionary highly conserved mechanisms are regulations of aging and cell death mechanism [1], [2]. In this paper I aim to review the possibilities of aging research with microfluidic devices as well as introduce the early results of our developmental process of our own aging device.

Microfluidic platforms have emerged as powerful tools in yeast aging research [3]. They offer precise control over environmental conditions and also the ability to monitor individual cells over extended periods, like the whole lifespan of a yeast cell [4]. This high-throughput capability results in the collection of extensive datasets, facilitating statistical analysis and recent developments of dedicated machine learning algorithms can automate these tasks [5]. By combining microfluidics with fluorescence microscopy a wide range of parameters, including cell morphology, gene expression, protein localization, and mitochondrial dynamics can be studied providing a comprehensive view of the aging processes [6].

## II. METHODS

BY7442 strain of *Saccharomyces cerevisiae* was used in this study. Double color-tagged strains were achieved by mating haploid  $\alpha$  HO::Tef1p-EGFP-KanMx4 with haploid a HO::Tef1p-mCherry-URA3 of the same strain, followed by double selection plating. Synthetic complete (SD) media with 2% glucose was used to grow cells overnight before the experiment as well as during the microfluidic measurement. Chambers were designed and fabricated by the biomicrofluidics research team on our faculty. Chips were prepared from PDMS mold on glass microscopy slides. Chamber height is 5  $\mu$ m. Preculture was prepared the day before the experiment and diluted 100-fold in the morning before loading into the chambers. Syringe pump was used to set flow rate specified in the Results section.

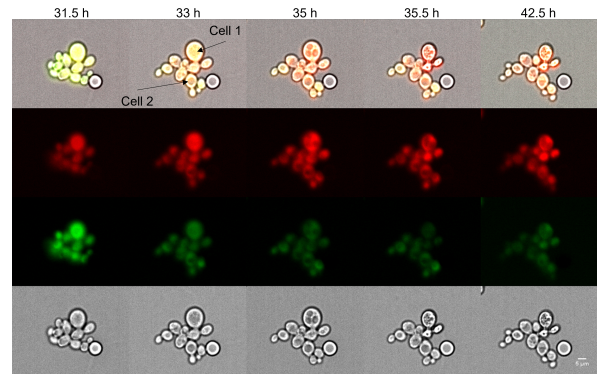


Fig. 1. Aging experiment in microfluidic chamber with media flow stopped at 32 hours. BY7442 strain is tagged with constitutively expressed EGFP and mCherry. Changes in cell morphology are shown between 30 and 40 hours

## III. RESULTS

Developing a full protocol for single-cell analysis is an iterative process with many steps to be optimized and improved along the road. The main focus of development was chamber geometry and optimizing flow rates and loading procedure. First important step in optimization was the shape of the traps. Throughout the iterations, more than 5 trap shapes were tested. Our improved desing has demonstrated the capability of retaining mother cells for over 50 hours. Further development is in progress to extend this to 3-5 days.

## ACKNOWLEDGEMENTS

I would like to thank András Laki and Mária Laki for designing and fabricating the microfluidic devices and Csaba Pongor for the support with microscopy. Experimental work was carried out with Bőborka Pillér, Helga Szakadati and Eszter Kegyes-Brassai. The research was supported by the Hungarian National Research, Development and Innovation Office (NKFI/NRDI) through the Hungarian Scientific Research Fund (OTKA-K20-134489) and the Thematic Excellence Programme grant no. TKP2021-EGA-42.

## REFERENCES

- [1] A. Denoth Lippuner, T. Julou, and Y. Barral, “Budding yeast as a model organism to study the effects of age,” *FEMS Microbiology Reviews*, vol. 38, no. 2, pp. 300–325, 2014.
- [2] A. A. Duina, M. E. Miller, and J. B. Keeney, “Budding yeast for budding geneticists: A primer on the *saccharomyces cerevisiae* model system,” *Genetics*, vol. 197, no. 1, pp. 33–48, 2014.
- [3] K. L. Chen, M. M. Crane, and M. Kaerberlein, “Microfluidic technologies for yeast replicative lifespan studies,” *Mechanisms of Ageing and Development*, vol. 161, pp. 262–269, 2017.
- [4] M. C. Jo and L. Qin, “Microfluidic platforms for yeast-based aging studies,” *Small*, vol. 12, no. 42, pp. 5787–5801, 2016.
- [5] T. Aspert, D. Hentsch, and G. Charvin, “Detecdiv, a generalist deep-learning platform for automated cell division tracking and survival analysis,” *eLife*, vol. 11, 2022, September 13, 2022.
- [6] P. Allard, F. Papazotos, and L. Potvin-Trottier, “Microfluidics for long-term single-cell time-lapse microscopy: Advances and applications,” *Frontiers in Bioengineering and Biotechnology*, vol. 10, 2022.



# Extraction of PDMS electromagnetic parameters at microwave frequencies

Máté KÁLOVICS

(Supervisors: Kristóf IVÁN, Zsolt SZABÓ)

Pázmány Péter Catholic University, Faculty of Information Technology and Bionics

50/a Práter street, 1083 Budapest, Hungary

kalovics.mate@itk.ppke.hu

**Keywords-microstrip, PDMS, microwave frequencies**

## I. INTRODUCTION

Determining the electromagnetic parameters of polydimethylsiloxane (PDMS) is an important task due to it is the most common material employed in fabrication and prototyping of microfluidics. However there is a group [1] who determined the complex permittivity of PDMS by coplanar transmission lines (CPW) from 1 to 220 GHz where the real part ( $\epsilon_r$ ) varies from 2.9 to 2.55 and the loss tangent ( $\tan\delta$ ) reaches 0.048 at 210 GHz frequency. It is important to specify the electromagnetic parameters of the PDMS substrate I am working with since those can be influenced by environmental effects, aging, the ratio of the liquid PDMS and the cross-linking agent, or the plasma treatment. In the full version of the document I present you the dielectric characterisation of PDMS from 1 to 12 GHz frequencies achieved by extracting the transmission lines with microstrips designed and manufactured by Electromagnetic Structures Research Group.

## II. DESIGN AND FABRICATION OF MICROSTRIP

The design and the actual device is shown on Fig. 1. The PCB laminate is Isola IS680 with a  $d = 0.76 \text{ mm}$ , copper weight of  $35 \mu\text{m}$ ,  $\epsilon_r = 3.45$  and  $\tan\delta = 0.0035$  at frequencies of 1 to 15 GHz. The length of the PCB is  $100 \text{ mm}$  horizontally an  $41.4 \text{ mm}$  vertically. The width of the microstrip is  $W = 1.7 \text{ mm}$  and the length  $l = 41.4 \text{ mm}$  which was the result of rastering a paint layer with a  $30 W$  laser cutter and chemical etching.

## III. SIMULATION

In preparation of determining  $\epsilon_r$  and  $\tan\delta$  of PDMS simulations were made in CST Studio Suite 2021 and AWR TXLine to validate the results of S-parameter measurements carried out by vector network analyser (VNA). The results are shown

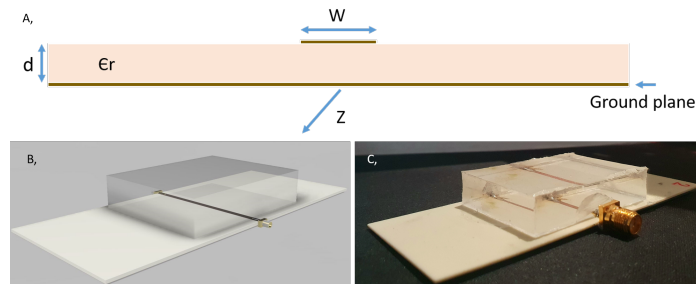


Fig. 1. A, Outline of the geometry of a microstrip with important parameters highlighted such as  $W$  for width of the microstrip,  $d$  for the height of the substrate,  $Z$  for the characteristic impedance and  $\epsilon_r$  for the relative permittivity of the substrate. B, Design of the structure with a block of PDMS on top of it made in AutoDesk Fusion360 for simulation purposes. C, An actual image of the manufactured microstrip and the PDMS block bound to it.

in Fig.2. The simulation results were compared to numerical method [2]:

$$\phi = \beta l, \quad (1)$$

where  $\phi$  is the phase delay,  $\beta$  is the propagation constant, and  $l$  is the length of the microstrip. Since the results show no significant differences the device is appropriate to the validation measurement and the extraction of PDMS electromagnetic parameters.

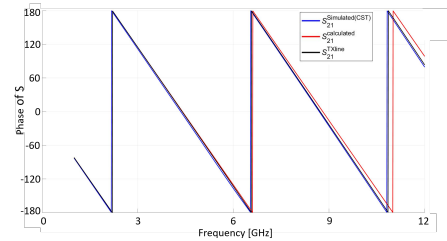


Fig. 2. Comparison of numerical and simulation results for phase of S-parameter from 1 to 12 GHz frequency. The blue line corresponds to simulation results of CST Studio Suite 2021 while the red line shows the result of an analytical model [2]. The black line is the result of AWR TXLine simulation package.

## IV. ACKNOWLEDGEMENT

This research was supported by the project NKFI K 132050 "Funkcionális elektromágneses metafelületek tervezése". In addition to the work of Zsolt Szabó and Kristóf Iván, I would also like to highlight the contribution of Balázs M. Bódis.

## REFERENCES

- [1] P.-Y. Cresson, Y. Orlic, J.-F. Legier, E. Paleczny, L. Dubois, N. Tiercelin, P. Coquet, P. Pernod, and T. Lasri, "1 to 220 ghz complex permittivity behavior of flexible polydimethylsiloxane substrate," *IEEE Microwave and Wireless Components Letters*, vol. 24, no. 4, pp. 278–280, 2014.
- [2] D. M. Pozar, *Microwave engineering*. John wiley & sons, 2011.

# Medial septal contributions to supra-theta oscillations

Barnabás KOCSIS

(Supervisor: István ULBERT)

Pázmány Péter Catholic University, Faculty of Information Technology and Bionics

50/a Práter street, 1083 Budapest, Hungary

kocsis.barnabas@itk.ppke.hu

**Abstract**—Medial septum (MS) was identified as an important player of hippocampal theta generation. Simultaneous recording of the CA1 local field potentials and septal single units in anaesthetized and awake rodents enabled us to perform a deep analysis of this mechanism [1]. Septal cells were classified by their rhythmic features during dominant theta and non-theta sections (See Methods, Figure 2). Putative pacemakers fired burst of action potentials, showed hippocampal theta phase-preference and were theta rhythmic during both states. They reduced relative rhythmicity frequency differences during theta. Optotagging experiments showed that more than half of them expressed parvalbumin. In contrast, always theta rhythmic tonically active cells fired single action potentials and were irrespective of hippocampal theta phase. Follower neurons fired theta or delta rhythmic bursts at specific phases of theta or delta dependent on the dominant hippocampal activity.

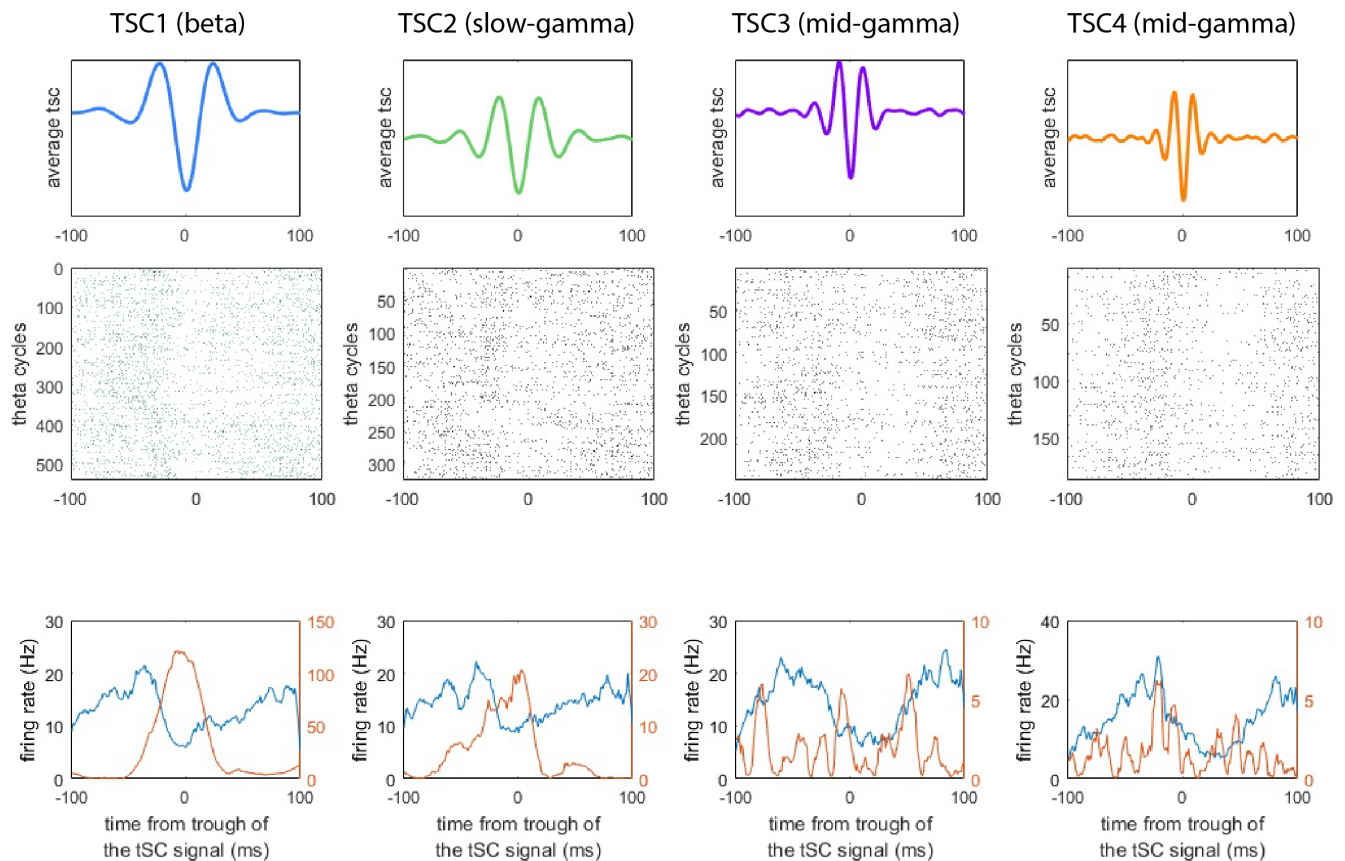
Recent studies have demonstrated, that certain theta cycles carry beta and gamma components (tSC, 'theta spectral components'), that are neglected if long recordings are not filtered specifically for them [2]. However, these short oscillation possibly reflect important operations dedicated to sensory information processing, coding and memory retrieval.

Since the MS has direct accessibility to the hippocampus and

contain a variety of rhythmic cells, our group supposed that it may contribute to the generation of supra-theta oscillation, too. Here we introduce the key points, resulting from the analysis of numerous electrophysiological rodent datasets ([3]), ranging from the tSC related MS activity to tSC coupled firing, temporal anticipation, tSC conveying cells and tSC generation with photostimulation -with emphasis on rhythmic MS neurons.

## REFERENCES

- [1] B. Kocsis, S. Martínez-Bellver, R. Fiáth, A. Domonkos, K. Sviatko, D. Schlingloff, P. Bartho, T. F. Freund, I. Ulbert, S. Kali, *et al.*, "Huygens synchronization of medial septal pacemaker neurons generates hippocampal theta oscillation," *Cell Reports*, vol. 40, no. 5, p. 111149, 2022.
- [2] V. Lopes-dos Santos, G. M. van de Ven, A. Morley, S. Trouche, N. Campo-Urriza, and D. Dupret, "Parsing hippocampal theta oscillations by nested spectral components during spatial exploration and memory-guided behavior," *Neuron*, vol. 100, no. 4, pp. 940–952, 2018.
- [3] A. Joshi, M. Salib, T. J. Viney, D. Dupret, and P. Somogyi, "Behavior-dependent activity and synaptic organization of septo-hippocampal gabaergic neurons selectively targeting the hippocampal ca3 area," *Neuron*, vol. 96, no. 6, pp. 1342–1357, 2017.



# Dermatological comparison of the skin of C57BL/6J hairy and SKH1 nude mice

Dorottya KOCSIS

(Supervisor: Franciska ERDŐ)

Pázmány Péter Catholic University, Faculty of Information Technology and Bionics

50/a Práter street, 1083 Budapest, Hungary

kocsis.dorottya@itk.ppke.hu

**Abstract**—Since *ex vivo* mouse skins are widely used in the field of dermatopharmacology, the characterisation of different skin parameters of model animals is inevitable. In the current study C57BL/6J hairy and SKH1 nude mouse skins were compared, with an emphasis on different parameters, such as skin thickness at different anatomical regions, permeability through the dermal barrier, transepidermal water loss, skin surface structure, morphology, and molecular composition. Based on our results, it can be concluded that the two mouse models are greatly different, which indicates a need for cautious usage of mouse strains in dermatological experiments.

**Keywords**—dermal barrier; skin-on-a-chip microfluidic device; confocal Raman spectroscopy

## I. SUMMARY

Although the 3R rule (replacement, reduction, refinement) is getting more and more important in the field of animal studies, still the physiologically relevant, predictive assessment of pharmacokinetic and pharmacodynamic characteristics of the drugs is not possible without animal studies. In dermatological research, the hairy C57BL/6 and the nude SKH1 mice are frequently used as models for inducing different diseases, such as psoriasisform dermatitis [1], allergic contact dermatitis, or photocarcinogenesis. As *ex vivo* studies are conducted in excised mouse skins, this study focused on the comparative dermatological analysis of a hairy and a hairless mouse strain, with an emphasis on 1) skin thickness, 2) transepidermal permeability of a hydrophilic model compound (caffeine), 3) transepidermal water loss, 4) skin surface structure detected by scanning electron microscopy 5) skin morphology visualised by histology and 6) molecular composition measured with confocal Raman spectroscopy.

The results indicate that skin thickness is higher, and consequently, the permeability is lower in hairless mice [2]. These findings correspond to previous expectations, since the skin lacking the defensive fur must act as a prominent physical and chemical barrier. In accordance with this, the mechanical sensitization (10 times repeated tape strippings) had a huge effect on the transepidermal water loss in C57BL/6J mice, whereas it had practically no influence in hairless mice [2]. On the scanning electron microscopic images remarkable differences were detected in the density and size of the pores, while the histology revealed that SKH1 skin is abundant in utriculi, i.e., degenerative sebaceous glands at the hair follicles, and dermal cysts [2]. As for the molecular composition, the surface of the hairy mouse skin is more lipophilic, but at the deeper layers, hairless skin is more abundant in lipid components like ceramides and cholesterol [2]. The lactate level was higher in C57BL/6J mice, while more protein and urea was found in the hairless skin [2].

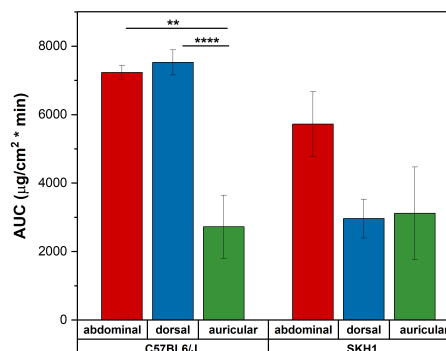


Fig. 1. Area under the curve values calculated from the cumulative mass-time profiles of caffeine absorption. Means  $\pm$  SE,  $n=3-5$ . \*\*:  $p<0.01$ , \*\*\*\*:  $p<0.0001$

Our observations suggest that the two mouse strains are greatly different, hence, before selecting an animal model for skin research, the findings of this study, and the previously published information [3], [4] should all be carefully considered, and for the evaluation of the experimental data, only the results collected in the same strains are comparable.

## ACKNOWLEDGEMENTS

The author thanks Dr Franciska Erdő, Dr Csaba Pongor, Anita Báthory-Fülöp, Brigitta Szöllösi, and Barnabás Bánfi from the Pázmány Péter Catholic University; Dr Roland Csépanyi-Kömi and Fabiola Kreis from the Semmelweis University; moreover Dr Emilie Munnier and Hichem Kichou from the University of Tours for the joint work.

## REFERENCES

- [1] D Kocsis, S Horváth, Á Kemény, Z Varga-Medveczky, C Pongor, R Molnár, A Mihály, D Farkas, BM Naszlady, A Fülöp, A Horváth, B Rózsa, E Pintér, R Gyulai, F Erdő, "Drug Delivery through the Psoriatic Epidermal Barrier-A "Skin-On-A-Chip" Permeability Study and Ex Vivo Optical Imaging", *Int J Mol Sci*, vol. 23, no. 4237, 2022.
- [2] D Kocsis, FE Kreis, A Fülöp, C Pongor, A Báthory-Fülöp, B Bánfi, MB Naszlady, K Lőrincz, R Csépanyi-Kömi, F Erdő, "Comparative dermatological analysis of the skin of C57BL/6J hairy and SKH1 hairless mice", submitted.
- [3] D Kocsis, H Kichou, K Döme, Z Varga-Medveczky, Z Révész, I Antal, F Erdő, "Structural and Functional Analysis of Excised Skins and Human Reconstructed Epidermis with Confocal Raman Spectroscopy and in Microfluidic Diffusion Chambers", *Pharmaceutics*, vol. 14, no. 1689, 2022.
- [4] D Kocsis, V Klang, EM Schweiger, Z Varga-Medveczky, A Mihály, C Pongor, Z Révész, Z Somogyi, F Erdő, "Characterization and ex vivo evaluation of excised skin samples as substitutes for human dermal barrier in pharmaceutical and dermatological studies", *Skin Res Technol*, vol. 28, pp. 664-676, 2022.

# Possibilities of multicellularity in yeast

Valentina MADÁR

(Supervisor: Attila CSIKÁSZ-NAGY)

Pázmány Péter Catholic University, Faculty of Information Technology and Bionics  
50/a Práter street, 1083 Budapest, Hungary  
madar.valentina@itk.ppke.hu

**Abstract**—Plethora of evolutionary innovation created the world we know today. Several lifestyle strategies have given advantage to organisms to adopt to continuously changing environment. One of these is the emergence of multicellularity, which provided an opportunity for more complex organisms to evolve. The way from unicellularity to multicellularity was a long journey. In this study we want to explore this process with the widely used unicellular model organism: baker's yeast (*Saccharomyces cerevisiae*).

Due to insufficient environmental conditions yeasts can form facultative multicellular secondary structures (e.g. pseudohyphae, flocs), that helps the colony to gain nutrients and reduce the deficient environmental impact. Our goal is to mutate this facultative multicellularity to obligate multicellularity and evolve a stay-together strategy in yeast.

**Keywords**—yeast; multicellularity; evolution;

## I. INTRODUCTION

The multicellular body structure has evolved through multiple pathways during the course of organism evolution [1]. This structure has provided numerous advantages over unicellular life forms. Different physiological functions became spatially separated within an organism, meaning that cell specialization and division of labor emerged, leading to increased complexity and size of organisms. In order for this to occur, the unicellular ancestor underwent numerous genetic modifications. Some functions disappeared while new ones emerged along the long journey to multicellularity. Our goal is to explore and recreate this path in yeast.

Previous studies have demonstrated that knockout of the ACE2 (Activator of CUP1 Expression 2) gene leads to significant phenotypic changes [2]. This activator is a DNA-binding transcription factor involved in the positive regulation of post-division septum digestion. In its absence, the daughter cell fails to fully separate from the mother cell, resulting in their remaining together in a clonal "snowflake" structure.

The previous studies focused on the widely used laboratory strain Y55. In this project, we have created this modification in multiple strains. By utilizing these strains, we can investigate the physiological effects of this mutation in different genetic backgrounds.

## II. DISCUSSION

### A. Phenotype without ACE2 gene

During the research, we are working with multiple yeast strains commonly used in laboratories. Using homologous recombination, we targeted the region encoding the *ace2* gene in these strains and replaced it with an antibiotic resistance marker gene. The resulting transformed strains do not contain the ACE2 gene but are resistant to antibiotics.

When comparing them to the unicellular variant, microscopic examination revealed that these strains exhibit a clonal snowflake morphology (Figure 1).

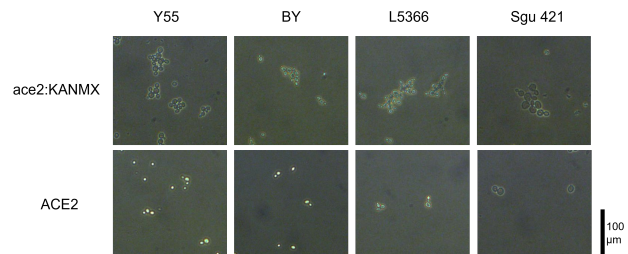


Fig. 1. Comparison of the phenotype of the ACE2 knocked out strains. The upper line represents the transformed strains, the second line the ancestor strains. Scale bar represents 100 µm.

### B. Comparing diploid and haploid strains

In one strain, we also transformed a haploid variant. This variant exhibits larger clustering compared to the diploid version (Figure 2). The underlying reason for this phenomenon may be that in most cases, the gene knockout was performed in diploid strains, so we cannot determine whether both alleles were affected by the modification. However, it is known that cluster size depends on ploidy [3], which explains the more pronounced phenotype observed in the haploid strain.

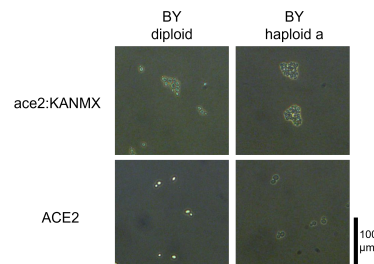


Fig. 2. Comparison of the phenotype of the ACE2 knocked out strains. The upper line represents the transformed strains, the second line the ancestor strains. Scale bar represents 100 µm.

## ACKNOWLEDGEMENTS

Some of the experimental work described was carried out together with Bőrkő Pillér and Tünde Gaizer. This work was supported by the National Research, Development and Innovation Office of Hungary (grant nr. K-20 134489).

## REFERENCES

- [1] A. H. Knoll, "The multiple origins of complex multicellularity," *Annual Review of Earth and Planetary Sciences*, vol. 39.
- [2] R. D. G. D. T. M. Ratcliff WC, Fankhauser JD, "Origins of multicellular evolvability in snowflake yeasts," *Nat Commun*, vol. 20, no. 6, p. 6102, 2015.
- [3] M. A. Barrere J, Nanda P, "Alternating selection for dispersal and multicellularity favors regulated life cycles," *Curr Biol*, pp. 1809–1817, 2023.

# Molecular pathological characterisation of lung cancer using PET/CT imaging

Vilmos MADARAS

(Supervisor: Csaba BENEDEK)

Pázmány Péter Catholic University, Faculty of Information Technology and Bionics

50/a Práter street, 1083 Budapest, Hungary

madaras.vilmos@itk.ppke.hu

**Abstract**—For the definitive diagnosis of non-small cell lung cancer (NSCLC), histological examination of the tumor is required. Considering that positron emission tomography/computed tomography (PET/CT) scans are used for the staging of patients, the question arises whether they can be used for estimating the molecular pathological status of the patient. In this paper, the results of the current state-of-the-art methods are concluded and the potential of a deep learning model is discussed.

**Keywords**—NSCLC; PET/CT; PD-L1; KRAS; Convolutional Neural Networks (CNN); Segmentation; Classification

## I. SUMMARY

In the choice of therapy for non-small cell lung cancer (NSCLC) the molecular phenotype of the tumor cells, i.e. the expression of Programmed Death Ligand 1 (PD-L1) and the mutation of the Kirsten rat sarcoma viral oncogene (KRAS) plays a crucial role, as explained in Figure 1. For the most favorable prognosis, different inhibitors need to be used depending on the molecular pathology of the tumor. For a definitive diagnosis, histological sampling is required.

Several studies have been concluded investigating a potential non-invasive alternative for biopsy to predict the molecular pathology of NSCLC. Most approaches use radiomics (i.e. extraction of quantitative metrics from within medical images) calculated from CT or from multimodal PET/CT images. Radiomics were collectively found to outperform predictive models solely based on clinical characteristics (such as age, smoking, etc.). There are a limited amount of studies, which investigate deep learning (DL) models as feature extractors, yet those findings indicate them to be potentially superior compared to radiomics-based methods.

Therefore, we aimed at developing DL models for predicting solely PD-L1 expression. Multimodal convolutional neural networks (CNN) and Residual CNNs (ResNet-10, ResNet-18, ResNet-50) were implemented and trained, trying to replicate the SoA performance on our dataset. Available pre-trained versions [1] of the ResNets was also fine-tuned for the task at hand, and a pre-trained ResNet-18 was modified and trained for tumor segmentation

The bottleneck of neural networks bear is the large amount of data they require for learning general features. This is suspected to be the reason, why our model could only fit the training and validation data but generated underwhelming predictions for the unseen test data. Fine-tuning pre-trained models did not increase the classification accuracy substantially either, but moderately accurate segmentations could be reached, which might not be satisfactory for calculating radiomic features, but perfectly applicable for automatizing the DL model, by detecting the tumor region

## ACKNOWLEDGEMENTS

The author is grateful to SZTAKI and the Institute of Nuclear Medicine for the opportunity to work on this project, particularly for Csaba Benedek for his guidance and support.

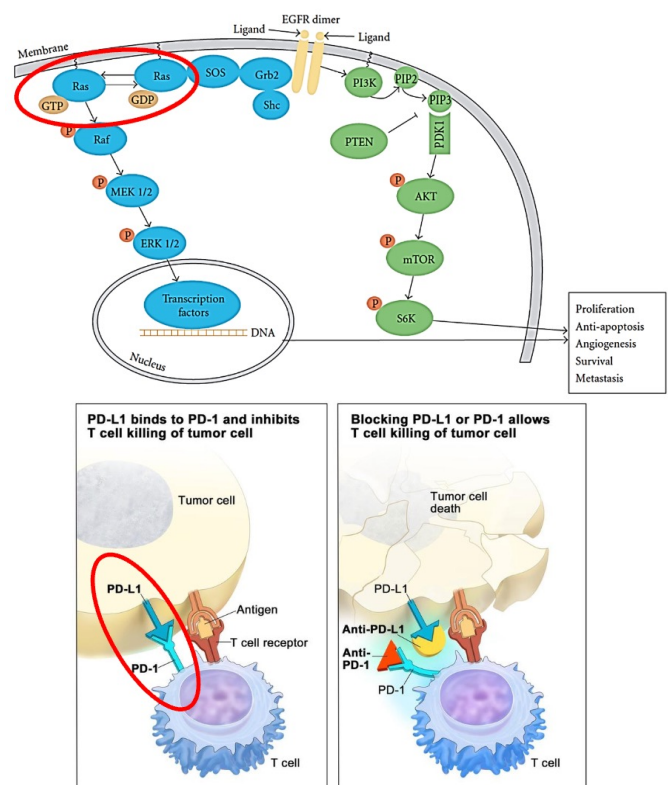


Fig. 1. (Top): K-Ras mutation can result in a constitutively active protein that gives cells a continuous growth signal [2]. (Bottom): PD-L1: a transmembrane protein that inhibits the immune cells that attack the tumor cell, thus improving the chances of tumor survival [3].

## REFERENCES

- [1] S. Chen, K. Ma, and Y. Zheng, “Med3d: Transfer learning for 3d medical image analysis,” 2019.
- [2] S. Jančík, J. Drábek, D. Radzioch, and M. Hajdúch, “Clinical relevance of kras in human cancers,” *Journal of Biomedicine and Biotechnology*, vol. 2010, p. 150960, Jun 2010.
- [3] A. F. Oliveira, L. Bretes, and I. Furtado, “Review of pd-1/pd-11 inhibitors in metastatic dmmr/msi-h colorectal cancer,” *Frontiers in Oncology*, vol. 9, 2019.

# Shared representations for microbiome data: empowering predictive disease classification through transfer learning

Zsófia MOLNÁR

(Supervisors: Sándor PONGOR, Balázs LIGETI)

Pázmány Péter Catholic University, Faculty of Information Technology and Bionics  
50/a Práter street, 1083 Budapest, Hungary  
molnar.zsofia@itk.ppke.hu

**Abstract**—Microbial communities, known as the microbiome, play a crucial role in various diseases and industrial applications. However, emerging challenges such as climate change, the rise of new diseases, and the emergence of drug-resistant bacteria demand innovative approaches. Many scientific investigations encounter limitations such as small sample sizes and high costs associated with labeled data production. Furthermore, the inherent noise and high dimensionality of data pose further challenges. Traditional machine learning frameworks are often constrained in such scenarios. To overcome these limitations, this study aims to develop a machine learning framework and data representation by harnessing the power of transfer learning using publicly available microbiome data.

**Keywords**—meta-learning, microbiome, transfer-learning, biomarker

## I. INTRODUCTION

The human microbiome, consisting of trillions of microorganisms residing in various body regions, plays a crucial role in maintaining overall health. Imbalances in the microbiome, known as dysbiosis, have been linked to various health conditions. Understanding this relationship has led to personalized medicine and therapeutic interventions. However, studying the microbiome presents challenges such as small sample sizes, costly data production, and noisy datasets. Transfer learning has emerged as a powerful approach to overcome these limitations. By leveraging pre-existing knowledge, transfer learning enhances the analysis of microbiome data and enables the development of robust machine learning models. Incorporating transfer learning techniques in microbiome analysis has the potential to revolutionize healthcare outcomes, improve diagnostics, and uncover new discoveries.

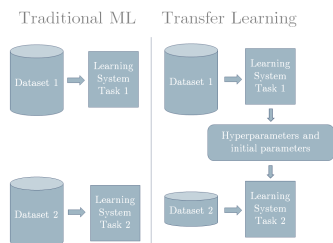


Fig. 1: A simplified data flow diagram of the designed pipeline. According to our plans, this pipeline will be complemented with at least a motility calculation stage, and possibly several other stages.

## II. SUMMARY

This study focused on analyzing microbiome data obtained from diverse cohorts, with a specific emphasis on colorectal cancer (CRC) patients. The dataset, sourced from the curated-MetagenomicData database, contained information on disease status, taxonomic abundance levels, and additional patient details. Thorough preprocessing steps were performed, including dataset selection, feature reduction, and transformation techniques such as zero replacement and central log ratio (CLR) transformation.

The resulting dataset consisted of seven CRC cohorts, enabling a targeted exploration of the microbiome dynamics associated with CRC. Three distinct approaches were employed for model implementation, incorporating nested cross-validation (CV) and transfer learning. The first approach compared classical machine learning algorithms and a fully connected neural network using a random train-test split. The second approach evaluated models using a studywise train-test split, accounting for cohort-specific characteristics. The third approach focused solely on neural networks and utilized transfer learning by initializing the model with weights and hyperparameters from a base model.

The methodology aimed to overcome challenges in microbiome data analysis and assess the effectiveness of transfer learning. Although the results did not show significant overall improvement, further investigations with additional cohorts, more data, and extended features hold promise for advancing the understanding and applicability of transfer learning in microbiome research. The creation of a shared representation that can be reused and extended to unseen datasets is a key objective for future studies.

## REFERENCES

- [1] Liwinski, Timur, Avner Leshem, and Eran Elinav. "Breakthroughs and bottlenecks in microbiome research." *Trends in molecular medicine* 27.4 (2021): 298-301.
- [2] Ma, Jianzhu, et al. "Few-shot learning creates predictive models of drug response that translate from high-throughput screens to individual patients." *Nature Cancer* 2.2 (2021): 233-244.
- [3] Hernández Medina, Ricardo, et al. "Machine learning and deep learning applications in microbiome research." *ISME Communications* 2.1 (2022): 98.

# Review on the applicability of postnatal phonocardiogram processing techniques for fetal signals

Kristóf MÜLLER

(Supervisor: Miklós KOLLER)

Pázmány Péter Catholic University, Faculty of Information Technology and Bionics  
50/a Práter street, 1083 Budapest, Hungary  
muller.kristof@itk.ppke.hu

**Abstract**—Phonocardiography processing is currently mainly developed with postnatal studies. Most processing algorithms are focused on problems which can be applied on fetal signals, but there are multiple differences between the two types of signals and the required methods for processing them. In this article we looked at postnatal techniques and evaluated their applicability for fetal phonocardiogram processing.

## I. INTRODUCTION

Monitoring the health of the heart is an important medical topic, especially the early detection of congenital heart defects (CHD) for a better long term outcome. Phonocardiography (PCG) techniques gained a lot more attention recently due to its ease-of-use and development in processing algorithms [1]. The normal heart produces two main heart sounds named S1 and S2, seen in Figure 1. These sounds consist of two impulses each, caused by the closure of different heart valves. The impulses are named M1, T1, A2, and P2 after the valve which causes them and the heart sound they belong to [2].

## II. REVIEWED WORKS

In our previous work we developed a method for murmur detection for the 2022 George B. Moody challenge [3]. The signal was first segmented with a wavelet decomposition and Shannon entropy based method. The murmur classification was achieved with a trained support vector machine (SVM), with multiple features calculated from the given segments. Our model achieved an accuracy of 57.4% on the validation set. Given that there were three classes, and we used a relatively simple method, this result can be considered good.

Had *et al.* showed a method for detecting the individual impulses in PCG signals [4]. They first segmented the heart sounds with a Hilbert envelope method, then decomposed the individual heart sounds with orthogonal matching pursuit (OMP) algorithm. The parameters for the OMP dictionary were estimated with other steps. They tested their method with simulated signals and later validated them with real life data.

Alkhodari and Fraiwan applied a special neural network (NN) architecture for detecting valvular heart diseases [5]. They combined a convolutional neural network (CNN) and a bi-directional long short-term memory network (BiLSTM). The inputs for the NN were the smoothed and normalized PCG signals. Their trained model achieved an average accuracy of 99,3%.

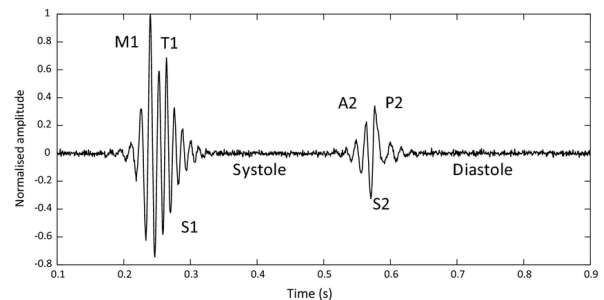


Fig. 1. PCG waveform of a normal heartcycle [4]

## III. CONCLUSION

Current PCG processing methods are quite diverse and most of them can be used for fetal signals, however modifications are almost always necessary. A main problem being that most fetal PCG signals are recorded with a 333 Hz sampling rate and 8 bit depth, compared to the unofficial PCG standard of 4000 Hz sampling frequency and 16 bit depth. This means that there are less possible representable values and frequencies in fetal PCG recordings, which can lead to less accurate results. Another complication is the noises present in the recordings. A significant amount of processing is required if the maternal heart sounds are also present in the recording. Also fetal movements and digestive noises cannot be easily removed from the signal, since their frequency range overlaps with the fetal heart sounds.

## IV. ACKNOWLEDGEMENTS

I would like to thank Dr. Janka Hatvani and Dr. Márton Áron Goda for their valuable insight and guidance.

## REFERENCES

- [1] G. D. Clifford, C. Liu, B. Moody, D. Springer, I. Silva, Q. Li, and R. G. Mark, "Classification of normal/abnormal heart sound recordings: The PhysioNet/Computing in Cardiology Challenge 2016," in *2016 Computing in Cardiology Conference (CinC)*, pp. 609–612, 2016.
- [2] J. M. Felner, *Clinical Methods: The History, Physical, and Laboratory Examinations*, ch. 22. Boston: Butterworths, 3 ed., 1990.
- [3] K. Müller and M. Á. Goda, "Heart Murmur Detection in Phonocardiographic Signals Using Breathing Noise Suppression," in *2022 Computing in Cardiology (CinC)*, vol. 498, pp. 1–4, 2022.
- [4] A. Had, K. Sabri, and M. Aoutoul, "Detection of Heart Valves Closure Instants in Phonocardiogram Signals," *Wireless Personal Communications*, vol. 112, 06 2020.
- [5] M. Alkhodari and L. Fraiwan, "Convolutional and recurrent neural networks for the detection of valvular heart diseases in phonocardiogram recordings," *Computer Methods and Programs in Biomedicine*, vol. 200, p. 105940, 2021.

# Structural modeling of the interaction between dynein light chain molecule and the postsynaptic density scaffold protein GKAP

Eszter NAGY-KANTA

(Supervisor: Zoltán GÁSPÁRI)

Pázmány Péter Catholic University, Faculty of Information Technology and Bionics  
50/a Práter street, 1083 Budapest, Hungary  
nagy-kanta.eszter@itk.ppke.hu

**Keywords-protein NMR; molecular dynamics**

## I. INTRODUCTION

GKAP is a scaffold protein involved in maintaining and organizing the post-synaptic density (PSD). Based on predictions, GKAP is mainly intrinsically disordered. Main regions include the GBR (GK-binding repeats) region, DYLL (dynein light chain binding) region, the GH1 domain and a short PDZ-binding domain on the C terminal [1]. The dynein light chain molecule (DYNLL2) forms homodimers. Two possible complexes might be considered: with 2:1 ratio, two DYNLL2 molecules binding to one GKAP molecule, or as a 2:2 complex, each GKAP binding motif associates with a different DYNLL2 dimer. Most likely a DYNLL2 dimer binds to two GKAP molecules, which could themselves bind to other molecules of DYNLL2 thanks to their second motif. This raises the possibility of forming hetero-oligomers [2].

## II. METHODS

We were using plasmid vector technology in BL21 *E. coli* bacteria for protein expression and affinity chromatography (IMAC), ion exchange chromatography and size-exclusion chromatography for the purification of GKAP-DYL and DYNLL2. We analyze the structural properties with NMR (nuclear magnetic resonance) spectroscopy. 2D, 3D and 4D experiments were executed to help the chemical shift assignment. GKAP-DYL was produced with <sup>15</sup>N- and <sup>13</sup>C- isotopic labeling. NMR titration experiments were also conducted with the binding partner. NMR measurements were executed at 25°C on a Bruker 800 MHz spectrometer, with the help of prof. Permi Perttu, at the University of Jyväskylä, Finland.

For molecular dynamics simulations, we performed model building with Chimera and MODELLER. The DYNLL2 dimer template was modified from the known X-ray structure (PDB ID: 2XQQ). Molecular dynamics simulation was performed with the software GROMACS 2020.

## III. RESULTS

Backbone (N, H, C', CA) and sidechain (CB, HA, HB) chemical shift assignment was successful on the GKAP-DYL protein construct. GKAP-DYL is disordered based on the CA and CB values, with slight structural preferences.

We calculated secondary chemical shifts, which describes the secondary structural preferences of the protein. Titration NMR experiments were performed and the affected residues were analyzed. GROMACS molecular dynamics simulation

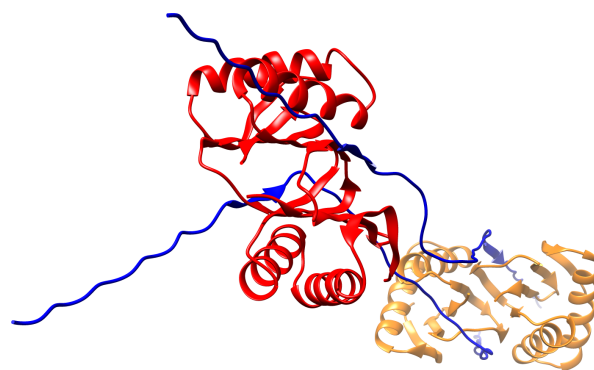


Fig. 1. A model of the GKAP:DYNLL2 complex was built with the stoichiometry 2:4. The initial GKAP model was built using Chimera.

was performed on the complex structure. However, mapping the conformational space accessible for the full complex needs further investigations. Also, structural ensembles will be filtered based on the obtained chemical shift data from the NMR measurements.

## ACKNOWLEDGEMENTS

The research has been supported by grants from the Hungarian Scientific Research Fund (NKFI 124363 & 137947). This research was supported by the National Research, Development and Innovation Office – NKFIH – through the grant no. TKP2021-EGA-42.

The author thanks Zoltán Gáspári, Permi Perttu, and all the current and former members of the collaborating research groups for their contribution to this work, and Enora Moutin for the GKAP and DYNLL2 cDNA.

## REFERENCES

- [1] Rasmussen AH, Rasmussen HB, Silahtaroglu A. *The DLGAP family: neuronal expression, function and role in brain disorders*. Mol Brain. 2017 Sep 4;10(1):43. doi: 10.1186/s13041-017-0324-9.
- [2] Moutin E, Compan V, Raynaud F, Clerfè C, Bouquier N, Labesse G, Ferguson ML, Fagni L, Royer CA, Perroy J. *The stoichiometry of scaffold complexes in living neurons - DLC2 functions as a dimerization engine for GKAP*. J Cell Sci. 2014 Aug 15;127(Pt 16):3451-62. doi: 10.1242/jcs.145748. Epub 2014 Jun 17.



# The role of extracellular vesicles in melanoma progression

Afrodité NÉMETH

(Supervisor: Tamás Márton GARAY)

Pázmány Péter Catholic University, Faculty of Information Technology and Bionics

50/a Práter street, 1083 Budapest, Hungary

nemeth.afrodite@itk.ppke.hu

**Abstract**—The small lipid-bilayered extracellular vesicles (EVs) are present in all body fluids and involved in intracellular communication. EVs play key role in several diseases, including the different stages of cancer progression. For this reason, our aim was to isolate extracellular vesicles from metastatic melanoma cell pairs and investigate their EVs effect on proliferation, spheroid growth and migration. EVs were isolated with ultracentrifugation and characterized by their size, particle, protein and lipid concentration and the commonly present EV-surface markers. After successful isolations cells were treated with EVs derived from their own supernatant or from their pairs' supernatant. EV treatment did not affect cell proliferation and spheroid growth markedly, however, migration of melanoma cells could be influenced by EVs. According to our experiments, EVs' metastasis-promoting role is more prominent than their involvement in primary tumor growth.

**Keywords**—extracellular vesicles, ultracentrifugation, proliferation, spheroids, single cell migration

## I. INTRODUCTION

EVs are the molecular fingerprints of their origin, they can be loaded with DNA, mRNA, noncoding RNA, transcription factors, signal molecules or growth factors. Moreover, their transferred macromolecules can influence the recipient cells' behaviour. Extracellular vesicles involvement in cancer progression become clear in the last decade [1]. Formation of metastasis in distant organs are the major cause of cancer-related deaths. Melanoma, which is derived from pigment-producing melanocytes forms the deadliest type of skin cancer, because of its high metastatic potential [2]. Therefore, to understand the metastasis formation of melanoma more deeply we investigated cell culture-derived EVs role in melanoma progression.

## II. METHODS

Cells were produced EVs for 72 hours, then their supernatant was centrifugated and filtered before EV isolation with ultracentrifugation. The isolates were characterized according to the ISEV2018 guideline [3]. EVs size, particle, protein, lipid concentration and their specific surface markers were measured. Cells were treated with EVs based on the isolates' protein concentration. Proliferation was investigated after 72 hours of EV treatment, migration was followed with video microscope for 24 hours and spheroid growth assay was performed for 7 days.

## III. SUMMARY

EV isolation from cell culture media was successful with ultracentrifugation. EV treatment of melanoma cells mainly induced migration, but did not alter proliferation prominently.

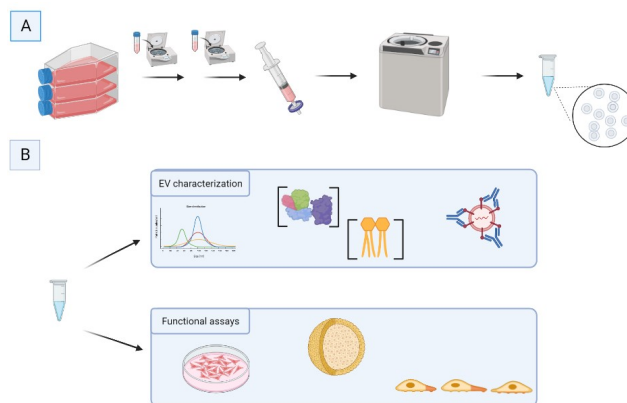


Fig. 1. Extracellular vesicles isolation, characterization and the investigated aspects of cancer progression; A) EV isolation with ultracentrifugation after collecting cell culture media and assessing the supernatant to centrifugation and filtration; B) EV characterization (based on their size, particle, protein, lipid concentration and specific surface markers' detection) and the investigated functional assays with melanoma cells

For this reason, we can suggest that EVs are promoting metastasis formation of melanoma over primary tumor growth.

## IV. ACKNOWLEDGEMENTS

This research was supported by the National Research, Development and Innovation Office - NKFI - through grant no. TKP2021-EGA-42.

## REFERENCES

- [1] T. S. et al, "Small extracellular vesicles and metastasis—blame the messenger," *Cancers*, 2021.
- [2] N. T. et al, "Genetics of metastasis: melanoma and other cancers," *Clin Exp Metastasis*, 2018.
- [3] C. T. et al, "Minimal information for studies of extracellular vesicles 2018 (misev2018): a position statement of the international society for extracellular vesicles and update of the misev2014 guidelines," *J Extracellular Vesicles*, 2018.

# Toxin production and sensitivity of different yeast strains

Biborka PILLÉR

(Supervisor: Attila CSIKÁSZ-NAGY)

Pázmány Péter Catholic University, Faculty of Information Technology and Bionics

50/a Práter street, 1083 Budapest, Hungary

piller.biborka@itk.ppke.hu

**Abstract**—Over the past few decades, there has been a significant increase in our understanding of intracellular processes. However, our knowledge regarding the interactions between cells remains limited. This is primarily because most laboratory experiments on microbial growth focus on individual strains, while in nature, microbial populations form complex communities comprising multiple strains. These strains possess the ability to influence one another, and these interactions can have a profound impact on the growth and future of the population. Within these mixed colonies, both cooperation and competition can arise among the strains, leading to the thriving of certain strains and the suppression of others. Our objective is to examine these interactions among different strains of *Saccharomyces cerevisiae* in order to gain a better understanding of the significance of coexistence and competition.

**Keywords**—yeast strains; yeast growth; toxin production

## I. INTRODUCTION

The *Saccharomyces* genus encompasses a diverse array of species, displaying variations in habitat, fermentation capabilities, metabolite production, environmental resilience, and toxin generation. Among these species, *Saccharomyces cerevisiae*, commonly known as Baker's yeast, holds considerable significance in research and industry [1]. Wine yeast strains derived from this species, isolated from different regions worldwide, exhibit unique characteristics. Apart from potential variations in toxin production, these strains differ in other crucial properties regarding the fermentation process.

Initially various strains that are present in grapes and in the air participate during the fermentation [2]. However, these strains become less dominant as *Saccharomyces* takes on the main role later in the process [2]. It is well-established that *Saccharomyces* strains can outcompete non-*Saccharomyces* strains. Nevertheless, a question about this achieved dominance arises when multiple *Saccharomyces* strains are co-cultivated, particularly when certain strains are known to possess killer activity.

Interactions between yeast strains were already observed in the 1970s [1]. While cooperation is often observed in populations as they work together to produce necessary substances for survival, the most prevalent interaction between strains is the competition for nutrients [3]. One specific form of competition arises from the production of toxins [4] by killer active yeast strains. This killer phenotype is the result of an infection by dsRNA viruses known as L-A and M [5]. Currently, we can discuss four distinct types of killer strains that exhibit similarities but also significant differences, namely K1, K2, K28, and Klus. [5] This toxin production has been proven to be significant in the fermentation of food and beverages, as well as in medical research [4].

Our objective is to expand upon this existing knowledge by studying the effects of different toxin-producing strains on the growth of other laboratory strains. We aim to accomplish this by determining the toxin types produced by each strain using a PCR based approach. After that our aim is to observe the growth of these strains in co-cultures in liquid media under different environmental conditions.

## I. DISCUSSION

### A. Testing toxin production and sensitivity

To determine the toxin production and sensitivity of the strains we used a technique based on colony growth described in the methods section. The results show that the strains that were originally known to be toxin producers are able to produce a killer toxin but it depends on the the medium.

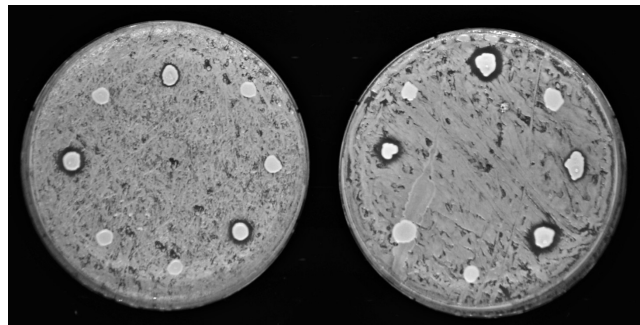


Fig. 1: The sensitivity of a non-toxin producer strain to the killer active strains on different media

## ACKNOWLEDGEMENTS

This research was supported by the National Research, Development and Innovation Office – NKFIH – through the grant no. TKP2021-EGA-42 .

## REFERENCES

- [1] M. Cavaliere, S. Feng, O. S. Soyer, and J. I. Jiménez, "Cooperation in microbial communities and their biotechnological applications," *Environmental Microbiology*, vol. 19, no. 8, pp. 2949–2963, 2017.
- [2] F. Zamora, M. V. Moreno-Arribas, and M. C. Polo, "Wine chemistry and biochemistry," 2009.
- [3] J. Friedman and J. Gore, "Ecological systems biology: The dynamics of interacting populations," *Current Opinion in Systems Biology*, vol. 1, pp. 114–121, 2017.
- [4] V. Palpacelli, M. Ciani, and G. Rosini, "Activity of different 'killer' yeasts on strains of yeast species undesirable in the food industry," *FEMS Microbiology Letters*, vol. 84, no. 1, pp. 75–78, 1991.
- [5] J. Quintero-Blanco, J. Jimenez, and A. Garzón, "A simple multiplex reverse transcription-pcr method for the diagnosis of la and m totiviruses in *saccharomyces cerevisiae*," *Applied and Environmental Microbiology*, vol. 88, no. 4, pp. e02213–21, 2022.

# Theoretical and applied studies on the cyclic movements of human limbs

Balázs RADELECZKI

(Supervisor: József LACZKÓ)

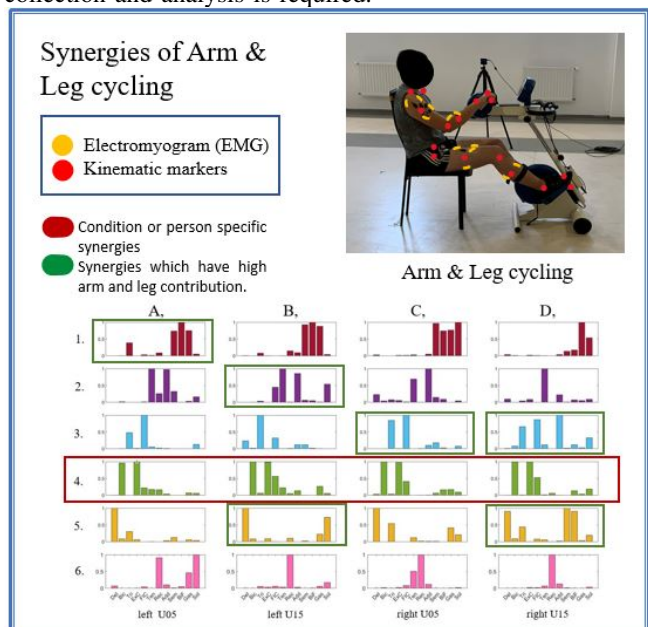
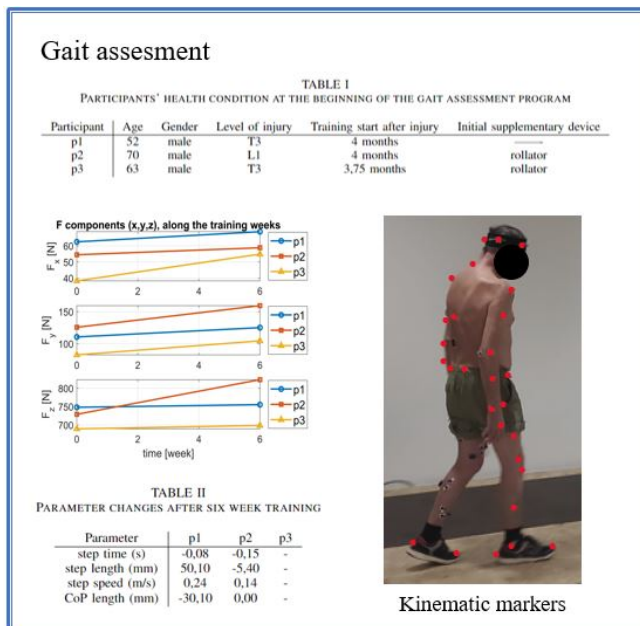
Pázmány Péter Catholic University, Faculty of Information Technology and Bionics

50/a Práter street, 1083 Budapest, Hungary

radeleczki.balazs@itk.ppke.hu

Our research group studies the application of Functional Electrical Stimulation (FES) assisted leg and simultaneous voluntary arm cycling training of incomplete Spinal Cord Injured (iSCI) participants to improve their walking ability. This idea is based on the concept of common movement control areas of the arms and legs by the Central Nervous System (CNS). We present a case study of inter-limb synergy calculation of simultaneous arm and leg cycling with a healthy adult participant. See left panel of the figure. We also measured the effect of the resistance changes of the cranks (from moderate to height resistance) to the muscle synergies. The muscle synergies are able to describe and model the muscles' cooperation. The signal processing is following our previous work [1]. We used a MATLAB implementation of Non-negative Matrix Factorisation for the synergy calculation [2]. We have found one common synergy across all conditions which implies a task or personal specific muscle cooperation. Muscle synergies were also found between upper and lower limbs activity for each measurement condition. The number of inter-limb synergies may increase with the resistance of the upper crank. If the inter-limb synergies are general phenomenon, it can also be used to create FES stimulation patterns where arm movements are also taken into account [3].

week. It seems that the gait parameters of all participants have beneficially changed or kept their values. These parameters are the step length, step height, step time, walking speed, Center of Pressure (CoP) trajectory length and maximum absolute force magnitude. These parameter changes were evaluated from the records of the start and the six weeks later data assessments. The kinematic data are inline with an independent American study [4]. To validate statistically the result of synergy calculation and FES assisted gait rehabilitation, further data collection and analysis is required.



## REFERENCES

- [1] L. Botzheim, J. Laczko, D. Torricelli, M. Mravcsik, J. L. Pons, and F. Oliveira Barroso, "Effects of gravity and kinematic constraints on muscle synergies in arm cycling," *Journal of neurophysiology*, vol. 125, no. 4, pp. 1367–1381, 2021.
- [2] F. O. Barroso, D. Torricelli, J. C. Moreno, J. Taylor, J. Gomez-Soriano, E. Bravo-Esteban, S. Piazza, C. Santos, and J. L. Pons, "Shared muscle synergies in human walking and cycling," *Journal of neurophysiology*, vol. 112, no. 8, pp. 1984–1998, 2014.
- [3] B. Radeleczi, M. Mravcsik, L. Bozheim, and J. Laczko, "Prediction of leg muscle activities from arm muscle activities in arm and leg cycling," *The Anatomical Record*, vol. 306, no. 4, pp. 710–719, 2023.
- [4] R. Zhou, L. Alvarado, R. Ogilvie, S. L. Chong, O. Shaw, and V. K. Mushahwar, "Non-gait-specific intervention for the rehabilitation of walking after sci: role of the arms," *Journal of Neurophysiology*, vol. 119, no. 6, pp. 2194–2211, 2018.

These sequels are inline with our preliminary result of three iSCI patients gait improvement after a six weeks FES assisted cycling training. The improvement in ground reaction force and in kinematic parameters are presented at the left Figure. The participants had two training sessions a

# Examination of protein phase separation via *in vitro* and *in silico* methods

András László SZABÓ

(Supervisor: Zoltán GÁSPÁRI)

Pázmány Péter Catholic University, Faculty of Information Technology and Bionics

50/a Práter street, 1083 Budapest, Hungary

szabo.andras.laszlo@itk.ppke.hu

**Abstract**—Protein phase separation is a complex biochemical process that results in the reversible formation of protein-rich cellular compartments, typically initiated by interactions between multivalent proteins. This phenomenon contributes to dynamic cellular processes such as the organization of postsynaptic densities (PSDs). My current work utilizes techniques from the fields of fluorescent microscopy, microfluidics and bioinformatics to study the phase separation of PSD proteins, while some of my previous work reveals correlations between liquid-liquid phase separation (LLPS) and certain charged sequence motifs.

**Keywords**—protein phase separation; charge-dense regions; microfluidics; fluorescent microscopy

## I. INTRODUCTION

The PSD is a complex multilayered cellular component on the internal surface of the postsynaptic membrane. Synaptic plasticity correlates with its structural changes, which in turn partially depend on the phase separation of its proteins. [1] This phenomenon is driven by multivalent interactions resulting in the reversible formation of so-called membraneless organelles. The computational part of my work shows that LLPS correlates with the presence of certain charged sequence motifs such as single  $\alpha$ -helices (SAHs). The experimental part of my work aims to develop a novel technique for the detection of protein phase separation, by approximating the size of solute particles based on their diffusion. This technique has been previously utilized by Arosio et al. for the distinction of solute nanobodies and  $\alpha$ -Synuclein fibrils. [2]

## II. METHODS

SAHs and other charged residue repeats were identified by the FT-CHARGE algorithm that calculates the charge correlation function of different segments within the given protein sequence, and then analyses the charge patterns of its Fourier transform. SAH regions have a typical frequency range of 1/9 to 1/6. [3] Custom scripts have been written to explore a wider range of proteins with regions of high charge-density, all of which depend on windowing functions to survey sequences for special motifs. Several online databases were reviewed to filter the members of the human proteome that are related to LLPS. Recently, multiple analyses have been carried out concerning the residue composition of certain sequences. As for the experimental part of my work, the size approximation of solutes requires three major steps. The first step is to apply a fluorescent marker to the individual solute particles. The second step is to run the fluorescent sample through a microfluidic channel where several images are recorded at predetermined measurement points along the length of the channel, from which fluorescent profiles are extracted. Step three is fitting Gaussian functions to the measured profiles,

from which diffusion coefficients and particle sizes are then approximated.

## III. RESULTS

A high through-put approach was developed for the recognition of specific sequence motifs, and a wide variety of human protein regions with high charge-density have been surveyed for plausible contributions to LLPS. Preliminary experiments are being conducted to hone the acquisition and processing of solute diffusion data. The results in case of particles on the nanometer scale are encouraging but further adjustments might be necessary in case of larger particles.

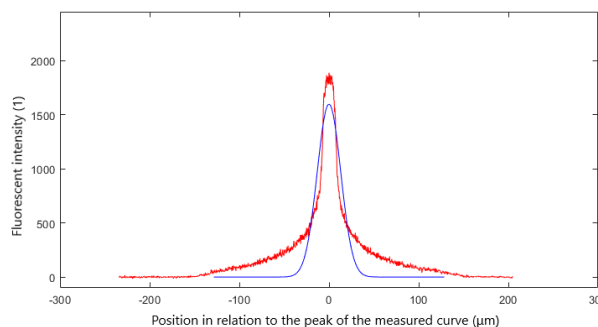


Fig. 1. The measured fluorescent intensity profile (red) and the fitted Gaussian function (blue) at the beginning of the microfluidic channel. The Gaussian function is fitted to the curve inside the 300  $\mu\text{m}$  wide channel.

## IV. ACKNOWLEDGEMENTS

This research was supported by the National Research, Development and Innovation Office – NKFIH – through the grant no. TKP2021-EGA-42 .

## V. PUBLICATIONS

A. L. Szabó, A. Sánta, R. Pancsa, and Z. Gáspári, "Charged sequence motifs increase the propensity towards liquid-liquid phase separation," *FEBS Letters*, vol. 596, no. 8, p. 1013-1028, 2022.

## REFERENCES

- [1] Z. Feng, X. Chen, M. Zeng, and M. Zhang, "Phase separation as a mechanism for assembling dynamic postsynaptic density signalling complexes," *Current Opinion in Neurobiology*, vol. 57, pp. 1–8, Aug. 2019.
- [2] P. Arosio, T. Müller, L. Rajah, E. V. Yates, F. A. Aprile, Y. Zhang, S. I. Cohen, D. A. White, T. W. Herling, E. J. De Genst, and et al., "Microfluidic diffusion analysis of the sizes and interactions of proteins under native solution conditions," *ACS Nano*, vol. 10, no. 1, p. 333–341, 2015.
- [3] Z. Gáspári, D. Süveges, A. Perczel, L. Nyitray, and G. Tóth, "Charged single alpha-helices in proteomes revealed by a consensus prediction approach," *Biochimica Et Biophysica Acta*, vol. 1824, pp. 637–646, Apr. 2012.

# Growth laws: from bacteria to yeast

Giorgio TALLARICO

(Supervisor: Andrea CILIBERTO)

Pázmány Péter Catholic University, Faculty of Information Technology and Bionics

50/a Práter street, 1083 Budapest, Hungary

tallarico.giorgio@itk.ppke.hu

**Abstract**—While bacterial models have provided insights in growth physiology and cellular resource allocation, limited research exists for eukaryotic cells. This study proposes a combination of mathematical modeling and experimental approaches for enabling a quantitative description of cellular macromolecular content and associated global regulations under growth inhibition and nutrient limitation. Preliminary results shows that a major trade-off between ribosome content and growth found the first time in bacteria is also observed in the budding yeast *Saccharomyces cerevisiae*, emphasizing the predictive capability and effectiveness of the models previously developed for prokaryotes. Simultaneously, the data reveals that budding yeast exhibits increased complexity, manifested through non-constant trends in dry mass and protein densities necessitating novel mathematical models capable of accurately describing the allocation of non-protein components across various conditions.

**Keywords**—Yeast; growth laws

## I. BACKGROUND

In bacteria, recent work has shown how growth physiology can be described by simple mathematical relationships (sometimes termed “growth laws”) which formalize complex emerging principles that connect environmental cues to growth and cell composition. These models are based on a broad description of cells, typically organizing proteins into groups based on their function (e.g., ribosomal proteins grouped as the “R class” or “R sector”) or shared regulation [1]. Such descriptions naturally reflect the idea that allocating excessive resources to one function can adversely impact others [2], [3].

These models have been instrumental in explaining how cells optimize the allocation of cellular resources to physiological processes and pathways, thereby influencing the molecular composition of the cell in response to specific environmental conditions, such as bacterial response to antibiotic drugs [2], and how they strive to minimize disruption [3]. For example, the linear relationship found between specific growth rate and ribosome content under translation inhibition can be explained by a simple model in which the whole proteome is divided in two distinct classes and the regulation of this two classes arise passively considering that the sum of their mass fractions is constant [2].

While there is a wealth of literature on bacterial growth laws [2], [3], the available body of research on eukaryotic cells is comparatively small. However, some seminal experimental studies have shown clear evidence of growth laws in both yeast and cancer cells [4], [5], [6] but at the same time, these studies often lack the experimental data required to validate their quantitative models or are more phenomenologically oriented. My PhD project aim is to perform “knowledge transfer” of powerful tools that emerge from work in bacteria to eukaryotic cells, in particular to the budding yeast *Saccharomyces cerevisiae*. The potential results of this project could be also relevant in the field of cancer research, because having a

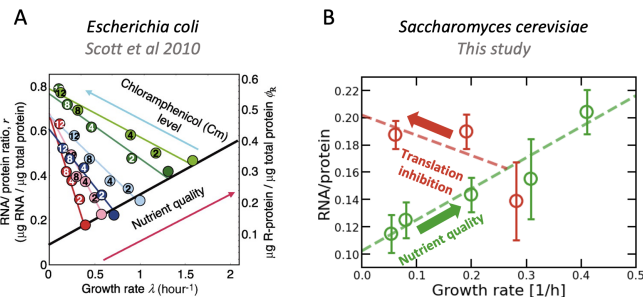


Fig. 1. Our preliminary data demonstrates the conservation of a significant trade-off between ribosome allocation and growth in bacteria and yeast. This trade-off is observed when translation inhibition occurs by reducing ribosome efficiency, such as with the use of cycloheximide. Ribosome content is measured with the RNA/protein ratio and growth as specific growth rate. Every point shown is the average of 3 replicates, green points in (B) are obtained using different carbon sources (in increasing order of growth rates: 2% lactate, 2% trehalose, 2% raffinose, 2% galactose and 2% glucose)

robust quantitative theory for cellular macromolecular content and proteome allocation for eukaryotic cells could unveil key trade-offs involved in how normal and cancer cells allocate their resources in response to drugs and help designate better treatments.

## REFERENCES

- [1] S. Hui, J. M. Silverman, S. S. Chen, D. W. Erickson, M. Basan, J. Wang, T. Hwa, and J. R. Williamson, “Quantitative proteomic analysis reveals a simple strategy of global resource allocation in bacteria,” *Molecular Systems Biology*, vol. 11, Feb. 2015.
- [2] M. Scott, C. W. Gunderson, E. M. Mateescu, Z. Zhang, and T. Hwa, “Interdependence of cell growth and gene expression: Origins and consequences,” *Science*, vol. 330, pp. 1099–1102, Nov. 2010.
- [3] A. Bren, D. S. Glass, Y. K. Kohanim, A. Mayo, and U. Alon, “Tradeoffs in bacterial physiology determine the efficiency of antibiotic killing,” Mar. 2022.
- [4] E. Metzl-Raz, M. Kafri, G. Yaakov, I. Soifer, Y. Gurvich, and N. Barkai, “Principles of cellular resource allocation revealed by condition-dependent proteome profiling,” *eLife*, vol. 6, Aug. 2017.
- [5] K. Kochanowski, T. Sander, H. Link, J. Chang, S. J. Altschuler, and L. F. Wu, “Systematic alteration of in vitro metabolic environments reveals empirical growth relationships in cancer cell phenotypes,” *Cell Reports*, vol. 34, p. 108647, Jan. 2021.
- [6] Q. Wang and J. Lin, “Environment-specificity and universality of the microbial growth law,” *Communications Biology*, vol. 5, Aug. 2022.

# A Hamiltonian representation of semi-discretized nonlocal flows

Mihály András VÁGHY

(Supervisors: Mihály KOVÁCS, Gábor SZEDERKÉNYI)

Pázmány Péter Catholic University, Faculty of Information Technology and Bionics

50/a Práter street, 1083 Budapest, Hungary

vaghy.mihaly.andras@itk.ppe.hu

This progress report is based on [1], [2]. We show that one-dimensional nonlocal flow models in PDE form with Lighthill-Whitham-Richards flux supplemented with appropriate in- and out-flow terms can be spatially discretized with a finite volume scheme to obtain formally kinetic models with physically meaningful reaction graph structure. The result is a subclass of so-called generalized flow models and based on the dynamics of the reaction network we can construct a port-Hamiltonian representation of the system in the original and also in the reduced state spaces with clear connection between the structure matrices and the compartmental graph topology.

Local conservation and balance laws have been widely used in aerodynamics and Eulerian gas dynamics [3], traffic flows [4], ribosome flows [5] in the past decades. In recent years nonlocality has been introduced in several applications, e.g., for modelling supply chains [6] and traffic flows [7]. Spatial nonlocality is often defined as a continuum average or convolution with an appropriate weight function, which, in many applications, can be interpreted as the velocity distribution of the flow.

We consider nonlocal flows of the following form:

$$\frac{\partial \rho}{\partial t} + \int_0^\delta \frac{F(\rho, \tau_h \rho) - F(\tau_{-h} \rho, \rho)}{h} \omega(h) dh = r - s; \quad (1)$$

$$\rho(x, 0) = \rho_0(x),$$

where  $\rho : \mathbb{R} \times (0, T) \mapsto \overline{\mathbb{R}}_+$  is the conserved quantity at a given point and at a given time,  $F : \mathbb{R} \times \mathbb{R} \mapsto \mathbb{R}$  is the flux function,  $\tau_{\pm h} \rho(x, t) = \rho(x \pm h, t)$  denotes a spatial shift and  $r, s : \mathbb{R} \times (0, t) \times \overline{\mathbb{R}}_+ \mapsto \overline{\mathbb{R}}_+$  are the source and sink terms, respectively. For the physical background and formal derivation of (1), we refer to [8].

With a novel finite volume scheme we obtain the so-called generalized NFRM. Let  $n_i$  and  $s_i$  denote the continuous number of particles and available spaces in the  $i$ th cell per unit length, respectively. The system of ODEs derived from the reactions are:

$$\dot{n}_i = \sum_{j=1}^{b_i} k_{i-j,i} n_{i-j} s_i - \sum_{j=1}^{f_i} k_{i,i+j} n_i s_{i+j} + k_{in,i} s_i - k_{out,i} n_i, \quad (2)$$

$$\dot{s}_i = - \sum_{j=1}^{b_i} k_{i-j,i} n_{i-j} s_i + \sum_{j=1}^{f_i} k_{i,i+j} n_i s_{i+j} - k_{in,i} s_i + k_{out,i} n_i.$$

Generalized NFRMs are formally kinetic, which ensures some advantageous properties of the model and most importantly, allows us to use the well-developed theory of chemical reaction networks [9]. Furthermore, the underlying CRN has physically meaningful compartments and topology. In fact, let  $N_i$  and  $S_i$  denote particles and available space slots for particles in the  $i$ th cell, respectively. Then the particle flow

can be represented as transformations of complexes (that is, as reactions) as follows:

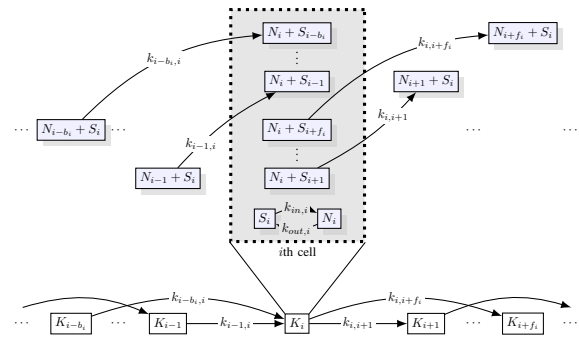


Fig. 1. Compartmental model of the generalized NFRM

Relying on the linear first integral of a closed system with strongly connected structure we can formalize the following Hamiltonian representation.

$$[\tilde{J}]_{ik}(n, s) = \begin{cases} \mathcal{K}_{ki}(n_k, s_i) - \mathcal{K}_{ik}(n_i, s_k) & k \in \mathcal{D}_i \cap \mathcal{R}_i, \\ \mathcal{K}_{ki}(n_k, s_i) & k \in \mathcal{D}_i \cap \mathcal{R}_i^C, \\ -\mathcal{K}_{ik}(n_i, s_k) & k \in \mathcal{D}_i^C \cap \mathcal{R}_i, \\ 0 & \text{otherwise.} \end{cases}$$

Observe that (2) is equivalent to

$$\begin{bmatrix} \dot{n} \\ \dot{s} \end{bmatrix} = \begin{bmatrix} \tilde{J}(n, s) & 0 \\ 0 & -\tilde{J}(n, s) \end{bmatrix} \cdot \nabla H = J(n, s) \cdot \nabla H(n, s).$$

## REFERENCES

- [1] M. A. Vághy, M. Kovács, and G. Szederkényi, “Kinetic discretization of one-dimensional nonlocal flow models,” *IFAC-PapersOnLine*, vol. 55, pp. 56–61, 2022. Presented at MATHMOD 2022.
- [2] M. A. Vághy and G. Szederkényi, “Hamiltonian representation of generalized ribosome flow models,” in *European Control Conference - ECC*, 2022.
- [3] R. J. LeVeque, *Numerical Methods for Conservation Laws.*, vol. 57. Basel: Birkhäuser, 1992.
- [4] F. Kessels, *Traffic Flow Modelling*. Springer, 2019.
- [5] S. Reuveni, I. Meilijson, M. Kupiec, E. Ruppin, and T. Tuller, “Genome-scale analysis of translation elongation with a ribosome flow model,” *PLoS Computational Biology*, vol. 7, no. 9, 2011.
- [6] A. Keimer, G. Leugering, and T. Sarkar, “Analysis of a system of nonlocal balance laws with weighted work in progress,” *Journal of Hyperbolic Differential Equations*, vol. 15, no. 3, pp. 375–406, 2018.
- [7] F. A. Chiarello and P. Goatin, “Global entropy weak solutions for general non-local traffic flow models with anisotropic kernel,” *ESAIM: Mathematical Modelling and Numerical Analysis*, vol. 52, pp. 163–180, 2018.
- [8] Q. Du, M. Gunzburger, R. B. Lehoucq, and K. Zhou, “A non-local vector calculus, non-local volume-constrained problems and non-local balance laws,” *Mathematical Models and Methods in Applied Sciences*, vol. 23, no. 3, pp. 493–540, 2013.
- [9] M. Feinberg, *Foundations of Chemical Reaction Network Theory*. Springer International Publishing, 2019.

# Structural characterization of the postsynaptic Drebrin protein

Soma VARGA

(Supervisor: Bálint Ferenc PÉTERFIA)

Pázmány Péter Catholic University, Faculty of Information Technology and Bionics

50/a Práter street, 1083 Budapest, Hungary

varga.soma@itk.ppke.hu

**Abstract**—The postsynaptic density (PSD) of excitatory synapses is a complex network of nervous system proteins involved in postsynaptic signaling. Our research group focuses on the function of proteins in PSD organization. Drebrin is a cytoskeleton-organizing protein of the PSD and its detailed structural and functional characterization is yet to be revealed. Our aim is to use several biophysical and spectroscopic methods for obtaining atomic level information of the protein which can lead to a better understanding of Drebrin's biological role.

**Keywords**—PSD, Drebrin, SAH domain, Circular dichroism spectroscopy, solution NMR, protein structure

## I. INTRODUCTION

Drebrin modulates and regulates several functions of the nervous system, thereby responsible for a few molecular mechanisms involved in learning and memory [1]. The Drebrin protein is an essential component of the cytoskeleton, and its presence is required for actin polymerization of synapses and recruitment of CXCR4 chemokine receptors [2], as well as for the morphogenesis of the dendritic spine. Drebrin also plays an important role in synaptic plasticity associated with hippocampal memory and establishes several key interactions with other proteins present in PSD [3].

In this work we aim to characterize the structure of three different Drebrin regions, namely the ADFH (Actin-Depolymerizing Factor Homology) domain and the actin-binding core at the N-terminal, the SAH (Single Alpha Helix) domain which was earlier predicted with bioinformatic methods [4], and the HBMs (Homer Binding Motifs) near the C terminus.

## II. METHODS

We performed the molecular cloning with pEV and pGEX4T1 vectors and the expression of the corresponding constructs with our competent DH5 alpha, XL-10 Gold and BL21 E. coli bacteria cells. Purification of the proteins were done by several chromatography methods, namely: IMAC (Immobilized Metal Affinity Chromatography), IEC (Ion Exchange Chromatography), and SEC (Size Exclusion Chromatography). We started the initial characterization of the successfully purified constructs with CD (Circular Dichroism) and NMR (Nuclear Magnetic Resonance) spectroscopy. Molecular interaction with F-actin was investigated with pull-down assay.

## III. RESULTS

The preparation of the pEV and pGEX plasmids for in total 11 constructions was successfully accomplished. The results were confirmed by Sanger DNA sequencing. The expression and purification protocols of the ADFH and SAH domains has been experimentally optimized and monitored by SDS-PAGE

(Sodium Dodecyl Sulfate-Polyacrylamide Gel Electrophoresis). For characterizing the secondary protein structure of the D233 and SAH domains, CD measurements were performed. The structural characterization of the SAH domain has been continued with 2D, 3D and 4D NMR techniques (Fig.1). We developed a Ni-NTA beam based pull-down assay, which successfully proved that our in-house D233 construct is able to bind F-actin.

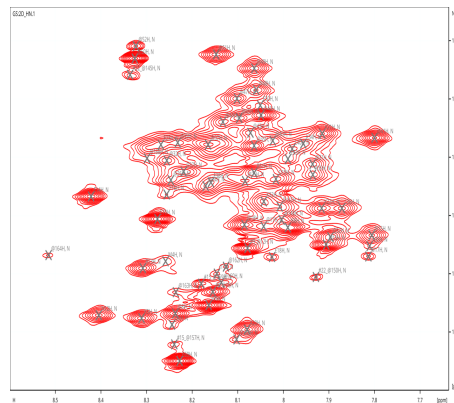


Fig. 1. Region of the 1H-15N HSQC spectra obtained from the SAH domain is showing that the similar amino acids are producing overlapping signals. 30 of the 74 residues were assigned with standard triple resonance experiments. With the help of 4D experiments, we were able to solve most of the previously appearing severe signal overlaps.

## ACKNOWLEDGEMENTS

I would like to thank my supervisor Dr. Bálint Ferenc Péterfia for his help and guidance with my laboratory work and to Dr. Zoltán Gáspári for his comprehensive help with my research and to Dr. Perttu Permi for performing the NMR measurements. The authors acknowledge the support of the National Research, Development and Innovation Office – NKFIH – through grant no. TKP2021-EGA-42.

## REFERENCES

- [1] V. M. Ho, J.-A. Lee, and K. C. Martin, “The Cell Biology of Synaptic Plasticity,” *Science*, vol. 334, pp. 623–628, Nov. 2011.
- [2] M. Pérez-Martínez, M. Gordón-Alonso, J. R. Cabrero, M. Barrero-Villar, M. Rey, M. Mittelbrunn, A. Lamana, G. Morlino, C. Calabia, H. Yamazaki, T. Shirao, J. Vázquez, R. González-Amaro, E. Veiga, and F. Sánchez-Madrid, “F-actin-binding protein drebrin regulates CXCR4 recruitment to the immune synapse,” *Journal of Cell Science*, vol. 123, pp. 1160–1170, Apr. 2010.
- [3] Y. Hayashi, “Drebrin-Homer Interaction at An Atomic Scale,” *Structure*, vol. 27, pp. 3–5, Jan. 2019.
- [4] Á. Kovács, D. Dudola, L. Nyitray, G. Tóth, Z. Nagy, and Z. Gáspári, “Detection of single alpha-helices in large protein sequence sets using hardware acceleration,” *Journal of Structural Biology*, vol. 204, pp. 109–116, Oct. 2018.

# Yeast models of neurodegenerative diseases using whole-cell simulations

Áron WEBER

(Supervisor: Attila CSIKÁSZ-NAGY)

Pázmány Péter Catholic University, Faculty of Information Technology and Bionics

50/a Práter street, 1083 Budapest, Hungary

weber.aron@itk.ppke.hu

**Abstract**—Neurodegenerative diseases - illnesses characterised by a progressive degradation and death of neurons - are becoming more and more prevalent as average ages and expected lifespans increase. With no effective treatment options available, they greatly burden both individual and society. Therefore, gaining further understanding of these illnesses is of high importance. And, since performing research on human patients is expensive and cumbersome, and also raises considerable ethical concerns, modeling these diseases in different organisms can speed up research aimed at elucidating their exact molecular mechanisms. During our work, we have used an *in vitro* budding yeast model of four illnesses - Alzheimer's, Parkinson's, and Huntington's diseases, and amyotrophic lateral sclerosis - to perform computational simulations aimed at investigating which protein complexes exhibit quantitative changes upon the expression of key aggregation-prone proteins of the aforementioned diseases.

**Keywords**-neurodegenerative diseases; complexomics; computational simulation

## SUMMARY

Neurodegenerative diseases - illnesses that are characterised by the gradual degradation, and later on, death of neurons - affect, as the mean age and expected lifespan of developed countries increase, an ever-rising number of patients worldwide. However, as of now, there are no effective treatments to them, leading to greater and greater burdens on societies and individuals alike. Thus, researching the exact molecular mechanisms of these illnesses, and finding points where one can intervene could help develop ways to alleviate their negative effects. In my research, I have focused on four such disorders, Alzheimer's, Parkinson's and Huntington's diseases, and amyotrophic lateral sclerosis, colloquially known by its abbreviation, ALS. A common motif in these is that in each of them, a specific protein is misfolded, and, instead of assuming their usual (sometimes intrinsically disordered, as is the case in alpha-synuclein) structures, they start forming aggregates with each other. These proteins are often called aggregation-prone proteins (APP). The APPs examined are as follows: amyloid beta (Alzheimer's), alpha-synuclein (Parkinson's), huntingtin (Huntington's), TAR-DNA binding protein and fused-in-sarcoma protein (both ALS). During this work, our group has attempted to provide an *in-silico* reproduction of an experiment aimed at modeling these four diseases in *Saccharomyces cerevisiae* [1]. In this experiment, the researchers have expressed the APPs of the disorders above in separate yeast colonies (and GFP as control), and made proteomics measurements 6, 12, 18 and 24 hours after APP expression. For the computational reproduction, I have performed cell simulations using the previously described proteomics data with the Cytocast Cell Simulator algorithm. I have selected the protein complexes that had abundances significantly dif-

fering from the control measurements, and analysed their functions, both using available literature and Gene Ontology enrichment analysis. While I have still not gained a complete understanding of the exact molecular pathophysiology of these four neurodegenerative diseases, I have found certain protein complexes and molecular functions that could be worthy of closer, more detailed investigation in the near future.

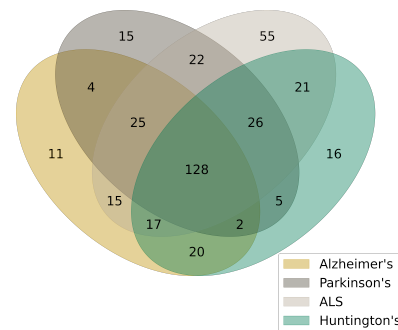


Fig. 1. Number of protein complexes with a significantly altered abundance, grouped by disease. Based on the simulation results corresponding to measurements 18 hours after induction. From [2]

## ACKNOWLEDGEMENTS

This work was done using the resources of Cytocast Hungary Kft. Other contributors to the project were Fruzsina Dvorzsák and Anna Zichy.

## REFERENCES

- [1] A. Melnik, V. Cappelletti, F. Vaggi, *et al.*, “Comparative analysis of the intracellular responses to disease-related aggregation-prone proteins,” eng, *Journal of Proteomics*, vol. 225, p. 103 862, Aug. 2020, ISSN: 1876-7737. DOI: 10.1016/j.jprot.2020.103862.
- [2] Á. Weber, F. Dvorzsák, A. Zichy, B. Keömley-Horváth, E. Fichó, and A. Csikász-Nagy, “Modeling neurodegenerative diseases in yeast through whole cell simulations,” *Hungarian Molecular Life Sciences* (poster), 2023.
- [3] S. Rizzetto, P. Moysesos, B. Baldacci, C. Priami, and A. Csikász-Nagy, “Context-dependent prediction of protein complexes by sicompre,” *npj Systems Biology and Applications* 2018 4:1, vol. 4, pp. 1–9, 1 Sep. 2018, ISSN: 2056-7189. DOI: 10.1038/s41540-018-0073-0.
- [4] H. Yang and H.-Y. Hu, “Sequestration of cellular interacting partners by protein aggregates: Implication in a loss-of-function pathology,” en, *The FEBS Journal*, vol. 283, no. 20, pp. 3705–3717, Oct. 2016, ISSN: 1742-464X, 1742-4658. DOI: 10.1111/febs.13722.
- [5] C. Hetz and S. Saxena, “Er stress and the unfolded protein response in neurodegeneration,” en, *Nature Reviews Neurology*, vol. 13, no. 8, pp. 477–491, Aug. 2017, ISSN: 1759-4766. DOI: 10.1038/nrneuro.2017.99.



**PROGRAM 2**  
**COMPUTER TECHNOLOGY BASED ON**  
**MANY-CORE PROCESSOR CHIPS, VIRTUAL**  
**CELLULAR COMPUTERS, SENSORY AND**  
**MOTORIC ANALOG COMPUTERS**

Head: Péter SZOLGAY

# Head restrained mouse behavior experiments

Boldizsár Zsolt BALOG

(Supervisors: Gábor NYÍRI, György CSEREY)

Pázmány Péter Catholic University, Faculty of Information Technology and Bionics

50/a Práter street, 1083 Budapest, Hungary

balog.boldizsar.zsolt@itk.ppke.hu

**Abstract**—Neuroscience experiments are critical for studying brain physiology and pathology. Head restrained experiments (HREs) and freely moving experiments (FMEs) are both used during behavioral studies. In FMEs subjects are allowed to explore and interact with the experimental setup voluntarily; in HREs the head of the animal is fixed. This article compares HREs and FMEs, contrasts their differences and similarities, evaluates their advantages and disadvantages, typical use cases, and latest developments in the field.

**Keywords**—keyword; freely moving; head restrained, mouse, behavior, experiment, neuroscience

## I. INTRODUCTION

Experimental neuroscience has a fundamental role in understanding brain function and dysfunction. The laboratory mouse is a well-established model animal for studying the mammalian brain, thus analysis of mouse behavior is essential for understanding mental disorders and cognitive deficits, which are among the largest social and economic burden of our society. In memory related neuroscience research, acquiring information about the memories of the subjects is almost exclusively done by analyzing their behavior. Behavior analysis is based on delivering well controlled stimuli to the subjects and simultaneously measuring their response.

## II. ADVANTAGES OF FMEs

To study mouse behavior, traditionally researchers used FMEs, as it yields natural behavior. The movement of animals is a fundamental measure of their behavior that can serve as a solid basis for evaluating the effects of a treatment. Spatial navigation tasks are well established in FMEs (for example Morris water maze).

Some neuroscience methods (for example two-photon microscopy, electrophysiology with high-density silicon probes, high resolution pupillometry) introduced problems: a) heavy devices, b) delicate instruments and c) devices with accuracy requirements. These problems were solved by the development of HREs. This compromise allows the experimenters to study awake mice with advanced methodology.

## III. ADVANTAGES OF HREs

By restraining the movement of the subject's head, even large devices can be precisely and rigidly positioned relative to the animal (Fig. 1.). Stimuli in HREs can be better controlled, measurements can be more accurate, experiments get more reproducible and more standardized [1]. An example of this is the utilization of water reward as a motivation for water restricted mice [2], [3]. In HREs, water droplets can be precisely delivered to the subjects. Similarly, olfactory, auditory, tactile [2] and visual cues can be more controllable in the HREs. In addition, some experiments, like the selective stimulation of certain whiskers, can only be carried out in HREs.

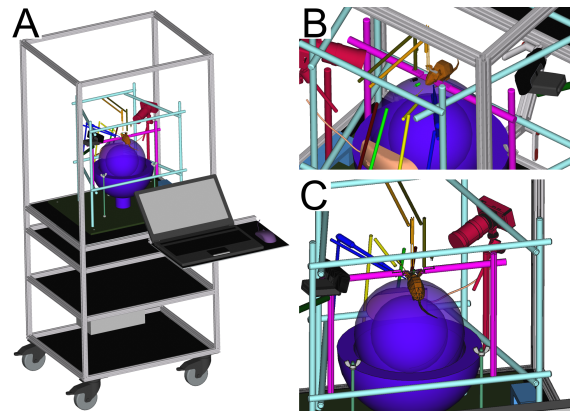


Fig. 1. CAD model of a head restrained experimental arrangement

Some research groups develop voluntary head restraint setups. In these experiments, animals move freely, but for some tasks, they voluntarily stabilize their head for a short period of measurement. This can facilitate automation of behavioral batteries, reduce time-demanding nature of head-restrained experiments and decrease the stress and variability caused by the researcher-subject interaction [1].

## IV. CONCLUSION

FMEs and HREs are both well established and widely used in modern behavioral neuroscience. When designing an experiment, researchers need to take FMEs' and HREs' capabilities into account and choose the best method for the experiment.

## ACKNOWLEDGEMENT

This research was supported by the National Research, Development and Innovation Office – NKFIH – through the grant no. TKP2021-NVA-27.

## REFERENCES

- [1] R. Aoki, R. Aoki, T. Tsubota, Y. Goya, and A. Benucci, "An automated platform for high-throughput mouse behavior and physiology with voluntary head-fixation.," *Nature Communications*, 2017.
- [2] Z. V. Guo, S. A. Hires, N. Li, D. H. O'Connor, D. H. O'Connor, T. Komiyama, E. Ophir, D. Huber, C. Bonardi, K. Morandell, D. A. Gutnisky, S. Peron, N. long Xu, J. C. Cox, J. D. Cox, and K. Svoboda, "Procedures for behavioral experiments in head-fixed mice.," *PLOS ONE*, 2014.
- [3] C. Barkus, C. Bergmann, T. Branco, M. Carandini, P. T. Chadderton, G. L. Galiñanes, G. Gilmour, D. Huber, J. R. Huxter, A. G. Khan, A. J. King, M. Maravall, T. O'Mahony, C. I. Ragan, E. S. Robinson, A. T. Schaefer, S. R. Schultz, F. Sengpiel, and M. J. Prescott, "Refinements to rodent head fixation and fluid/food control for neuroscience," *Journal of Neuroscience Methods*, 2022.

# Progress report on robust epidemic model control by feedback linearization and state estimation

Balázs CSUTAK

(Supervisor: Gábor SZEDERKÉNYI)

Pázmány Péter Catholic University, Faculty of Information Technology and Bionics

50/a Práter street, 1083 Budapest, Hungary

csutak.balazs@itk.ppke.hu

**Abstract**—In this progress report, I present my recent contributions in the field of state estimation and control of epidemiological models, using classical techniques typically applied to electromechanical systems. Using our previously published and validated epidemic simulation toolbox, we achieve robust asymptotic output tracking with a modified version of feedback linearization, accurate even in case of serious model and parameter mismatch. We ensure a realistic setup by estimating the model states using an Extended Kalman Filter.

**Keywords**—epidemic, feedback linearization, robust control, Extended Kalman Filter

## I. INTRODUCTION

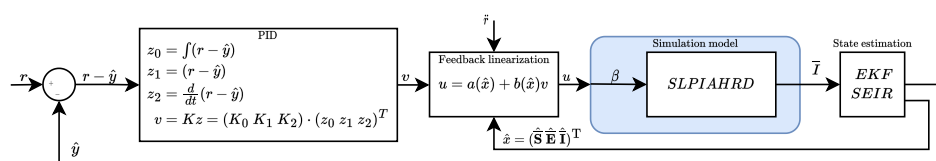
Since the winter of 2020, the whole world has been struggling with the COVID-19 pandemic, posing a formidable problem to economies and healthcare systems in each country. In the initial stages, when effective treatments and vaccines were not available, policymakers resorted to implementing restrictive measures in an attempt to limit the spread of the virus. To facilitate informed decision-making, the construction of accurate simulation and control frameworks is inevitable.

As a direct sequel to my previous research [1], I present our newly developed building blocks suitable for such a decision support system: a technique for robust control of epidemic processes based on feedback linearization, used in conjunction with an Extended Kalman Filter based state estimation algorithm. Given a reference (or target) curve for the number of infected individuals over time, our method is capable of computing the reproduction number  $\beta$  required to reach that prescribed trajectory, even if some of the initial assumptions are not entirely correct (eg. model inaccuracies, mismatched parameters, imprecisely estimated states).

As the reproduction number is strongly influenced by governmental restrictions (social distancing, banning public events, closing schools, etc), implementing the computed input translates to a mapping problem between levels of  $\beta$  and the actual action to be taken (solvable by eg. agent-based models).

## II. MODELS

In order to prove the robustness of our approach, we used different models for estimation/control, and for simulation (ie. observing the actual effect of the computed input). The whole setup of our experiments can be seen in figure 2 (below).



For simulation, we use our previously published 8-compartment compartmental model (*SLPIAHRD*)[1]. The estimation and control process is based on a much simpler model, the *SEIR*, which is widely used for modeling epidemic processes, even though it lacks the ability to capture the fine details of COVID-19 (eg. the high proportion of asymptomatic infections). The parameters of the two models were only matched intuitively, based on their approximate effect on the epidemic dynamic.

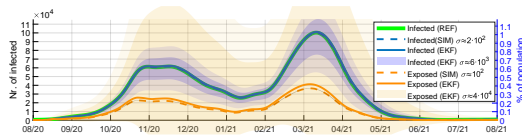


Fig. 1. Comparison of simulated and estimated trajectories

## III. ROBUST CONTROL AND RESULTS

We realize robust control by introducing an extra integrator step into the classic feedback linearization scheme of Isidori [2, Chap 4.3]. That is, by defining the transformed model states as  $\dot{z} = r - y$ , we obtain a PID-like control structure, effectively handling all kinds of disturbances.

To test our setup, we ran  $9 \times 9$  simulations, altering the two parameters of the SEIR control model on a grid, between 10% – 300% of their nominal value. The results, as presented in detail in [3], [4] show a reduction by two magnitudes in the deviation of simulated model states compared to the estimation (see figure 1).

## ACKNOWLEDGEMENTS

Parts of this research were supported by grants TKP2021-NVA-27, ÚNKP-22-3-I-PPKE-79, NKFIH-131545 and RRF-2.3.1-21-2022-00006.

## REFERENCES

- [1] B. Csutak, “Progress report on epidemic model inversion using feedback linearization,” *PPCU-FIT PhD Proceedings*, 2022.
- [2] A. Isidori, *Nonlinear control systems*. Springer, 1995.
- [3] B. Csutak, M. K. Jenei, and G. Szederkényi, “Linearization based robust reference tracking control of a compartmental epidemiological model,” in *24th International Conference on Process Control*, 2023. To be published.
- [4] B. Csutak and G. Szederkényi, “Reference tracking control of a nonlinear epidemiological model with state estimation,” in *9th International Conference On Control, Decision And Information Technologies*, 2023. To be published.

# Improvement possibilities of SVM algorithms for open-set recognition

Lóránt DAUBNER

(Supervisors: Tamás ZSEDROVITS, Kálmán TORNAI)

Pázmány Péter Catholic University, Faculty of Information Technology and Bionics

50/a Práter street, 1083 Budapest, Hungary

daubner.lorant.szabolcs@itk.ppke.hu

Support Vector Machine (SVM) is a great machine learning algorithm widely used in pattern recognition and classification. SVM maps training examples to points in space and constructs a hyperplane which represents the largest separation (maximizes the margin) between the two classes. In other words, SVM allows maximizing the generalization ability of a model. [1] SVMs have empirically shown strong performance on various recognition or categorization problems in multiple fields of application. SVM was introduced by Vapnik [2] as a kernel based machine learning model and due to its good generalization capability it has become one of the most used methods in classification.

Beyond the obvious benefits, the SVM algorithms have several limitations too. In this summary I try to collect various methods to overcome these limitations and propose further development of the SVM algorithms based on papers related to current research.

One important objective in pattern classification is to develop a model which maximizes the performance for the training data. SVMs can become computationally expensive when dealing with large datasets. To handle this, dimension reduction techniques like Principal Component Analysis [4] or feature selection [8] or utilizing distributed computing on subsets [5] [7] are used.

When dealing with real-world recognition problems, we usually cannot have knowledge of the entire set of possible classes. In such cases, we need to think of classification methods able to deal with the “unknown” and reject samples belonging to classes never seen during training (generally called Open-Set Recognition).

This semester I started to work on planning and developing improved SVM algorithms based on the following three main ideas (taking also the SVM limitations into account):

- Using SVM for Multi-view learning. Multi-view learning considers learning with multiple views to improve the generalization performance. Multi-view learning is also known as data fusion or data integration from multiple feature sets. [13][14] (Fig.1)
- Incremental Learning Algorithm with SVM, which is one of the most effective methods of learning large-scale data [15]
- Dataset shift and dynamic data (to include time parameter in the SVM algorithm)

The improved classifier for Open-Set Recognition should be a hybrid classifier (e.g. by combining multiple SVM models or SVM and other learning methods). To boost SVM’s performance parallelization could be used as well: e.g. training multiple SVMs on different subsets of the training data and running SVMs with different kernels

on selected features. We could also train multiple SVMs sequentially, where each subsequent SVM works on the output data of the previous SVM.

## ACKNOWLEDGEMENT

This research was supported by the National Research, Development and Innovation Office – NKFIH – through the grant no. TKP2021-NVA-26.

## REFERENCES

- [1] Cervantes, J., García-Lamont, F., Rodríguez, L., Lopez-Chau, A. A comprehensive survey on support vector machine classification: Applications, challenges and trends. *Neurocomputing* 408, 189-215, 2020.
- [2] Cortes, C., Vapnik, V. Support-vector networks. *Machine Learning* 20, 273-297, 1995.
- [3] Fathi Hafshejani, S., Moaberfard, Z. A new trigonometric kernel function for support vector machine. *Iran Journal of Computer Science* 6, 137-145, 2023.
- [4] Heng Lian, On feature selection with principal component analysis for one-class SVM. *Pattern Recognition Letters* 33, 137-145, 2012.
- [5] E. Osuna, R. Freund and F. Girosit, Training Support Vector Machines: an Application to Face Detection. *Proceedings of IEEE Computer Society Conference on Computer Vision and Pattern Recognition*, 130-136, 1997.
- [6] L. Mohan, J. Pant, P. Suyal and A. Kumar, Support Vector Machine Accuracy Improvement with Classification. *12th International Conference on Computational Intelligence and Communication Networks (CICN)*, 477-481, 2020.
- [7] Zhi-Qiang Zeng, Hong-Bin Yu, Hua-Rong Xu, Yan-Qi Xie and Ji Gao, Fast Training Support Vector Machines Using Parallel Sequential Minimal Optimization. *12th International Conference on Computational Intelligence and Communication Networks (CICN)*, 997-1001, 2008.
- [8] Kamel, S.R., YaghoobZadeh, R., Kheirabadi, M. Improving the performance of support-vector machine by selecting the best features by Gray Wolf algorithm to increase the accuracy of diagnosis of breast cancer. *Journal of Big Data* 6, Article number: 90, 2019.
- [9] Anderson Rocha and Siome Goldenstein. Multiclass from binary: Expanding one-vs-all, one-vs-one and ECOC-based approaches. *IEEE Transactions on Neural Networks and Learning Systems*, vol. 25, no. 2, pp. 289-302, 2014.
- [10] W. J. Scheirer, A. D. R. Rocha, A. Sapkota, and T. E. Boult, Toward Open Set Recognition. *IEEE Transactions on Pattern Analysis and Machine Intelligence*, vol. 35, no. 7, pp. 1757-1772, 2013.
- [11] P. Ribeiro Mendes Júnior, T. E. Boult, J. Wainer and A. Rocha, Open-Set Support Vector Machines. *IEEE Transactions on Systems, Man, and Cybernetics: Systems*, vol. 52, no. 6, pp. 3785-3798, 2022.
- [12] C. Geng, S. -J. Huang and S. Chen, Recent Advances in Open Set Recognition: A Survey. *IEEE Transactions on Pattern Analysis and Machine Intelligence*, vol. 43, no. 10, pp. 3614-3631, 2021.
- [13] Jing Zhao, Xijiong Xie, Xin Xu, Shiliang Sun, Multi-view learning overview: Recent progress and new challenges. *Information Fusion* 38, 43-54, 2017.
- [14] Ruxin Xu, Huiru Wang, Multi-view learning with privileged weighted twin support vector machine. *Expert Systems with Applications* 206, 2022.
- [15] Hongwei Jiang, Bin Zou, Chen Xu, Jie Xu, Yuan Yan Tang, SVM-Boosting based on Markov resampling: Theory and algorithm. *Neural Networks* 131, 276-290, 2020.
- [16] Chang Xu and Dacheng Tao and Chao Xu, A Survey on Multi-view Learning. 2013.

# Automatic stencil program generation from C++ to OPS DSL

Balázs DRÁVAI

(Supervisor: István Zoltán REGULY)

Pázmány Péter Catholic University, Faculty of Information Technology and Bionics

50/a Práter street, 1083 Budapest, Hungary

dravai.balazs@itk.ppke.hu

**Abstract**—We introduce a compiler/code generator to enhance C++ stencil program performance. Our pipeline translates C/C++ to MLIR for loop information extraction and provides a utility for interpreting loop metadata. This approach aims to optimize stencil programs without learning a DSL.

**Keywords**—HPC; automatic parallelisation; source-to-source compiler

## I. INTRODUCTION

Stencil computations, key to scientific and engineering applications involving multi-dimensional arrays or grids, modify elements through nested loops in an n-dimensional grid following a predetermined pattern. Performance improvements typically focus on fine-grained and coarse-grained parallelism, optimizing SIMD parallelization and restructuring computational loops for simultaneous large data block calculations. Despite advancements in compiler technology, certain algorithm transformations remain challenging, which could potentially be mitigated by using specialized compilers and domain-specific languages, albeit possibly compromising universality.

In our paper, we introduce the core components of a new compiler/code generator that converts C++ stencil programs to the OPS DSL [2].

## II. MLIR FRONTEND FOR STENCIL PROGRAMS

In the process of representing high-level structures and data flow graphs in MLIR [3], we are finding that there’s a need for a fitting front-end to compile and present the source code. Currently, no fully functional solution for representing C/C++ structures exists, despite various attempts such as the discontinued CIL dialect and the still-under-development Clang IR (CIR).

We are employing Polygeist [1], or `cgeist` as it’s also known, which serves as a front-end for polyhedral C/C++ codes. It depicts this code by merging `arith`, `scf`, `memref`, and `affine` dialects. Stencil computations often have loops with a regular and deterministic structure, which pairs well with the polyhedral model, making it a practical approach for enhancement. Hence, we can make it possible to compile stencil programs into MLIR using this method.

## III. C TO OPS CONVERTER

The process of the compiler [1] pipeline can be delineated as follows: Initially, the C implementation is translated into MLIR via the utilization of ‘`cgeist`’, which subsequently generates a segment of code in the `affine` dialect that necessitates further lowering to `scf` and `memref` dialects. The selected architecture of the system preferentially extracts pertinent information from the `scf` dialect as opposed to the `affine`, a decision that provides the potential to later

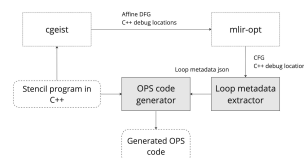


Fig. 1. Pipeline of the code generation process from naive C++ to OPS

integrate with an alternative frontend, under the condition that the compiled MLIR can be further lowered to `scf` and `memref` dialects.

To begin, it is imperative to recognize the loop nests within the coding structure. This can be accomplished by navigating the Multi-Level Intermediate Representation (MLIR) abstract graph. Each loop, devoid of a parent loop operation, indicates the initiation of a loop nest. The association of loops with array indices can be systematically arranged from the external to the internal, thus enabling the extraction of the loop induction variables, as well as the loop bounds.

Usually in stencil kernels the multi-dimensional arrays are treated as a one-dimensional array or a flattened version of itself. This approach requires a flat-array indexing expression to access the elements of the array. This simplification often facilitates easier manipulation of the data, allowing for quicker computations and more streamlined code. However, this method sometimes leads to less intuitive indexing, particularly when working with arrays that originally have more than two dimensions. We also need to determine every argument the extract the indexing offsets. The necessity of analyzing the expression tree of the indexing expression arises from the inherent difficulty in directly accessing the offsets. Leveraging the gathered metadata, we developed a Python-based utility which interprets the extracted loop metadata. This tool discretely encapsulates each kernel into an independent function, administrates the sequence of execution, and establishes the iteration domain.

## REFERENCES

- [1] Moses, W., Chelini, L., Zhao, R. & Zinenko, O. Polygeist: Raising C to Polyhedral MLIR. *2021 30th International Conference On Parallel Architectures And Compilation Techniques (PACT)*. pp. 45-59 (2021)
- [2] Regulý, I., Mudalige, G., Giles, M., Curran, D. & McIntosh-Smith, S. The OPS Domain Specific Abstraction for Multi-block Structured Grid Computations. *2014 Fourth International Workshop On Domain-Specific Languages And High-Level Frameworks For High Performance Computing*. pp. 58-67 (2014)
- [3] Lattner, C., Pienaar, J., Amini, M., Bondhugula, U., Riddle, R., Cohen, A., Shpeisman, T., Davis, A., Vasilache, N. & Zinenko, O. MLIR: A Compiler Infrastructure for the End of Moore’s Law. *ArXiv*. **abs/2002.11054** (2020)

# Adapting the open-set recognition method to various time-series data

András Pál HALÁSZ

(Supervisors: Kálmán TORNAI, Péter Norbert SZOLGAY)

Pázmány Péter Catholic University, Faculty of Information Technology and Bionics

50/a Práter street, 1083 Budapest, Hungary

halasz.andras@itk.ppke.hu

Nowadays, various machine learning methods provide excellent results in different classification and recognition tasks, reaching or even exceeding the human level in numerous cases. The experiments yielding these results were conducted in a closed-set scenario, i.e., the assumption that all classes are known during training. A more realistic situation is the open-set case when new classes can appear during testing, and our model has to reject them, which is a great challenge. The problem of Open Set Recognition (OSR) was formalized by Scheirer et al. [1]

In my former research, I implemented a well-performing OSR method. The main idea is to model the space of unknowns - to the best of our abilities - by generating fake samples using the real ones. Experiments showed that training the model to reject the generated samples helps to prepare it to reject the real unknown samples later. Moreover, I created the fake samples in a hidden feature layer instead of creating fake inputs. It proved advantageous in terms of accuracy: Due to the much smaller generative model (the feature layer is of a much simpler structure than the input layer), the extra computational costs of generating samples are virtually eliminated. Generative Adversarial Networks still do the sample generation [2], but the generator and discriminator networks are replaced with much simpler ones.

The model was initially constructed to process image datasets and convolutional networks were used. However, it is important to process data of different natures. The same approach can be adapted to different kinds of data by replacing the feature-extraction part. Once appropriate features are obtained, the generative and feature classifier models work similarly. I have adapted the model to classify multi-channel time series. The dataset I have processed consists of biometric signals. The task is to classify the user based on the vibration of their hand. The vibration is recorded via the accelerometer and gyroscope sensors of a mobile phone in the hand of the subject. [3]

To extract the features, I have used two different approaches. The first approach is to use a neural network as it was done for images. Of course, for time series, we need a different network structure. The backbone of the feature extractor consists of 3 residual blocks, but one-dimensional convolutional layers are used. After the residual blocks, follow a linear layer with ReLU activation to decrease the number of features. The data had to be preprocessed. I used some of the guidance from the authors to create the dataset for this. The data were resampled with fixed sampling frequency, aligning the values from the two sensors on identical timestamps. After that, the data were cut into shorter slices and normalized.

The other method is not to train a model but to use

predefined features. These are calculated before training. After that, the training itself starts with the generative part right away. The data are preprocessed the same way described above, except for the normalization. The features include some statistical aggregates (min, max, variance, deviation, the signal's energy, etc.), Fourier coefficients and their aggregates, entropy, and auto-correlation values. These are concatenated into a single vector.

The script was adapted to accommodate both methods, and the initial tests were run. The preliminary results are quite promising: trained on 20 known classes, the closed-set performance is almost flawless (0.994) using predefined features, while the open-set AUC values is 0.883. Using neural networks as feature-extractor, I was not able to get good results yet.

Future works include combining the finetuned versions of the two approaches.

## ACKNOWLEDGEMENT

*This research was supported by the National Research, Development and Innovation Office – NKFIH – through the grant no. TKP2021-NVA-26.*

## REFERENCES

- [1] W. J. Scheirer, A. Rocha, A. Sapkota, and T. E. Boult, "Toward open set recognition," *IEEE Transactions on Pattern Analysis and Machine Intelligence*, vol. 35, pp. 1757–1772, 2013.
- [2] I. J. Goodfellow, J. Pouget-Abadie, M. Mirza, et al., "Generative adversarial nets," in *Proceedings of the 27th International Conference on Neural Information Processing Systems - Volume 2*, ser. NIPS'14, Montreal, Canada: MIT Press, 2014, pp. 2672–2680.
- [3] K. Jiokeng, G. Jakllari, and A.-L. Beylot, "I want to know your hand: Authentication on commodity mobile phones based on your hand's vibrations," *Proc. ACM Interact. Mob. Wearable Ubiquitous Technol.*, vol. 6, no. 2, Jul. 2022. DOI: 10.1145/3534575. [Online]. Available: <https://doi.org/10.1145/3534575>.

# Comparison of the effect of combinations of non-pharmaceutical restrictions on the spread of COVID-19

Gergely HORVÁTH

(Supervisor: Gábor SZEDERKÉNYI)

Pázmány Péter Catholic University, Faculty of Information Technology and Bionics  
50/a Práter street, 1083 Budapest, Hungary  
horvath.gergely@itk.ppke.hu

**Abstract**—Throughout this semester, we quantified the impact of non-pharmaceutical interventions (NPIs) on the spread of COVID - both individually and in various combinations. We make use of the previously developed PanSim agent-based model to accurately capture various aspects of the pandemic and the interventions and show how the transmission rate ( $\beta$ ) commonly used in compartmental ODE models can be matched to PanSim and used to compare interventions. Through a specific example of targeting a desired and constant level of peak hospitalization, we give several equivalent restriction packages that can be imposed at various times during a single wave to achieve this goal. By mapping out the effect of different combinations of interventions on the transmission rate, we pave the way for coupling our agent-based model with advanced feedback control.

**Keywords**-epidemic models, agent-based models

## I. INTRODUCTION

This work is a PhD research summary, and [1] accepted conference article is its basis. The COVID-19 pandemic transformed certain parts of our lives fundamentally [2]. It also showed more work is needed to be done to be ready for potential, similar, future pandemic events. Many countries have tackled the pandemic differently, therefore their success rates were - in some cases - significantly different, even from one wave to another [3]. A delicate balance had to be maintained, to minimize the casualties and the number of people hospitalised due to serious symptoms while not damaging the society and economy significantly. This turned out to be a very difficult challenge which led to the varying success rates of pandemic response. Such events can be controlled with bottom-up and top-down approaches. The so-called bottom-up approaches are about developing the right vaccines to treat/prevent the disease and also the accurate testing method which helps to detect who has already been infected. The top-down approaches target studying the event on a phenomenological level to be able to predict certain pandemic trajectories and even shift them towards a mild wave.

To tackle this issue, we have developed PanSim [4], an agent-based simulation model, to address the issue of simulation on a human (agent) level. Agent-based models have agents as their fundamental components, and these agents have their own states, dynamics and drives in predefined state space. This discrete and stochastic type of modelling serves as a simple quantitative description of the real world by only taking the most important aspects of the issue to be tackled into account.

Our ability to use agent-based models efficiently for pandemic simulation lies in their inner dynamics, the possible

states and state transitions of the agents, which is an alternative to the traditional ordinary differential equations-based (ODE-based) methods. On a microscopic level, the agent-based model will significantly differ from the outputs of the traditional, phenomenological models, but on a statistical level, its behaviour (or rather the expected value of its behaviour) should converge to theirs.

PanSim closely models the city of Szeged, having a population of about 180.000 people, to simulate the conditions in Szeged, and the spread of the virus in this case. It has been thoroughly validated on measurement data [4]. The specific data structures inside the simulator only include the interactions of agents and their given state, but the simulator can compute the number of agents in each state, therefore it can give the required phenomenological descriptors of an ODE model, which is how the connection between the phenomenological and stochastic modelling approach can be made.

In this work, we would like to take the first steps toward connecting these two approaches, by quantifying the effects of NPIs on the spread of the disease, and by showing how multiple restrictions interact with each other in further reducing transmission

## REFERENCES

- [1] G. Horváth, I. Reguly, and G. Szederkényi, "Quantifying and comparing the impact of combinations of non-pharmaceutical interventions on the spread of covid-19," *Accepted to MED 2023 conference*, 2023.
- [2] I. Chakraborty and P. Maity, "COVID-19 outbreak: Migration, effects on society, global environment and prevention," *Science of The Total Environment*, vol. 728, p. 138882, aug 2020.
- [3] F. Cascini, G. Failla, C. Gobbi, E. Pallini, J. Hui, W. Luxi, L. Villani, W. Quentin, S. Boccia, and W. Ricciardi, "A cross-country comparison of covid-19 containment measures and their effects on the epidemic curves," *BMC Public Health*, vol. 22, sep 2022.
- [4] I. Z. Reguly, D. Csercsik, J. Juhász, K. Tornai, Z. Bujtár, G. Horváth, B. Keömley-Horváth, T. Kós, G. Cserey, K. Iván, S. Pongor, G. Szederkényi, G. Röst, and A. Csikász-Nagy, "Microsimulation based quantitative analysis of covid-19 management strategies," *PLOS Computational Biology*, vol. 18, pp. 1–14, 01 2022.

# Remote Cardio-Respiratory Monitoring of Neonate Rats under Asphyxia with Combined Photo- and Speckleplethysmography

Imre Gergely JÁNOKI

(Supervisor: Péter FÖLDESZ)

Pázmány Péter Catholic University, Faculty of Information Technology and Bionics

50/a Práter street, 1083 Budapest, Hungary

janoki.imre.gergely@itk.ppke.hu

**Abstract**—In this article a complete system for remote, non-contact monitoring of the vital signs of neonate rats during an asphyxia scenario is described. These rats are used as model animals for the investigation of neonatal asphyxia-induced conditions and treatments, and the task to keep the model animals alive and in similar condition are not yet solved. The method uses a combination of remote photoplethysmography and laser speckle contrast imaging to obtain and monitor the heart rate and breath rate of the rats, as we found that the accuracy and quality of these are heavily affected by the heart rate, ultimately enabling a better measurement over the wide range of such physiological conditions. The validation of our approach was done during an inhalational anesthesia and asphyxia.

**Keywords**—laser speckle contrast imaging, non-contact vital sign monitoring, photoplethysmography, speckle plethysmography, asphyxia

## I. INTRODUCTION

The literature is sparse in the field of vital sign monitoring of rats and similar model animals, especially in an asphyxia scenario, for which the monitoring of the model rodents for their survival is needed. Studies suggest that for heart rate extraction, photoplethysmography (PPG) and speckleplethysmography (SPG) yield similar results [1], even showing some advantages, such as a better signal-to-noise ratio of SPG [2]. At the same time the classical methods for respiration extraction often use optical flow methods, however the large homogeneous surface of the rats poses a disadvantage as there are less regions for breath information extraction, being salient points and the edges of the trunk.

## II. METHODS

The bases of laser speckle contrast imaging [3], [4] is using a coherent laser light source, which scatters on a surface generating an amplification-attenuation pattern from the superposition of the light. During the exposure of a camera - among several other factors -, the speckle pattern decorrelates if the scatterers move. This way, a correlation between contrast and flow speed can be estimated.

We have created a measurement system of an RGB and a monochrome camera with a thermally stabilized laser illumination for laser speckle contrast imaging. The proposed method for the respiration rate and the heart rate extraction creates a segmentation of the animal, followed by contrast and compensated perfusion calculation, then peak detection and envelope extraction is performed with normalization, and finally the calculation of respiration rate, and in the case of

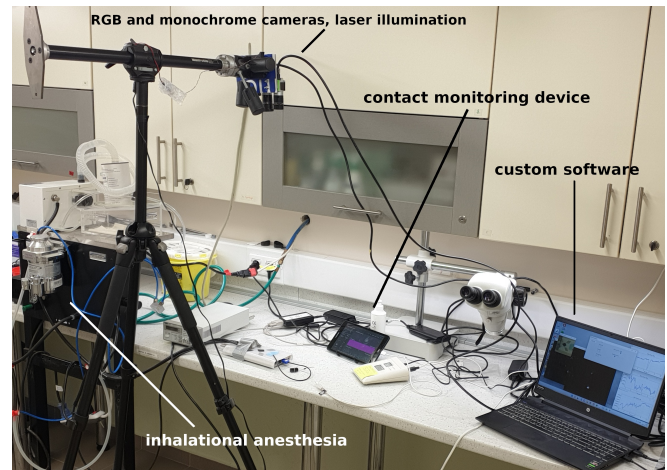


Fig. 1. Monitoring setup for simultaneous ECG, PPG and SPG measurements of an anesthetized rat model animal.

heart rate, a continuous 1-D wavelet transformation and weighting with the scalogram of the final normalized respiratory waveform is also performed with a final step of maximum amplitude frequency search.

We have performed experiments to validate our method in a controlled scenario with an anesthetized animal using a contact monitor device.

## ACKNOWLEDGEMENTS

The author would like to express gratitude to Máté SIKET, Ádám NAGY, Hanga KELEMEN, Kornél DEMETER, Éva MIKICS, Ákos ZARÁNDY and Péter FÖLDESZ.

## REFERENCES

- [1] J. Herranz Olazábal, F. Wieringa, E. Hermeling, and C. Van Hoof, "Camera-Derived Photoplethysmography (rPPG) and Speckle Plethysmography (rSPG): Comparing Reflective and Transmissive Mode at Various Integration Times Using LEDs and Lasers," *Sensors*, vol. 22, p. 6059, Jan. 2022. Number: 16 Publisher: Multidisciplinary Digital Publishing Institute.
- [2] P. V. Rouast, M. T. Adam, R. Chiong, D. Cornforth, and E. Lux, "Remote heart rate measurement using low-cost rgb face video: a technical literature review," *Frontiers of Computer Science*, vol. 12, pp. 858–872, 2018.
- [3] R. Bonner and R. Nossal, "Model for laser doppler measurements of blood flow in tissue," *Applied Optics*, vol. 20, no. 12, pp. 2097–2107, 1981.
- [4] A. Fercher and J. Briers, "Flow visualization by means of single-exposure speckle photography," *Optics Communications*, vol. 37, no. 5, pp. 326–330, 1981.



# Development of a soft resistive sensor to measure the arterial blood pressure waveform

Rizal MAULANA

(Supervisor: György CSEREY)

Pázmány Péter Catholic University, Faculty of Information Technology and Bionics

50/a Práter street, 1083 Budapest, Hungary

rizal.maulana@itk.ppke.hu

**Abstract**—This research aims to develop a noninvasive continuous blood pressure measurement system. The component of the proposed system consists of a resistive yarn, base material, an applanation object and a covering layer integrated as a wristband for measuring the arterial blood pressure waveform on the radial artery. The designed system is still in the development stage. Several parameters related to sensor sensitivity were evaluated in this research. Even though the system has not acquired a stable arterial blood pressure waveform, it has been able to detect a pressure signal with a frequency corresponding to the heartbeat.

**Keywords**-arterial blood pressure; continuous; non-invasive; resistive yarn

## I. SUMMARY

Continuous blood pressure monitoring is essential, especially for hypertension patients. Medical professionals can prevent unanticipated complications by providing patients with the appropriate treatment if they are aware of sudden changes in blood pressure directly [1]. Research on continuous blood pressure measurement has been conducted by Choi et al. [2]. This study determined blood pressure by analyzing an electrocardiogram and a photoplethysmogram signal. The solution offered in this research becomes less applicable if implemented as a home health monitoring device since measuring blood pressure requires two sensor channels.

A single-channel pressure sensor can measure pressure directly at one of the accessible arterial pulse sites. This pressure measuring technique tries to measure the pressure pulse wave (PPW), which represents variations in pressure in the blood vessels of the arteries. A flexible material like a resistive pressure sensor can measure PPW. Resistive pressure sensors are available in the form of flexible sheets [3], textiles [4] or yarn. Resistive pressure sensors in the form of yarn are commonly referred to as resistive yarn. Resistive yarn is a yarn whose resistance value varies under mechanical tension. In response to the need for a non-invasive device capable of continuously measuring blood pressure, we propose an arterial blood pressure (ABP) waveform measuring system that employs resistive yarn as its primary component. The developed technology is integrated into a wristband to measure blood pressure in the radial artery on the wrist.

The system's primary component is the sensing component, which detects changes in radial artery pressure. The sensing component comprises resistive yarn woven in a specific pattern onto the base material. The pressure generated by the radial artery is extremely low and difficult to detect directly by the sensing component. This pressure can be increased by adding an applanation object. In addition, there are several additional components, including a solid cover that surrounds the base material and a covering layer designed to increase the sensor's

sensitivity. The integration of all system components in the form of a wristband is shown in Fig 1.

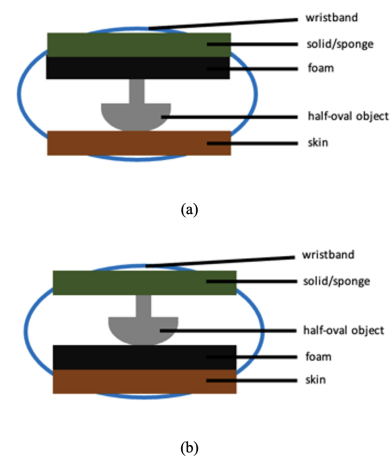


Fig. 1. Integration of all system components in the form of a wristband. (a) The applanation object is placed below the sensing component. (b) The applanation object is placed above the sensing component

The experiment in this study is intended to determine the best sensing and additional component configuration for ABP waveform measurement. Based on test results, sensing components with tight stitch patterns and short yarn are more sensitive. While for other configurations, using applanation objects with additional block objects, placing applanation objects above the sensing component, and using a covering layer made of sponges all offer better sensitivity than each comparison configuration.

## ACKNOWLEDGEMENTS

The author would like to thank Prof. György Cserey and Dr. Sándor Földi for their significant advice on the development of this research.

## REFERENCES

- [1] S. Földi, T. Horváth, F. Zieger, P. Sotonyi, and G. Cserey, "A novel non-invasive blood pressure waveform measuring system compared to millar applanation tonometry," *Journal of Clinical Monitoring and Computing*, vol. 32, pp. 717-727, 2018.
- [2] Y. Choi, Q. Zhang, and S. Ko, "Noninvasive cuffless blood pressure estimation using pulse transit time and hilbert-huang transform," *Computer and Electrical Engineering*, vol. 39, pp. 103-111, 2013.
- [3] N. Luo, W. Dai, C. Li, Z. Zhou, L. Lu, C.C.Y. Poon, S.C. Chen, Y. Zhang, and N. Zhao, "Flexible piezoresistive sensor patch enabling ultralow power cuffless blood pressure measurement," *Advanced Functional Materials*, vol. 26, pp. 1178,1187, 2015.
- [4] N.A. Choudhry, A. Rasheed, S. Ahmad, L. Arnold, and L. Wang, "Design, development and characterization of textile stitch-based piezoresistive sensors for wearable monitoring," *IEEE Sensors Journal*, vol. 20, pp. 10485-10494, 2020

# A torque measurement process to compare biological and exosuit assisted wrist strength

Katalin SCHÄFFER

(Supervisors: György CSEREY, Miklós KOLLER)

Pázmány Péter Catholic University, Faculty of Information Technology and Bionics

50/a Práter street, 1083 Budapest, Hungary

[schaffer.katalin@itk.ppke.hu](mailto:schaffer.katalin@itk.ppke.hu)

**Abstract**—There are an increasing number of soft upper limb wearable devices, also called exosuits, that based on different designs but serve a similar purpose. The lack of detailed evaluation and unified metrics make it difficult to compare the existing solutions and select the best design for a specific application. The 'strength' of a wearable device can be evaluated by measuring the static torque applied to the actuated joint. In this paper we introduce a torque measurement procedure for measuring the torque applied by an exosuit to the wrist. The setup is also used to collect biological peak torque data. The biological torque can serve as the reference to examine if the exosuit can provide full assistance over the range of movement. Also we will discuss what are the limitations of using the presented method as unified metric to evaluate the performance of a wrist exosuit.

**Keywords**—wearable devices; torque measurement; biological wrist torque

## I. INTRODUCTION

Over the last decade soft wearable devices, also called soft exosuits, gained popularity in the research community. Although there are a large variety of exosuit designs that aim to provide assistance of the upper limb [1], the evaluation of these devices are often over-viewed and not unified. Besides the design and prototyping, it is an important part of the exosuit development process to explore the benefits of the design and provide evaluation of the performance of the exosuit. Even if some of these devices have a specific application, there are some general properties that the exosuit has such as range of movement, speed or response time and strength. We consider the measurement of the peak torque applied to the actuated joint as one of the evaluation methods that can provide a quantitative measure of the strength of the device. Collected biological torque data helps to interpret the measurement results by comparing it with the applied torque when the device passively moves the wrist.

## II. RESULTS

Through our research work we explored the possible ways to acquire the biological data including of relying on data from the literature [2] and designing our own measurement setup. The results of ergonomics studies show that the measured wrist torque around one axis depend on the exact position of the upper arm [3] which indicates that the specific design of the used measurement setup effects the measured torque. For this reason the same measurement setup should be used to collect biological reference data and measure the torque applied by the wrist exosuit.

We introduced a torque measurement setup design which is based on measuring the linear force perpendicular to the line of the hand. This arrangement allowed us to use simple and low cost force sensors and it was used to measure both



Fig. 1. The torque measurement setup for collecting biological and exosuit assisted wrist torque data. The forearm plate and the hand plate helps to securely fix the position of the lower arm. As the hand plate rotates in a given joint angle by connecting the plate to a force sensor (MARK10 M3-100) positioned perpendicularly to the plate and fixed to the base plate along the circular groove.

biological and exosuit assisted wrist torque. By comparing the measured torques the fPAM actuated exosuit proved to provide better assistive force over the extension angles and gradually decreasing torque when the wrist was flexed. In the current state the exosuit can be used to provide small assistive torques. This can be utilized to reduce the physical strain on workers doing demanding and repetitive physical tasks. Our future work aims to improve the exosuit design to achieve higher assistive torques over the whole flexion/extension range. This include the improvement of the mounting methods to reduce fabric stretching and increasing the contraction ratio of the used artificial muscle.

## ACKNOWLEDGEMENTS

The research was conducted in the IRIS Lab of the University of Notre Dame. The authors acknowledge the support of the National Research, Development and Innovation Office – NKFIH – through grant no. TKP2021-NKTA-66.

## REFERENCES

- [1] C. Thalman and P. Artemiadis, "A review of soft wearable robots that provide active assistance: Trends, common actuation methods, fabrication, and applications," *Wearable Technologies*, vol. 1, p. e3, 2020.
- [2] M. Hallbeck, "Flexion and extension forces generated by wrist-dedicated muscles over the range of motion," *Applied ergonomics*, vol. 25, no. 6, pp. 379–385, 1994.
- [3] K. Plewa, J. R. Potvin, and J. P. Dickey, "Wrist rotations about one or two axes affect maximum wrist strength," *Applied ergonomics*, vol. 53, pp. 152–160, 2016.

# Utilizing the OP2 Domain Specific Library for Adaptive Multi-Precision Computing

Bálint SIKLÓSI

(Supervisor: István REGULY)

Pázmány Péter Catholic University, Faculty of Information Technology and Bionics

50/a Práter street, 1083 Budapest, Hungary

siklosi.balint@itk.ppke.hu

## ABSTRACT

This study explores the utilization of the OP2 domain-specific library for adaptive multi-precision computing. With the advent of exascale computing systems, the need for efficient and accurate simulations has become increasingly crucial. Mixed precision computing has emerged as a promising approach to address the challenges associated with these systems. This paper investigates the application of adaptive precision reduction techniques using the OP2 library and demonstrates the potential of achieving significant speedup without sacrificing simulation accuracy.

## I. INTRODUCTION

Exascale computing systems offer tremendous computational power but pose challenges in terms of memory capacity and energy consumption. Mixed precision computing has shown promise in addressing these challenges by leveraging lower precision data formats for certain computations. This study focuses on the utilization of adaptive precision reduction techniques enabled by the OP2 domain-specific library [1]. By dynamically adjusting the precision of computations based on accuracy requirements, the potential for achieving speedup without accuracy loss can be explored.

## II. MATERIALS AND METHODS

The IEEE-754 standard for representing floating point numbers serves as the foundation for mixed precision computing. Previous research has demonstrated the efficacy of mixed precision in various applications, such as neural network training and automatic recognition algorithms. The OP2 library, designed for parallel computations on unstructured meshes, offers a powerful tool for achieving high-performance simulations. In this study, we employ code generation techniques using OP2 for mixed execution and an adaptive precision choice algorithm.

## III. EXPERIMENTAL SETUP

To evaluate the effectiveness of adaptive multi-precision computing, we employed the Airfoil mini-application as a benchmark. The baseline tests were conducted by comparing simulations using single-precision (FP32) and double-precision (FP64) floating point formats. The hardware specifications of the tested systems, including CPU and memory configurations, are provided.

FP32	FP64	Time (s)	Speedup
180k	0	2389.17	1.32x
0	180k	3142.25	1x
34.4k	145.6k	3007.94	1.04x
60k	0	797.27	1.31x
0	60k	1045.76	1x
34.4k	25.6k	904	1.16x

TABLE I

AIRFOIL RUNTIMES ON CPUS COMPARED TO ITERATION NUMBERS IN DIFFERENT PRECISIONS. PRECISION GOALS ARE 1.6E-16 AND 1E-10. SPEEDUP COMPARED TO FULL FP64 RUN.

FP32	FP64	Time (s)	Speedup
180k	0	255.73	1.51x
0	180k	387.25	1x
33.7k	146.3k	362.81	1.07x
60k	0	85.04	1.52x
0	60k	129.04	1x
35.8k	24.2k	102.88	1.25x

TABLE II

AIRFOIL RUNTIMES ON GPUS COMPARED TO ITERATION NUMBERS IN DIFFERENT PRECISIONS. PRECISION GOALS ARE 1.6E-16 AND 1E-10. SPEEDUP COMPARED TO FULL FP64 RUN

## IV. RESULTS AND DISCUSSION

The experimental results demonstrate the effectiveness of adaptive multi-precision computing using the OP2 library in achieving significant speedup without accuracy loss. By dynamically adjusting the precision based on local accuracy requirements, we observed a speedup of 4.27% to 20.28% compared to the baseline double-precision simulations. The results indicate that precision reduction can be applied to specific computations without compromising the overall simulation fidelity. Tables I and II present the speedup achieved across different simulation scenarios.

## V. CONCLUSION

In this study, we have investigated the utilization of adaptive multi-precision computing using the OP2 library. By intelligently selecting data for precision reduction, significant speedup without accuracy loss was achieved. The experiments conducted on the Airfoil mini-application highlight the potential of adaptive multi-precision computing in the context of exascale computing systems. Future research can explore additional applications and optimizations in the realm of adaptive precision reduction techniques to further enhance simulation performance and energy efficiency.

## REFERENCES

- [1] "OP-DSL: The Oxford Parallel Domain Specific Languages," 2015. <https://op-dsl.github.io>.

# Time symmetric tracking of yeast cells using convolutional neural networks

Gergely SZABÓ

(Supervisor: András HORVÁTH)

Pázmány Péter Catholic University, Faculty of Information Technology and Bionics

50/a Práter street, 1083 Budapest, Hungary

szabo.gergely@itk.ppke.hu

**Abstract**—Tracking of live cells in video microscopy remains a challenging task for object tracking methods. Recent attempts to integrate deep-learning frameworks have relied on consecutive frame tracking on an architectural level or other systematic limitations. To overcome this, we developed a new deep-learning method that tracks cells based on a large temporal neighborhood, without restricting it to consecutive frames. Our approach enables learning motion patterns without assumptions and can handle an increased number of video frames with artifacts utilizing skip-connections. The aim of this short progress report is to give insight for the considerations and the principal from a high-level perspective.

## I. BACKGROUND AND MOTIVATION

In recent years, many cell tracking softwares and libraries started the adoption of machine learning based methods, particularly convolutional neural networks (CNNs). While some tools focus on high-quality segmentation using deep learning, they frequently rely on classical methods for tracking, such as the Kalman filter or bipartite graph matching. Other tools employ deep learning either in an end-to-end manner or combined with segmentation, but almost all currently known methods rely on frame-by-frame identity matching, overlooking valuable information in the temporal neighborhood.

To overcome these limitations, we developed a comprehensive tracking pipeline that separates segmentation and tracking stages. Our method leverages deep learning for both stages, utilizing the temporal neighborhood for prediction and enabling frame skipping. Our tracking approach improves robustness and minimizes methodological assumptions by employing metrics solely between different predictions for the same cell on the same frame. [1][2]

## II. INSTANCE SEGMENTATION

While further advancements are still possible in the field of instance segmentation of living cells especially in case of niche applications, the introduction of robust Mask R-CNN-based [3] solutions has enabled high-quality segmentation in most scenarios. Thus, we opted against developing a new architecture, instead we used the state-of-the-art Detectron2 environment. Our most successful model is based on a Mask R-CNN architecture with a ResNet-50 feature pyramid network backbone, pretrained on the COCO instance segmentation dataset. During training, we incorporated biologically inspired artificial data augmentation strategies, leveraging both the built-in transformations of the Detectron2 environment and the Albumentations library. Overall, the instance segmentation phase showed great performance, as confirmed by expert evaluation and quantitative metrics.

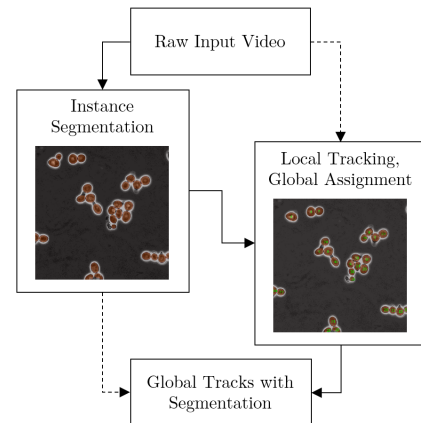


Fig. 1. A high-level data flow diagram of the designed pipeline. For the showcased sample both segmentation and tracking turned out to be flawless.

## III. LOCAL AND GLOBAL TRACKING

Our objective in tracking was to create a novel pipeline that reduces the reliance on systematic assumptions compared to existing solutions. To achieve this, we designed our pipeline based on the insight that incorporating all available information from the local temporal neighborhood can enhance cell tracking. For the temporally local tracking of individual cell instances, we employed the DeepLabV3+ [4] architecture. Subsequently, we optimized the assignment and combination of local tracks using similarity metrics that specifically compare predictions for the same temporal position. The tracking phase also demonstrated great performance, as validated through expert evaluation and quantitative metrics.

## REFERENCES

- [1] Dietler, Nicola, et al. "A convolutional neural network segments yeast microscopy images with high accuracy." *Nature communications* 11.1 (2020): 5723.
- [2] Chen, Yuqian, et al. "CellTrack R-CNN: A novel end-to-end deep neural network for cell segmentation and tracking in microscopy images." 2021 IEEE 18th International Symposium on Biomedical Imaging (ISBI). IEEE, 2021.
- [3] He, Kaiming, et al. "Mask r-cnn." *Proceedings of the IEEE international conference on computer vision*. 2017.
- [4] Chen, Liang-Chieh, et al. "Encoder-decoder with atrous separable convolution for semantic image segmentation." *Proceedings of the European conference on computer vision (ECCV)*. 2018.

**PROGRAM 3**  
**FEASIBILITY OF ELECTRONIC AND OPTICAL**  
**DEVICES, MOLECULAR AND**  
**NANOTECHNOLOGIES,**  
**NANO-ARCHITECTURES, NANOBIONIC**  
**DIAGNOSTIC AND THERAPEUTIC TOOLS**

Head: Árpád CSURGAY

# A Design and measurement of a compact retrodirective array

András ESZES

(Supervisor: Zsolt SZABÓ)

Pázmány Péter Catholic University, Faculty of Information Technology and Bionics

50/a Práter street, 1083 Budapest, Hungary

esz.es.andras@itk.ppke.hu

**Abstract**—Retrodirective structures have the exceptional property, that they reflecting back the incident wave to the direction where the wave is coming from. They have increasing importance owing to the fast improvement of RFID technologies. Retrodirective phenomena can be obtained with the utilization of classical antenna array theory, based on optical lenses or based on metamaterials.

In this manuscript design steps, full wave simulation results and measurement results have been presented for a compact Van Atta array, that have designed to operate at 9.75 GHz with 100 MHz operation bandwidth. Minkowski fractal insets have been utilized for the 8 radiator elements in order to achieve considerable size reduction. The radiator elements have been excited with microstrip lines via H shaped apertures. Then the designed structure have been fabricated with PCB etching. The designed and measured Van Atta array due to its compact size can be placed on UAV's or road lanes.

**Keywords**—Van Atta array, Retrodirective surface, Minkowski fractal, Aperture coupled patch antenna

## I. DESIGN

During design closed form equations have been utilized, then Ansys-HFSS and CST-MWS full wave numerical solvers have been used in order to obtain the final design.

In the initial design the components of the array been modeled and sized separately. The interconnection lines were initially designed with closed form equations, then they have fine tuned to achieve a more optimal monostatic radar cross section of the overall array. The performance of the complete structure have been checked by exciting the array with a plane wave.

## II. MEASUREMENT RESULTS

The designed structure have been fabricated with conventional PCB etching technique. The designed structure based on Isola 680-345 substrate and the different layers have been bonded together with the application of Isola Tera 3313 MT45 prepreg material. The designed structure have been measured in an anechoic chamber. The efficiency of the structure have been checked with the help of the monostatic RCS response of the structure. The measurement have preformed with 4 units and 10 units of arrays. The measurement have been carried out with continuous RF wave source, therefore considerable mutual coupling have been experienced between the transmitter and receiver antennas, hence deteriorating the dynamic range of the measurement setup. In order to mitigate this negative effect 10 array units have been utilized during the measurements.

## III. CONCLUSION

A compact Van Atta array have been designed and measured. To the best of the author's knowledge this structure is

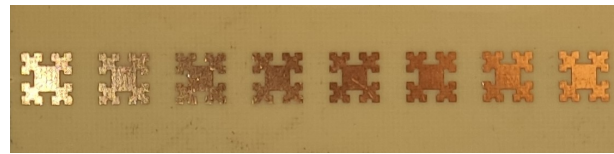


Fig. 1. Fabricated Van Atta array-top face

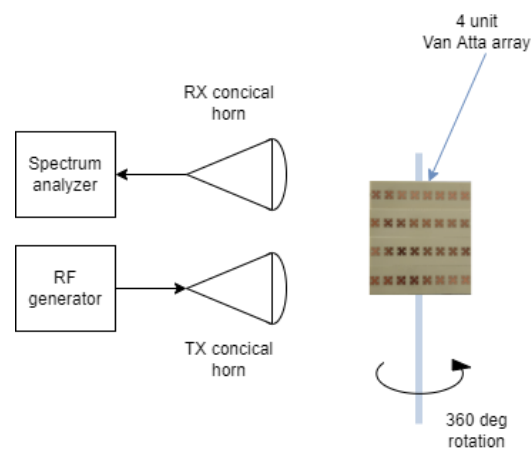


Fig. 2. Van Atta array measurement

the first VA array that utilizes Minkowski fractals as radiator elements.

## REFERENCES

- [1] Atta, L. C. V., "Electromagnetic reflector," U.S. Patent, Vol. 2908, 1959."
- [2] M. Kalaagi and D. Seetharamdoo, "Retrodirective metasurface operating simultaneously at multiple incident angles," 12th European Conference on Antennas and Propagation (EuCAP 2018), London, 2018, pp. 1-5, doi: 10.1049/cp.2018.0545.
- [3] Alharbi, M.; Alyahya, M.A.; Ramalingam, S.; Modi, A.Y.; Balanis, C.A.; Birtcher, C.R. Metasurfaces for Reconfiguration of Multi-Polarization Antennas and Van Atta Reflector Arrays. *Electronics* 2020, 9, 1262. <https://doi.org/10.3390/electronics9081262>
- [4] Nanfang Yu et. al. "Light Propagation with Phase Discontinuities: Generalized Laws of Reflection and Refraction" *Science* 21 Oct 2011: Vol. 334, Issue 6054, pp. 333-337 DOI: 10.1126/science.1210713
- [5] Alharbi, M.; Alyahya, M.A.; Ramalingam, S.; Modi, A.Y.; Balanis, C.A.; Birtcher, C.R. Metasurfaces for Reconfiguration of Multi-Polarization Antennas and Van Atta Reflector Arrays. *Electronics* 2020, 9, 1262. <https://doi.org/10.3390/electronics9081262>
- [6] S. Gupta, A. Parsa, E. Perret, R. V. Snyder, R. J. Wenzel and C. Caloz, "Group-Delay Engineered Noncommensurate Transmission Line All-Pass Network for Analog Signal Processing," in *IEEE Transactions on Microwave Theory and Techniques*, vol. 58, no. 9, pp. 2392-2407, Sept. 2010, doi: 10.1109/TMTT.2010.2058933.
- [7] Y. Liu, K. Li, Y. Jia, Y. Hao, S. Gong and Y. J. Guo, "Wideband RCS Reduction of a Slot Array Antenna Using Polarization Conversion Metasurfaces," in *IEEE Transactions on Antennas and Propagation*, vol. 64, no. 1, pp. 326-331, Jan. 2016, doi: 10.1109/TAP.2015.2497352.

# Modeling of VO<sub>2</sub> oscillator-based devices

Mitra MOAYED

(Supervisor: György CSABA)

Pázmány Péter Catholic University, Faculty of Information Technology and Bionics

50/a Práter street, 1083 Budapest, Hungary

Mitra.moayed@itk.ppke.hu

**Abstract**—this paper presents a focused study on the modeling of VO<sub>2</sub> oscillator-based devices and its properties. Vanadium dioxide (VO<sub>2</sub>) has attracted significant attention due to its unique properties, particularly the metal-insulator transition (MIT) near room temperature. VO<sub>2</sub> oscillators, which exploit the rapid change in resistivity during the MIT, hold great promise for various electronic applications. This paper specifically addresses the fundamental principles, modeling techniques, and potential applications of VO<sub>2</sub> oscillators. By adopting a systematic approach, valuable insights into the design and optimization of VO<sub>2</sub>-based devices for enhanced performance are provided. Moreover, the challenges associated with modeling and future research directions in this specific context are discussed.

**Keywords:**VO<sub>2</sub> Oscillator, ONN, oscillator-based computing.

## I. DISCUSSION

Vanadium dioxide (VO<sub>2</sub>) is a highly promising material due to its phase transition behavior near room temperature, which enables the development of VO<sub>2</sub> oscillator-based devices. These devices exhibit remarkable changes in their electrical and optical properties, making them valuable for a wide range of applications, including communication, sensing, and energy harvesting. To ensure reliable performance and optimize the operation of VO<sub>2</sub> oscillators, careful attention must be given to fabrication, characterization, and modeling techniques. The quality of the VO<sub>2</sub> material, electrode design, and interconnects play crucial roles in achieving desired performance and behavior. Understanding the dynamics of this phase transition is essential for accurately modeling and predicting the behavior of VO<sub>2</sub> oscillators [1]. Neural networks have emerged as effective tools for modeling VO<sub>2</sub> oscillators. By training neural networks with experimental or simulated data, it becomes possible to make accurate predictions about the oscillation behavior based on various input parameters such as temperature and voltage. This neural network-based modeling approach enables a deeper understanding of the complex relationships between variables and facilitates the optimization and design of VO<sub>2</sub> oscillator-based devices. By applying a bias voltage, these devices enter a self-sustained oscillatory state, switching between high and low resistance states. The frequency and stability of the oscillations depend on several factors, including the phase transition temperature, bias voltage, device geometry, material characteristics, and doping. Experimental characterization and modeling techniques are employed to optimize these parameters and achieve the desired oscillation performance [2]. In conclusion, the phase transition of VO<sub>2</sub> and the unique properties it exhibits make it a promising material for the development of VO<sub>2</sub> oscillator-based devices. Through fabrication, characterization, and modeling approaches, these devices can be optimized for various applications, opening up new possibilities in electronic systems.

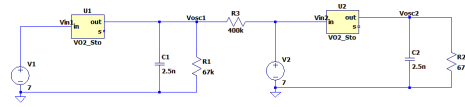


Fig. 1. Circuit scheme of two coupled oscillators for out-of-phase

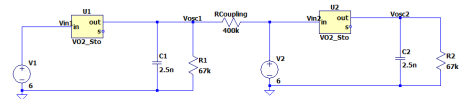


Fig. 2. Circuit scheme of two coupled oscillators for in-phase

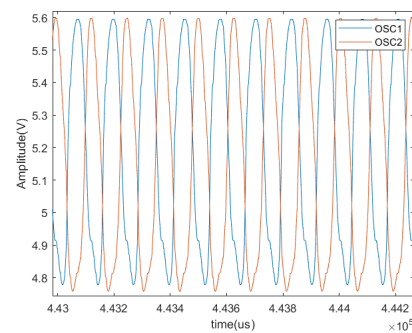


Fig. 3. Output waveform from Fig.6(Out-of-phase)

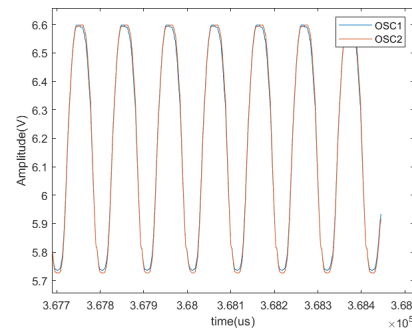


Fig. 4. Output waveform from Fig.7(in-phase)

The phase configuration (in-phase or out-of-phase) of two-coupled oscillators, as shown in figures (1, 2, 3, 4), can be programmed by changing the value of the Voltage (V1).

## REFERENCES

- [1] Csaba, Gy., and Porod, W. (2020). Coupled oscillators for computing: a review and perspective. *Appl. Phys. Rev.* 7:011302. doi: 10.1063/1.5120412. Clarendon, 1892, pp.68–73.
- [2] Jean-Paul Pouget. Basic aspects of the metal–insulator transition in vanadium dioxide VO<sub>2</sub> – a critical review. *Comptes Rendus. Physique*, Volume 22 (2021) no. 1, pp. 37-87. doi: 10.5802/crphys.74.

# Processing of time-independent and time-dependent signals using Oscillatory Neural Networks

Tamás RUDNER

(Supervisor: György CSABA)

Pázmány Péter Catholic University, Faculty of Information Technology and Bionics

50/a Práter street, 1083 Budapest, Hungary

rudner.tamas@itk.ppke.hu

**Abstract**—There are several proposed architectures which are utilising the advantages of physics. Our research is aimed at using coupled oscillators to perform computation. These oscillators can be used as various devices, such as logic gates or even as Hopfield networks. The computation is driven by the couplings between the oscillators but the setting of these couplings is not trivial to solve the tasks, so in order to figuring out these values, we use machine learning to learn the parameters of the system to make the coupled oscillatory architecture solve the problems at hand. In the results section, we show that we can set physical parameters for a coupled oscillator system to solve multi-class prediction problems on the MNIST datasets. Our results demonstrate that machine learning yields to higher circuit performance compared to standard ways of training the network such a fully connected neural network. Also, to show that not even time-independent, static data can be processed using these oscillatory neural networks, like images, we are experimenting with the processing of time-dependent data, such as waveform generation and vowel recognition.

**Keywords**—coupled oscillators, machine learning, circuit design, ground state computing, classification, time-dependent data processing

## I. INTRODUCTION

Today the need for new computing paradigms is highly sought after as we are approaching the limits of the conventional computational architectures [1]. To solve this problem, we can leverage physics to do computations for us which might be advantageous in the future [2].

## II. COUPLED OSCILLATORY CIRCUITS

The mathematical formulation of Ring-oscillator based coupled oscillatory circuits' dynamics contains three parts, namely the internal dynamics of the oscillators; the external dynamics due to the input current generators and coupling dynamics. The ODE derived for these architectures is the following:

$$\frac{dV}{dt} = \frac{1}{RC} \mathbf{A}' (f(\mathbf{P}_\pi V) - V) + \frac{1}{C} \mathbf{B}' u + \frac{1}{R_c C} \mathbf{C}' V, \quad (1)$$

Unfortunately the task of setting the values of the primed matrices is hard for complex problems, so we must use machine learning to train these parameters by simulating the ODEs then using backpropagation through time algorithm to change the values according to a loss function.

## REFERENCES

- [1] G. E. Moore, "Progress in digital integrated electronics [technical literature, copyright 1975 ieee. reprinted, with permission. technical digest. international electron devices meeting, ieee, 1975, pp. 11-13.]," *IEEE Solid-State Circuits Society Newsletter*, vol. 11, pp. 36–37, 09 2006.
- [2] K. Zuse, "The computing universe," *Int. J. Theor. Phys.*, vol. 21, pp. 589–600, 1982.

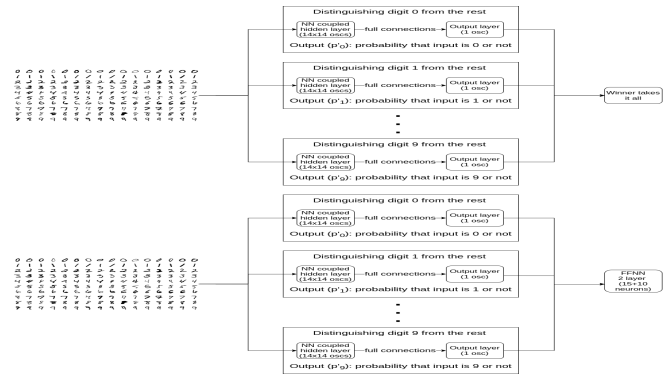


Fig. 1: Here it can be seen the two of the three tested architecture for the time-independent MNIST classification. Both consists the individually trained, nearest neighbour connected subnetworks which were designed to distinguish between a single class and the rest of the classes using binary cross-entropy loss function. The top block diagram describes the algorithm where to pick the prediction we took the maximum of individual network output probabilities. The more sophisticated version can be seen on the bottom block diagram. Here we took the output probabilities of the individual classifiers and feed them as inputs to a small, regular FFNN and trained it as it were a 10-class classification problem using binary cross-entropy.

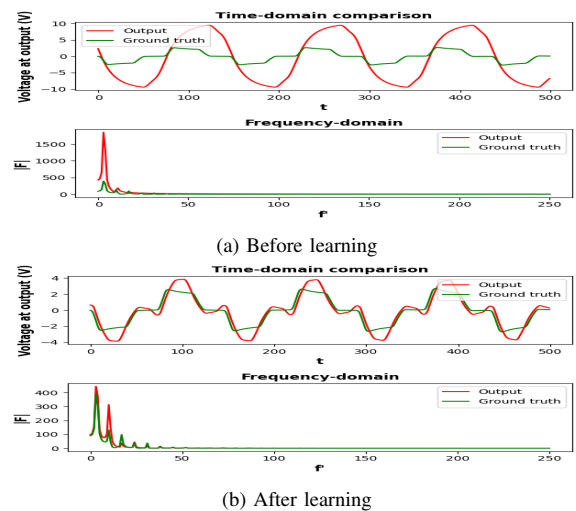


Fig. 2: On a) we can see the initial output of the sum of the oscillator's and the ground truth voltage in time domain and frequency domain as well. On b) we can see that the convergence took place and we managed to qualitatively close both in time and frequency domain



**PROGRAM 4**  
**HUMAN LANGUAGE TECHNOLOGIES,**  
**ARTIFICIAL UNDERSTANDING,**  
**TELEPRESENCE, COMMUNICATION**

Head: Gábor PRÓSZÉKY

# Gathering dataset for abstractive question answering using ChatGPT

Kamran IBIYEV

(Supervisor: Gábor PRÓSZÉKY)

Pázmány Péter Catholic University, Faculty of Information Technology and Bionics

50/a Práter street, 1083 Budapest, Hungary

ibiyev.kamran@itk.ppke.hu

**Abstract**—Because of improvements in learning technologies, artificial intelligence communities have focused primarily on question-answering. Our goal is to create a Question Answering dataset for the Azerbaijani language and to train various models on it. The creation of the dataset will be helped by a Question Generation model. We use a model that is trained on multilingual data and see how it performs. We use ChatGPT tool for creating the questions and answers based on the provided paragraphs.

**Keywords**—keyword; Question Answering; ChatGPT, M-BERT; Question Generation; Question analysis; Natural language processing

## I. INTRODUCTION

Question answering (QA) is a difficult task in natural language understanding. Grasping the question and the environment in which it is formed is one of the most important aspects of QA. The dynamic character of natural languages has made quality assurance difficult [1]. With the development of large-scale language models, conversational AI has made significant strides forward. OpenAI’s ChatGPT is one such model that has garnered significant attention for its capacity to generate coherent and contextually pertinent responses in conversational settings [2].

## II. LITERATURE REVIEW

Since the 2010s [3], QA has been widely researched, following the success of intelligent QA systems, such as Siri and Watson. ChatGPT is built upon the GPT (Generative Pre-trained Transformer) architecture, which utilizes a transformer-based neural network model. The model is trained using unsupervised learning on a massive corpus of text from the internet, allowing it to learn grammar, factual knowledge, and contextual patterns [2].

## CORPUS ANNOTATION METHOD

In this paper, we will use the Abstractive Question Answering method. Abstractive question answering is a type of quality assurance in which we want the system to generate an abstractive answer that includes all of the knowledge from the chapters necessary to respond to the questions. [4].

In our research instead of the manual question creators, we are using the ChatGPT tool. We provide a paragraph and ask the tool to create 5 questions and their answers based on the provided paragraph. We gather the paragraphs from Wikipedia Featured articles in the Azerbaijani language because it is public and well-written. We will also cover the option that the paragraph does not contain the answer to the asked question. For annotating, I will use the tool implemented by Attila Novak, a member of the Natural Language Processing Group at Pázmány Péter Catholic University, Faculty of Information Technology and Bionics.

## TRAINING THE MODEL

For training our model we will use the Multilingual-MiniLM model. Experimental data show that its monolingual model outperforms state-of-the-art baselines. It preserves over 99 percent accuracy on SQuAD 2.0 and various GLUE benchmark problems, while only employing half of the Transformer parameters and calculations of the instructor model. We also get satisfactory performance using multilingual pre-trained models and deep self-attention distillation. [5] This model also can be trained to generate text. Therefore we can use this model to generate questions.

Model	#Layers	#Hidden	Average
mBERT	12	768	57.7 / 41.6
XLM-15	12	1024	61.6 / 43.5
XLM-R <sub>BASE</sub> †	12	768	62.9 / 45.7
XLM-R <sub>BASE</sub> ‡	12	768	64.9 / 46.9
MINILM <sup>a</sup>	12	384	63.2 / 44.7
MINILM <sup>b</sup> (w/ TA)	6	384	53.7 / 36.6

Source: Adapted from [5]

Fig. 1: Cross-lingual question answering results on MLQA.

In Figure 1, F1 and EM scores are indicated. Results of mBERT and XLM15 are taken from Lewis [6]. † indicates results taken from Conneau [7]. The fine-tuned results of XLM-RBASE are indicated with symbol ‡. MiniLM team used SQuAD 1.1 as training data. It is indicated in Figure 1 that the 12x384 outperforms mBERT and XLM in terms of performance. MINILM 6-layer also delivers promising results.[5]

## REFERENCES

- [1] L. Kodra and E. K. Meçe, “Question answering systems: A review on present developments, challenges and trends,” *International Journal of Advanced Computer Science and Applications*, vol. 8, no. 9, 2017.
- [2] G. M. Currie, “Academic integrity and artificial intelligence: is chatgpt hype, hero or heresy?,” *Seminars in Nuclear Medicine*, 2023.
- [3] L. Yu, K. M. Hermann, P. Blunsom, and S. Pulman, “Deep learning for answer sentence selection,” *arXiv preprint arXiv:1412.1632*, 2014.
- [4] R. Mitra, “An abstractive approach to question answering,” *arXiv preprint arXiv:1711.06238*, 2017.
- [5] W. Wang, F. Wei, L. Dong, H. Bao, N. Yang, and M. Zhou, “Minilm: Deep self-attention distillation for task-agnostic compression of pre-trained transformers,” *Advances in Neural Information Processing Systems*, vol. 33, pp. 5776–5788, 2020.
- [6] P. Lewis, B. Oğuz, R. Rinott, S. Riedel, and H. Schwenk, “Mlqa: Evaluating cross-lingual extractive question answering,” *arXiv preprint arXiv:1910.07475*, 2019.
- [7] A. Conneau, K. Khandelwal, N. Goyal, V. Chaudhary, G. Wenzek, F. Guzmán, E. Grave, M. Ott, L. Zettlemoyer, and V. Stoyanov, “Unsupervised cross-lingual representation learning at scale,” *arXiv preprint arXiv:1911.02116*, 2019.

# Abstractive Arabic text summarization with reinforcement learning

Mram KAHLA

(Supervisors: Gábor PRÓSZÉKY, Zijian Győző YANG)

Pázmány Péter Catholic University, Faculty of Information Technology and Bionics

50/a Práter street, 1083 Budapest, Hungary

kahla.mram@itk.ppke.hu

**Abstract**—In this paper, we present the first work of applying reinforcement learning from human feedback on Arabic to train language models that are better at abstractive summarization. Reinforcement Learning from Human Feedback is a powerful technique that can be used to train Large Language Models to perform a wide range of tasks by providing the Language Models with feedback. The results on the English language show that it is possible to significantly improve summary quality by training a model to optimize for human preferences. The human feedback models outperform much larger supervised models across every dimension of quality.

This study presents the current phase of our research. In our previous research, we created the first corpus in the Arabic language for abstractive summarization "AraSum". The AraSum corpus has been used to fine-tune the mT5 language model for abstractive Arabic text summarization. We ask human annotators to judge and compare the summary quality and implement quality control after providing them with different samples. This step is still in progress. After collecting the comparison data, we will use it to train a reward model which itself will be used as a reward function to optimize a policy using The (PPO) reinforcement learning algorithm.

**Keywords**—Arabic, Abstractive summarization, mT5, human feedback, reinforcement learning

## I. SUMMARY

The aim of our work is to improve the abstractive summarization task for the Arabic language. Particularly train and fine-tune pre-trained language models for an abstractive summarization task.

Using the AraSum corpus which we created previously, two experiments have been conducted [1] and [2]. In both of the experiments, the results demonstrated that most of the models surpassed the models which were considered to be state-of-the-art for abstractive Arabic text summarization at the time they were published.

In the present research, we continue the work on the same NLP task which is the abstractive text summarization task, and apply reinforcement learning to this task for the Arabic language. We will apply reinforcement learning from human feedback to train language models that are better at summarization. The results on the English language show that it is possible to significantly improve summary quality by training a model to optimize for human preferences. The human feedback models outperform much larger supervised models across every dimension of quality as shown in figure 1. The used approach contains 3 main steps.

- **Step 1: Collect demonstration data, train a supervised policy, and send comparisons to humans.**

Humans are provided with references and samples resulting from finetuning a language model and asked to select the best summary of the given samples.

- **Step 2: Collect comparison data, and train a reward model (RM).**

A reward model will be trained using the results from the first step. This reward model will predict the log odds that this summary is the better one, as judged by the human annotators.

- **Step 3: Optimize a policy against the reward model using PPO.**

The output of the RM will be used as a scalar reward. The supervised policy will be fine-tuned to maximize this reward using reinforcement learning, specifically, the policy is Proximal Policy Optimization (PPO) algorithm.

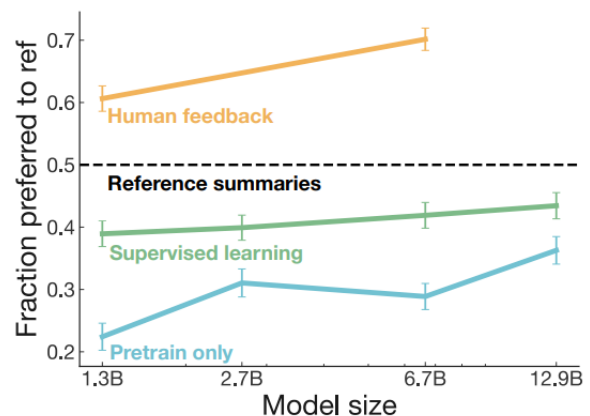


Fig. 1. Main results evaluating human feedback policies[3].

## ACKNOWLEDGEMENTS

I would like to express the deepest gratitude to Professor Gábor Prószéky, the main supervisor, and Zijian Győző Yang for their unrelenting support.

## REFERENCES

- [1] M. Kahla, Z. G. Yang, and A. Novák, "Cross-lingual fine-tuning for abstractive Arabic text summarization," in *Proceedings of the International Conference on Recent Advances in Natural Language Processing (RANLP 2021)*, (Held Online), pp. 655–663, INCOMA Ltd., Sept. 2021.
- [2] M. Kahla, A. Novák, and Z. G. Yang, "Fine-tuning and multilingual pre-training for abstractive summarization task for the arabic language," *Annales Mathematicae et Informaticae*, 2022.
- [3] N. Stiennon, L. Ouyang, J. Wu, D. M. Ziegler, R. Lowe, C. Voss, A. Radford, D. Amodei, and P. F. Christiano, "Learning to summarize from human feedback," *CoRR*, vol. abs/2009.01325, 2020.

# Topology management and control in multipath wireless sensor networks

Bálint Áron ÜVEGES

(Supervisor: András OLÁH)

Pázmány Péter Catholic University, Faculty of Information Technology and Bionics

50/a Práter street, 1083 Budapest, Hungary

uveges.balint.aron@itk.ppke.hu

**Abstract**—Wireless sensor networks are suitable to monitor diverse spatial phenomena in natural and artificial environments. Sensor nodes that constitute such network, convey local measurement information to a distinguished node called sink by utilizing multihop routing. A common technique to increase communication reliability is the application of multipath routing, where different paths are established from each node to the sink. While such approach increases connection redundancy, the quality of available paths heavily depend on the path construction strategy utilized by the corresponding routing algorithm. Unreliable transmission medium, individual node failures, and hazardous operating environment can render working paths unavailable at any point in time, leaving affected nodes disconnected from the network and associated spatial area unsupervised. To establish paths that meet certain quality of service criteria, and to detect and mitigate scenarios that can cause path failures, we present different topology management and control methods that incorporated into the Self-healing Multipath Routing Protocol aim to meet the outlined requirements.

**Keywords**—Multipath; Multihop; Wireless Sensor Networks, Disjoint, Graph, Path, Routing, Failure, Redundancy

## I. SELF-HEALING MULTIPATH ROUTING PROTOCOL

Wireless sensor networks (WSN) consist of computing, sensing and communicating devices, that's main purpose is to monitor different physical phenomena, and deliver sensed information to a central device, known as sink or base station. These devices are designed to function autonomously without the need for infrastructure. While these attributes make WSNs suitable to be deployed in remote or inaccessible outdoor and indoor areas, the network must be robust enough to handle and mitigate failure scenarios. WSN nodes are deployed in a scattered manner, requiring nodes closer to the sink to forward information from distant nodes, i.e., multihop routing is performed [1]. A single node failure can render multiple nodes disconnected, thus a commonly used technique to enhance a multihop WSN's reliability is to establish multiple paths towards the sink, to increase the connection's redundancy available to a node [2]. Most multipath related WSN publications focus on initial network construction and cover in-operation topology management and control to a limited extent. Scenarios caused by unreliable transmission medium, single node malfunction, and mass failure by hazardous environment are considered only partially. To cover such scenarios we propose the Self-healing Multipath Routing Protocol (ShMRP). Initial works showed promising results [3], however the centralized link and path control mechanism left room for improvement. To enhance the original design we introduce different techniques to improve network robustness, i.e., to handle link outages, node malfunction and massive node failures with reactive and proactive topology management. Such a technique is second learn, presented in Fig. 1.

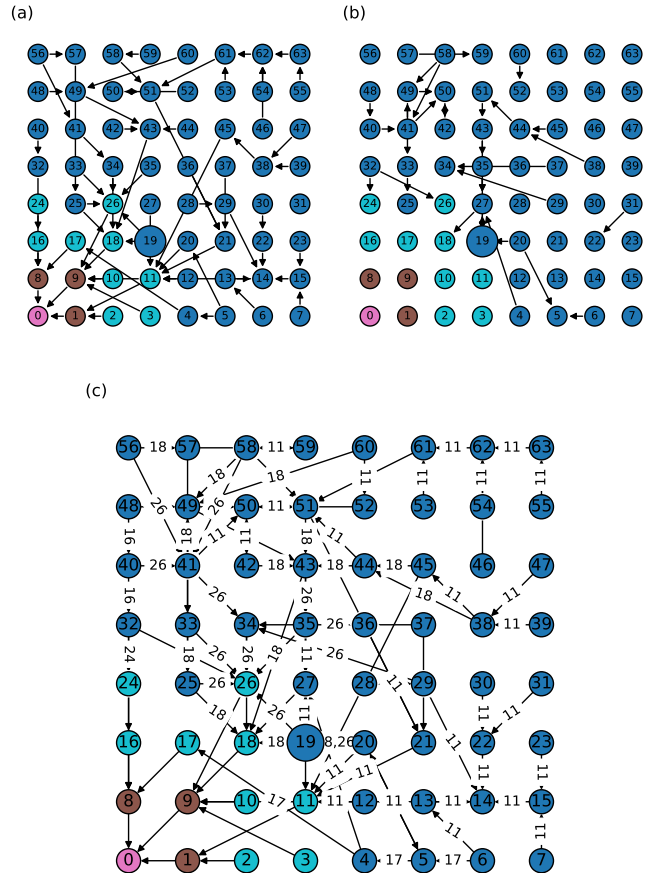


Fig. 1. Different roles in an ShMRP network: *Sink* (pink) aggregates information, *Internal* (brown) nodes are connected in mesh, *Border* (cyan) nodes terminate paths, *External* (blue) nodes are organized connect to one or more disjoint path. *Master* node is denoted with a large sphere. Initially constructed paths (a) are expanded during second learn (b), that results in robust multipath network (c).

## ACKNOWLEDGEMENTS

This research was supported by the National Research, Development and Innovation Office – NKFIH – through the grant no. TKP2021-NVA-27.

## REFERENCES

- [1] A. Förster, *Introduction to Wireless Sensor Networks*, ch. Multi-Hop Communications, pp. 77–97. John Wiley & Sons, Ltd, 2016.
- [2] S. Chaudhari, “A survey on multipath routing techniques in wireless sensor networks,” *International Journal of Networking and Virtual Organisations*, vol. 24, no. 3, p. 267, 2021.
- [3] B. A. Üveges, M. Lőrincz, and A. Oláh, “Self-healing multipath routing protocol to assist wireless sensor network based hazardous event monitoring,” in *2022 30th Telecommunications Forum (TELFOR)*, pp. 1–4, Nov 2022.

# PROGRAM 5

## ON-BOARD ADVANCED DRIVER ASSISTANCE SYSTEMS

Heads: Csaba REKECZKY, Ákos ZARÁNDY

# Real-time foreground segmentation for surveillance applications in NRCS Lidar Sequences

Marcell KÉGL

(Supervisor: Csaba BENEDEK)

Pázmány Péter Catholic University, Faculty of Information Technology and Bionics

50/a Práter street, 1083 Budapest, Hungary

kegl.marcell@itk.ppke.hu

## I. INTRODUCTION

Foreground-background separation is a crucial task in surveillance applications, requiring accurate and real-time results. Range sensors, such as laser-based LIDAR sensors, provide direct spatial geometrical information and offer advantages over conventional optical cameras.

While previous works have proved that LIDAR sensors are adequate for dynamic scene analysis [1], the limited vertical resolution and high cost of traditional sensors restrict their application in static configurations. An alternative LIDAR sensor called Livox Avia, which implements a Non-repetitive Circular Scanning (NRCS) technique, offers higher resolution, and better object detection and detail within the FoV [2]. This NRCS LIDAR sensor provides real-time measurements at affordable prices, making it suitable for various use cases, including not just surveillance but mapping and autonomous driving.

In this paper, we present a new method for foreground-background separation using measurement sequences from an NRCS LIDAR sensor deployed in a fixed position for surveillance. By generating and maintaining a high-resolution background model of the scene, combined with low integration time for dynamic object analysis, the spatial accuracy of the measurements is preserved. This allows for the extraction of sparse but accurate point cloud segments representing moving objects, enabling higher-level scene analysis in surveillance systems.

## II. THE PROPOSED METHOD

The proposed surveillance method detects and segments the foreground objects of the examined area. The algorithm then track the individual objects through the scene, so as further research, higher-level analysis is applicable.

Our method pipeline consists of 3 main steps, applied for all consecutive frames:

- 1) Foreground segmentation using a modified Mixture of Gaussians (MoG) approach [3]. Thanks to the non-repetitive movement of the LIDAR sensor, a high resolution background model can be created.
- 2) The noisy foreground point cloud is filtered by examining the second Gaussian components and applying pixel level noise filtering.
- 3) The segmented foreground points are clustered, and the individual objects are tracked with the Hungarian assignment algorithm and Kalman filter.

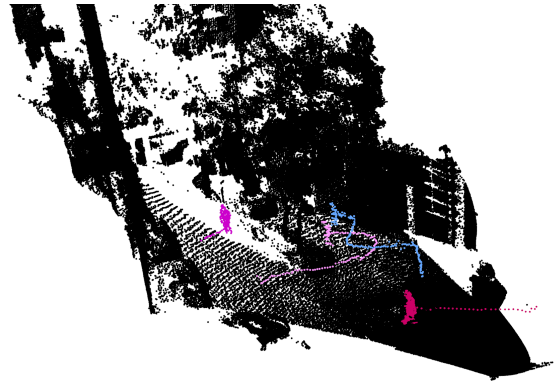


Fig. 1. Tracked foreground objects (colors) displayed over the high-resolution background model (black)

The developed method is able to detect and continuously track the foreground objects as long as they do not move out of the field of view. Thanks to the accurate spatial data the output of our algorithm can serve as an adequate data for further surveillance analysis.

## REFERENCES

- [1] C. Benedek, “3d people surveillance on range data sequences of a rotating lidar,” *Pattern Recognition Letters*, vol. 50, pp. 149–158, 2014. Depth Image Analysis.
- [2] L. Kovács, M. Kégl, and C. Benedek, “Real-time foreground segmentation for surveillance applications in nrsc lidar sequences,” *The International Archives of the Photogrammetry, Remote Sensing and Spatial Information Sciences, Proceedings of the XXIV ISPRS Congress*, 2022.
- [3] C. Stauffer and W. E. L. Grimson, “Learning patterns of activity using real-time tracking,” *IEEE Transactions on Pattern Analysis and Machine Intelligence*, vol. 22, pp. 747–757, 2000.

# Right ventricle segmentation in 3D echocardiographic recordings using deep neural networks

Bálint MAGYAR

(Supervisor: András HORVÁTH)

Pázmány Péter Catholic University, Faculty of Information Technology and Bionics  
50/a Práter street, 1083 Budapest, Hungary  
magyar.balint@itk.ppke.hu

**Abstract**—Deep learning algorithms are widely used tools for medical image processing tasks due to their outstanding performance and generalization capabilities. In this work, a deep neural network was applied for the segmentation of the right ventricle (RV) of the heart in 3-dimensional (3D) echocardiographic recordings.

The implemented method utilizes a deep neural network. The novelty of this method lies in its approach to predict the shape of the RV. Unlike previous techniques, the algorithm directly predicts the vertices of an anatomically defined mesh.

**Keywords**—echocardiography, right ventricle, image segmentation, deep learning

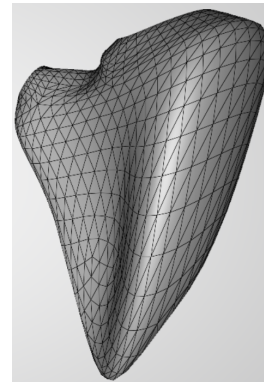


Fig. 1. Annotation sample from the dataset. Anatomical model of the right ventricle as a triangle mesh.

## I. SUMMARY

Echocardiograms are extensively utilized for evaluating cardiac functions. In the past, much of the research emphasis was placed on the left ventricle. However, recent studies have demonstrated the independent prognostic significance of RV function, even among patients with left-sided heart disease [1].

By analyzing the 3D shape of the RV, vital measures such as the ejection fraction and longitudinal strains can be computed. These measures are pivotal for estimating the patient's condition, assessing the risk of heart failure, and determining the appropriate treatment course [2].

In this paper we propose an end-to-end, encoder-decoder style deep learning-based method that predicts the 3D shape of the RV using 3D echocardiogram videos. In contrast to previously proposed methods that construct a 3D model by combining segmented 2D slices [3] or predicting a transformation from an anatomical model [4], our segmentation model directly predicts the vertices of a triangle mesh that accurately represents the anatomical shape of the RV (Figure 1).

We have collected a substantial dataset (more than 45 thousand 3D images) of 3D echocardiographic recordings, with manual annotation specifically focusing on the RV. Our model achieved a mean absolute error of 3.99 millimeters in predicting the mesh vertex coordinates and a mean absolute error of 16.78 milliliters in estimating the mesh volume in the test set.

## PUBLICATIONS OF THE AUTHOR

B. Magyar, M. Tokodi, A. Soós, et al., “Rvenet: A large echocardiographic dataset for the deep learning-based assessment of right ventricular function,” in *Computer Vision—ECCV 2022 Workshops: Tel Aviv, Israel, October 23–27, 2022, Proceedings, Part III*, Springer, 2023, pp. 569–583.

M. Tokodi, B. Magyar, A. Soós, et al., “Deep learning-based prediction of right ventricular ejection fraction using 2d echocardiograms,” *JACC: Cardiovascular Imaging*, 2023.

## REFERENCES

- [1] E. Surkova, D. Muraru, D. Genovese, P. Aruta, C. Palermo, and L. P. Badano, “Relative prognostic importance of left and right ventricular ejection fraction in patients with cardiac diseases,” *Journal of the American Society of Echocardiography*, vol. 32, no. 11, pp. 1407–1415, 2019.
- [2] A. Kovacs, B. Lakatos, M. Tokodi, and B. Merkely, “Right ventricular mechanical pattern in health and disease: Beyond longitudinal shortening,” *Heart failure reviews*, vol. 24, no. 4, pp. 511–520, 2019.
- [3] S. Dong, G. Luo, K. Wang, S. Cao, Q. Li, and H. Zhang, “A combined fully convolutional networks and deformable model for automatic left ventricle segmentation based on 3D echocardiography,” *BioMed research international*, vol. 2018, 2018.
- [4] S. Dong, G. Luo, C. Tam, et al., “Deep atlas network for efficient 3D left ventricle segmentation on echocardiography,” *Medical image analysis*, vol. 61, p. 101638, 2020.

# Spatial completion of sparse lidar point cloud sequences

Örkény Ádám H. ZOVÁTHI  
(Supervisor: Csaba BENEDEK)

Pázmány Péter Catholic University, Faculty of Information Technology and Bionics  
50/a Práter street, 1083 Budapest, Hungary  
h.zovathi.orkeny.adam@itk.ppke.hu

**Abstract**—This paper introduces a novel method for the spatial completion of point cloud sequences captured by a non-repetitive circular scanning (NRCS) Lidar sensor. In our approach, we utilize consecutive sparse measurements captured by NRCS Lidars in the depth image domain, and we propose a U-Net-like spatio-temporal deep network for producing spatially precise high-density depth data from the sparse depth image sequences. For the training and validation of the proposed method, a synthetic dataset is introduced as well, which contains various simulated urban scenarios from the CARLA virtual world.

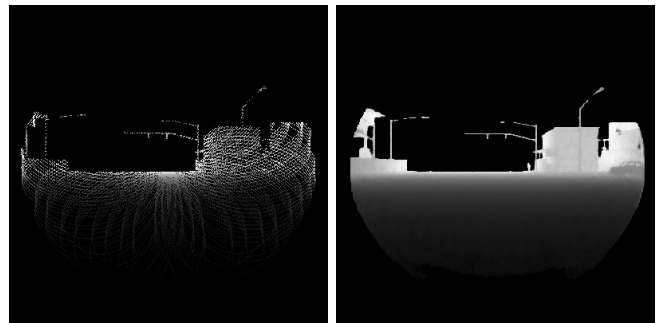
## I. INTRODUCTION

Recent scientific and engineering progress in autonomous driving and mobile robotics make us believe that cars will be able to drive without human intervention in the near future. Up-to-date intelligent robot and vehicle platforms are often equipped with real-time Lidar sensors as they are capable of providing accurate depth information about their environment. Although, in general, rotating multi-beam (RMB) Lidars [1] are the most widespread choices, recent non-repetitive circular scanning (NRCS) Lidar sensors are also increasingly applied for dynamic environment perception and recognition tasks such as advanced scene analysis and understanding. Unlike RMB Lidars, NRCS Lidars (e.g., the Livox AVIA sensor) [2] are able to densely map large areas from a given scanning position due to their special non-repetitive scanning patterns, at a lower cost compared to the rotating technology. The main challenge is here to optimally balance between the spatial and the temporal resolution of the recorded range measurements using an effective temporal integration window [3].

The main motivation of this research is to improve on the imperfect onboard perception of intelligent robots and vehicles that are equipped with a single NRCS Lidar sensor. In this context, we propose a novel deep learning based approach for densifying the sparse NRCS Lidar data while keeping its spatial accuracy and temporal resolution high.

## II. THE PROPOSED METHOD

The goal of the proposed solution is to produce a high-quality, dense and spatially precise point cloud sequence from measurements of a single NRCS Lidar sensor, with the same temporal resolution as the original sensor stream. Our approach consists of three main steps: *First*, the consecutive measurements of the NRCS Lidar are grouped by a narrow integration window, which results point cloud sets that are spatially precise, but notably sparse. Thereafter, the points within each group are converted onto a high-resolution depth image. *Second*, by each actual time frame, the last five collected depth images are fed to the proposed spatio-temporal deep network, which composes a high-quality range image



(a) Raw sensor data

(b) Proposed densification

Fig. 1. Depth image samples from the raw (a) and the densified (b) depth image stream from the CARLA virtual world [4], using a NRCS Lidar sensor

as output, with minimal motion blurring artifacts. This deep network can be trained on the introduced virtual dataset, which consists of realistic urban scenarios. *Third*, the output high-quality range image can be backprojected to the 3D space in a straightforward manner.

## III. SUMMARY

Using an effective spatio-temporal deep architecture, data-driven methods can help to efficiently balance between the spatial and the temporal resolution of NRCS Lidar measurements and therefore improve on the overall data quality (see Fig. 1). Although our ultimate future goal to use the proposed algorithm in real intelligent robot and vehicle platforms, effective training and evaluation can be enhanced by utilizing realistic scenarios from virtual worlds as well.

## ACKNOWLEDGEMENTS

This work was partially supported by the KDP-2020 Cooperative Doctoral Program (KDP-977852) from the source of the NRDI Fund.

## REFERENCES

- [1] Ö. Zováthi, B. Nagy, and C. Benedek, “Point cloud registration and change detection in urban environment using an onboard lidar sensor and MLS reference data,” *Int. J. Appl. Earth Obs. Geoinf.*, vol. 110, p. 102767, 2022.
- [2] Ö. Zováthi, B. Pálffy, Z. Jankó, and C. Benedek, “ST-DepthNet: A spatio-temporal deep network for depth completion using a single non-repetitive circular scanning lidar,” *IEEE Robotics and Automation Letters*, vol. 8, no. 6, pp. 3270–3277, 2023.
- [3] L. Kovács, M. Kégl, and C. Benedek, “Real-time foreground segmentation for surveillance applications in NRCS lidar sequences,” *ISPRS Arch. Photogramm. Remote Sens. Spatial Inf. Sci.*, vol. XLIII-B1-2022, pp. 45–51, 05 2022.
- [4] A. Dosovitskiy, G. Ros, F. Codevilla, A. Lopez, and V. Koltun, “CARLA: An open urban driving simulator,” in *Proc. Ann. Conf. Rob. Learn.*, pp. 1–16, 2017.



# APPENDIX

---

<b>PROGRAM 1: Bionics, Bio-inspired Wave Computers, Neuromorphic Models</b>	
<b>Name</b>	<b>Supervisor</b>
Zsófia BALOGH-LANTOS	Zoltán FEKETE PhD
Gréta Lilla BÁNYAI	Tamás GARAY PhD
Eszter BIRTALAN	Miklós KOLLER PhD
Camilla CANCRINI	Andrea CILIBERTO PhD
Fanni FARKAS	Zoltán GÁSPÁRI PhD
Gábor FARKAS	Szabolcs KÁLI PhD
Tünde Éva GAIZER	Attila CSIKÁSZ-NAGY DSc
Máté KÁLOVICS	Kristóf IVÁN PhD, Zsolt SZABÓ DSc
Barnabás KOCSIS	István ULBERT MD DSc
Dorottya KOCSIS	Franciska ERDŐ PhD
Valentina MADÁR	Attila CSIKÁSZ-NAGY DSc
Vilmos MADARAS	Csaba BENEDEK PhD
Zsófia MOLNÁR	Sándor PONGOR MHAS, Balázs LIGETI PhD
Kristóf MÜLLER	Miklós KOLLER PhD
Eszter NAGY-KANTA	Zoltán GÁSPÁRI PhD
Afrodité NÉMETH	Tamás GARAY PhD
Bíborka PILLÉR	Attila CSIKÁSZ-NAGY DSc
Balázs RADELECZKI	József LACZKÓ PhD
András László SZABÓ	Zoltán GÁSPÁRI PhD
Giorgio TALLARICO	Andrea CILIBERTO PhD
Mihály András VÁGHY	Mihály KOVÁCS DSc, Gábor SZEDERKÉNYI DSc
Soma VARGA	Bálint PÉTERFIA PhD
Áron WEBER	Attila CSIKÁSZ-NAGY DSc

---

---

**PROGRAM 2: Computer Technology Based on Many-core Processor Chips, Virtual Cellular Computers, Sensory and Motoric Analog Computers**

---

<b>Name</b>	<b>Supervisor</b>
Boldizsár Zsolt BALOG	György CSEREY PhD, Gábor NYÍRI PhD
Balázs CSUTAK	Gábor SZEDERKÉNYI DSc
Lóránt Szabolcs DAUBNER	Kálmán TORNAI PhD, Tamás ZSEDROVITS PhD
Balázs DRÁVAI	István Zoltán REGULY PhD
András Pál HALÁSZ	Péter SZOLGAY DSc, Kálmán TORNAI PhD
Gergely HORVÁTH	Gábor SZEDERKÉNYI DSc
Imre Gergely JÁNOKI	Péter FÖLDESZ DSc
Rizal MAULANA	György CSEREY PhD
Katalin SCHÄFFER	Miklós KOLLER PhD
Bálint SIKLÓSI	Péter SZOLGAY DSc, István Zoltán REGULY PhD
Gergely SZABÓ	András HORVÁTH PhD

---

---

**PROGRAM 3: Feasibility of Electronic and Optical Devices, Molecular and Nanotechnologies, Nano-architectures, Nanobionic Diagnostic and Therapeutic Tools**

---

<b>Name</b>	<b>Supervisor</b>
András ESZES	Zsolt SZABÓ DSc
Mitra MOAYED	György CSABA PhD
Tamás RUDNER	György CSABA PhD

---

---

**PROGRAM 4: Human Language Technologies, Artificial Understanding, Telepresence, Communication**

---

<b>Name</b>	<b>Supervisor</b>
Kamran IBIYEV	Gábor PRÓSZÉKY DSc
Mram KAHLA	Gábor PRÓSZÉKY DSc, Zijian Győző YANG PhD
Bálint Áron ÜVEGES	András OLÁH PhD

---

---

**PROGRAM 5: On-board Advanced Driver Assistance Systems**

---

<b>Name</b>	<b>Supervisor</b>
Marcell KÉGL	Csaba BENEDEK PhD
Bálint MAGYAR	András HORVÁTH PhD
Örkény Ádám H. ZOVÁTHI	Csaba BENEDEK PhD

---